# Efficient Numerical Methods Based on Integral Transforms to Solve Option Pricing Problems

Edgard Ngounda



A Thesis submitted in partial fulfillment of the requirements for the degree of Doctor of Philosophy in the Department of Mathematics and Applied Mathematics at the Faculty of Natural Sciences, University of the Western Cape

Supervisor: Prof. Kailash C. Patidar

June 2012

# KEYWORDS

Computational finance

Partial differential equations

American and European options

Barrier options

Jump-diffusion model


Heston's volatility model

Contour integrals

Spectral methods

Laplace transforms

Domain decomposition.

# ABSTRACT

**Efficient Numerical Methods Based on Integral Transforms to Solve Option Pricing Problems**

by

**Edgard Ngounda**

**PhD thesis, Department of Mathematics and Applied Mathematics, Faculty of Natural Sciences, University of the Western Cape**

In this thesis, we design and implement a class of numerical methods (based on integral transforms) to solve PDEs for pricing a variety of financial derivatives. Our approach is based on spectral discretization of the spatial (asset) derivatives and the use of inverse Laplace transforms to solve the resulting problem in time. The conventional spectral methods are further modified by using piecewise high order rational interpolants on the Chebyshev mesh within each sub-domain with the boundary domain placed at the strike price where the discontinuity is located. The resulting system is then solved by applying Laplace transform method through deformation of a contour integral. Firstly, we use this approach to price plain vanilla options and then extend it to price options described by a jump-diffusion model, barrier options and the Heston's volatility model. To approximate the integral part in the jump-diffusion model, we use the Gauss-Legendre quadrature method. Finally, we carry out extensive numerical simulations to value these options and associated Greeks (the measures of sensitivity). The results presented in this thesis demonstrate the spectral accuracy and efficiency of our approach, which can therefore be considered as an alternative approach to price these class of options.



June 2012

# DECLARATION

I declare that *Efficient Numerical Methods Based on Integral Transforms to Solve Option Pricing Problems* is my own work, that it has not been submitted before for any degree or examination at any other university, and that all sources I have used or quoted have been indicated and acknowledged by complete references.



Edgard Ngounda June 2012

Signed .....

# ACKNOWLEDGEMENT

Lévè lé wè Ndjiami, mô dousou na mpari é wè no soumbou à wè a kielè mè mô nà djandja yi.

This work would not have been possible without the financial support from the La Direction Générale des Bourses et Stages du Gabon (DGBS) now called Agence Nationale des Bourses du Gabon (ANBG), from the first year of tertiary studies to the completion of this thesis.

I am grateful to Professor Kailash C. Patidar for accepting me as a PhD student in his research team. Throughout this thesis work, he has been very instrumental in finding the right balance between independence and supervision, trust and test, support and challenge. Thank you prof for the good working relationship that you created over the years, your prompt response in helping to secure financial support from sponsors and in welcoming me in your family environment for late consultations whenever required.

The next person I am indebt to is my PhD fellow Edson Pindza with whom I had the privilege to share the 'ups' and 'downs' moments during the time of my study in South Africa. Thank you for lifting me up during my down moments, for your incentive during countless discussions and interactions.

I am grateful to the love and support of my family. I would like to thank them for their generosity and the part they have played in making the person I am today, without their support I would not have had all that it takes to succeed. To my Mother who always trust and believe in me and never questioned the relevance of my long stay here in South Africa. Great thanks to my uncles Ompigui Thacien and Jules Anoumba

and their respective families for the warm welcome every time I had the opportunity to go home. To my brothers and sisters, Ya Seraphine, Lydie, David (and his wife Sandrine), Sandra, Zita, Aude, Gael, Ralph, and my nephew Odi, Owen, Stephanie, Dane for the numerous calls, sms' and emails of supports and encouragements. I also extend my gratitude to my beloved fiancé Aurixiane for her support at the beginning of this undertaking and to her sister Ya Delphine with her family for their enthusiasm and kindness. I would never forget her efforts in helping to get funding for this undertaking. Special words of gratitude to Prof Patidar's wife and their children for their warm welcome at all time at their home. Their warm and tasteful indian tea always made me wanted to come back.

I would like to thank the University of the Western Cape, and the Department of Mathematics and Applied Mathematics for the opportunity to pursuit this thesis. Thanks to the office of Dean of Research for the laptop acquired for the duration of the thesis. My profound appreciation also goes to Prof. John P. Boyd for his input on decomposition methods during emails communication we had at an early stage of this thesis. A heartfelt thanks to friends and PhD candidates in the mathematics postgraduate lab, thank you for the passionate discussions we had on various topics which very often helped to ease the overload of study. Special thanks to Raji and Runke for accommodating me in HPR for two months.

Last but not the least, I wish to thank the small Gabonese community of the Western Cape.

# DEDICATION

I dedicate this work to all those who have contributed in one way or other in building the person I am and ought to be, to my mother and late father who instilled in me the notions of respect, discipline, love and the desire for success in my early years.

# Contents

# List of Tables

# List of Figures

# List of Publications

Part of this thesis has been submitted for publications to various international journals in the form of the following research papers:

1. E. Ngounda and K.C. Patidar, Numerical application of the Laplace transform for pricing European options, submitted for publication.

2. E. Ngounda, K.C. Patidar and E. Pindza, Improved Laplace transform method for the numerical solution of European option pricing problems, submitted for publication.



3. E. Ngounda, K.C. Patidar and E. Pindza, A robust Laplace transformed method for pricing American options, submitted for publication.

4. E. Ngounda, K.C. Patidar and E. Pindza, Contour integral method for European options with jumps, submitted for publication.

5. E. Ngounda, K.C. Patidar and E. Pindza, Pricing barrier options using Laplace transforms, submitted for publication.

6. E. Ngounda, K.C. Patidar and E. Pindza, A contour integral methods for solving Heston's model, submitted for publication.

# Chapter 1

# General introduction

The increasing interest in pricing financial derivatives has led to the development of many models that can best describe the evolution of options in the market place. As a result the pricing of these financial instruments has become an active research area in mathematical modeling. Analytical solutions of some of these models either do not exist or are difficult to obtain in a closed-form. Because of this numerical methods have become a fundamental tool for practitioners when pricing these options.



Some of the numerical methods most used in option pricing include finite difference, finite element and Runge-Kutta. However an alternative method which has emerged in recent years for numerically solving linear parabolic problems is based on Laplace transform [1, 50, 125]. In this thesis, we explore the utility of this method for pricing options.

Below we present some basic notions used in the option pricing theory. Then we proceed with the analysis of the Laplace transform method followed by the literature review and outline of the rest of the thesis.

## 1.1 A quick tour to option pricing

An option is a financial instrument which gives its holder the right without any obligation to buy or sell an asset at the predetermined price known as strike price within

a specified period of time (expiration time). If the option gives its holder the right to buy the underlying asset, it is a call option. In contrast, if the holder can only exercise his/her right to sell then it is a put option. Choosing to sell or buy an underlying option is termed as exercising the option. The nature of the option is largely dependent on the exercise date. When the option's holder is only allowed to exercise his/her right at expiration time, the option is called a European option. On the other hand if the holder can exercise the option at any convenient time prior to expiry, the option is called a American option. These two types of options are often classified as plain vanilla options. Besides these, there are other types of options very widely used in the financial market, namely, the exotic options. In this thesis, we will explore methods for pricing some of these options.

Options are mainly used for speculation and hedging. Speculators trade the options to make money according to their judgment of the trend of the asset prices. For example, if the underlying stock is subjected to market's fluctuations, the holder of the call option is likely to make money if at the exercise date the asset is worth more than the strick price and decides to sell it. On the other hand, the option is worthless if at the exercise date, the stock price is less than the strike price. The hedging takes place when investors want to secure the investment by reducing the risk of unpredictable events in the financial market.



Since its development in the 1970s by F. Black and M. Scholes, the Black-Scholes equation has become a fundamental model for pricing financial derivatives [12], in particular, options. For European and American options, the Black-Scholes equation is given by

$$\frac{\partial V}{\partial t} + \frac{1}{2}\sigma^2 S^2 \frac{\partial^2 V}{\partial S^2} + rS\frac{\partial V}{\partial S} - rV = 0, \qquad S \in (0, \infty), \quad t \in (0, T), \tag{1.1.1}$$

where $V(S, t)$ is the value of the option, $S$ the underlying asset, $0 \leq t \leq T$ the time at which the option is obtained, $T$ is the expiry date of the option, $r$ is the interest rate, $\sigma$ the volatility of the underlying asset and $K$ the strike price. At maturity, the payoff

of European and American options is given by

$$\left.\begin{array}{ll} \max(S-K,0) & \text{for a call option,} \\ \\ \max(K-S,0) & \text{for a put option.} \end{array}\right\} \tag{1.1.2}$$

American option pricing PDEs differ from their European counterpart due to the possibility of an early exercise (before the maturity) of the option which translates the American option pricing models to free boundary PDEs. On one side of the free boundary (known as the continuation region) it is optimal to hold the option. On the other side of the free boundary (known as the stoping region), it is optimal to exercise it. For a put (call) option, the stoping region is located on the left (right) of the free boundary whereas the continuation region is on the right (left). Therefore, determining the free boundary becomes a crucial part when one wishes to solve these type of options. To this end, let $S_f$ be the free boundary, $S_f$, divides the domain $(S,t)$ into two parts, the continuation region



$$\{(S,t) \in \mathbb{R}_+ \times [0,T] : V(S,t) > \max(K-S,0)\},$$

which is the region where the option is suppose to be alive, and the stopping region which is the region where early exercise is advisable, and is defined as

$$\{(S,t) \in \mathbb{R}_+ \times [0,T] : V(S,t) = \max(K-S,0)\}.$$

The price of the American option $V(S,t)$ satisfies (1.1.1) when

$$\begin{cases} S < S_f(t), \quad 0 \le t < T, & \text{for call option,} \\ \\ S > S_f(t), \quad 0 \le t < T, & \text{for a put option.} \end{cases}$$

On the free boundary $S_f$, the value of the option is

$$V(S_f(t), t) = K - S_f(t).$$

Analytical solutions for European options (1.1.1)-(1.1.2) are relatively easy to obtain. For these, we refer the reader to [64, 71] or any other standard text book on the financial engineering. Unlike European options, the free boundary makes pricing American options very challenging. The difficulty in pricing American options is finding the early exercise boundary associated with the possibility of an early trade prior to the expiration date of the option. As a result, finding the unknown boundary becomes an integral part of the solution of American options.

The Black-Scholes model is derived based on the assumption that the underlying asset follows a geometric Brownian motion process and has a continuous sample path which indicates that small changes in stock price occur in short intervals. However, on the stock market, jumps are regularly observed in the discrete movements of the stock price $S(t)$ [19, 62, 70]. These movements cannot be capture by the log-normal distribution characteristic of the stock price in the Black-Scholes setting and therefore alternative models which address these shortcoming are necessary. Alternative models include but not limited to the stochastic volatility models [62], Lévy models [21], Jump-diffusion model [100]. With the introduction of jumps, the market becomes incomplete and the derivation of the fair price of the derivatives becomes somewhat more involved. In such cases, the application of the Itŏ calculus [80] translates the problem to a partial integro-differential equation (PIDE) of the form

$$\frac{\partial V}{\partial t} = \frac{1}{2}\sigma^2 S^2 \frac{\partial^2 V}{\partial S^2} + (r - \lambda\kappa) S \frac{\partial V}{\partial S} - (r + \lambda) V + \lambda \int_0^\infty V(S\eta)\psi(\eta) d\eta, \qquad (1.1.3)$$

where $r$ is the risk free interest rate ($r \geq 0$), $\lambda$ is the intensity of the Poisson process ($\lambda > 0$), $\kappa$ is the expected jump size, $t$ is the current time, $\psi(\eta)$ is the probability function of the jump amplitude $\eta$, where $\psi(\eta) \geq 0$, for all $\eta$.

In addition to these options we will also consider barrier options which have expanded rapidly in recent years. These options are mostly traded in the over-the-counter market in which financial institutions sell a variety of exotic options tailored to meet the demands of various clients. They are characterized by the dependence of their payoffs on the path of the underlying asset throughout their life time. When the asset price reaches a specified barrier level, these options are either exercisable (activated), in this case, they are called knock-in options or they expire (extinguish) in which, case they are called knock-out options.

Another class of option pricing problem is the model under the stochastic volatility known as the Heston's volatility model. This model leads to a more realistic valuation of options than the celebrated Black-Scholes model constituting its extension to the case of a variable volatility [70, 100]. Semi-close formula for solving the Heston's model exists [62] but its implementation is not a straightforward exercise which makes Heston's model difficult to price.

The semi-discrete versions of the problems that one usually encounters in option pricing can be solved using a variety of numerical integrators, including classical Runge-Kutta methods. However, in view of the fact that the method of Laplace transform was quite successful for solving some other class of problems, we decided to explore it for problems in computational finance. To this end, let us discuss some of the basic results concerning the Laplace transform of a function of one variable which can be useful in the construction and analysis of this method.



## 1.2 Laplace transform and its applications in solving differential equations

Over the last two decades, Laplace transform has established itself as a major numerical method for solving linear partial differential equations arising in many area, such as physics, engineering, epidemiology, and in a growing areas such as computational

finance. It solves the PDE by removing the time variable, leaving an ordinary differential equation (ODE) in Laplace space. After solving the ODE in the Laplace space, the resulting solution is inversed to recover the solution in the usual time and space variables. Unlike time stepping methods such as the classical finite difference methods, which usually require small time steps to accurately solve PDEs, the Laplace transform solve the PDE directly at specific time and offers high accuracy. In addition, it can be easily parallelized [50, 51, 93, 138].

In view of the fact that the applications of the Laplace transform will be explore in this thesis, let us discuss some of its basic properties. To begin with, we note that the Laplace transform of a function $f(t)$ is defined as

$$F(z) = \int_0^\infty e^{-zt} f(t) dt, \qquad \operatorname{Re} z > \widetilde{\sigma}_0, \tag{1.2.1}$$

where $\widetilde{\sigma}_0$ is the convergence abscissa of the Laplace transform with $\widetilde{\sigma} \geq \widetilde{\sigma}_0$. The following theorem from [37] gives the domain of convergence of the Laplace transform.



**Theorem 1.2.1** ([37]) *The exact domain of convergence of the Laplace transform (1.2.1) is the right half-plan* $\operatorname{Re} z > \widetilde{\sigma}_0$*, possibly including none, part, or all of the line,* $\operatorname{Re} z = \widetilde{\sigma}_0$*; admitting the possibilities* $\widetilde{\sigma}_0$*.*

*Proof.* See [37].

The open half-plane $\operatorname{Re} z > \widetilde{\sigma}_0$ is referred to as the half-plane of convergence of the Laplace transform; the vertical line $\operatorname{Re} z = \widetilde{\sigma}_0$ is called the line of convergence.

**Theorem 1.2.2** ([37]) *Laplace transform (1.2.1) is an analytic function in the interior of its half-plane of convergence,* $\operatorname{Re} z = \widetilde{\sigma}_0$*.*

*Proof.* See [37].

Furthermore, we assume that $f(t)$ is a function of exponential order as $t \to +\infty$, and $\widetilde{\sigma}_0$ is such that $e^{-\widetilde{\sigma}_0 t}|f(t)| \leq +\infty$. In addition, if $f(t)$ is absolutely integrable for $t > 0$, then the Laplace integral (1.2.1) converges for all $\operatorname{Re} z > \widetilde{\sigma}_0$.

The main difficulty, however, in the use of the Laplace transform comes from the recovery of the original function $f(t)$ for a given Laplace transform $F(s)$, i.e., the evaluation of the inverse formula (1.2.2). Analytical solutions are often hard to obtained, and one has to rely on numerical methods to evaluate (1.2.2). An inventory of some of the most significant numerical methods developed in the last three decades using this idea can be found in [36, 40, 102]. These methods were classified by Abate and Valko [1] as Fourier series expansion method, Laguerre function expansion method, method based on the combination of Gaver functionals, and method based on the deformation of the Bromwich contour. In this thesis, we use the last of these four methods.

The Bromwich integral is given by

$$f(t) = \frac{1}{2\pi i}\int_{\mathcal{C}} e^{zt}F(z)dz, \qquad t > 0, \tag{1.2.2}$$

where $\mathcal{C}$ is a contour known as the Bromwich contour. Originally, $\mathcal{C}$ represents the vertical line from $\widetilde{\sigma}_0 - i\infty$ to $\widetilde{\sigma}_0 + i\infty$ with $\widetilde{\sigma} > \widetilde{\sigma}_0$. Formula (1.2.2) is valid if all singularities of $F(z)$ are located to the left of the vertical line $x = \widetilde{\sigma}$, i.e., $\operatorname{Re} z < \widetilde{\sigma}$ which is the case for linear parabolic PDEs.



For the numerical evaluation of (1.2.2), the contour $\mathcal{C}$ can be parameterized by

$$z = \widetilde{\sigma} + iy, \quad -\infty < y < \infty. \tag{1.2.3}$$

Then the integral (1.2.2) takes the form

$$f(t) = \frac{e^{\widetilde{\sigma}t}}{2\pi i}\int_{-\infty}^{\infty} e^{iyt}F(\widetilde{\sigma} + iy)dy. \tag{1.2.4}$$

Unfortunately, in most cases, the above integral is difficult to evaluate numerically for a number of reasons: firstly, the integrand is highly oscillatory on the Bromwich contour (1.2.3), when $y \to \pm\infty$. Secondly, the transformed function $F(\widetilde{\sigma} + iy)$ may decay slowly as $y \to \pm\infty$ ([39]).

Our numerical method for inverting the Laplace transform is based on the method

developed by Talbot [125] and uses the deformation of the Bromwich contour. Talbot's idea was to deform the Bromwich line into a contour which starts and ends in the left half-plane (see Figure 1.2.1 page 9 for an example of such a contour). Such a deformation of the contour is possible by the Cauchy's integral theorem [123]. This theorem is applicable provided that all singularities of the transformed function $F(z)$ are contained in the interior of the new contour and that $|F(z)| \to 0$ as $|z| \to \infty$ in the half-plane $\operatorname{Re} z < \widetilde{\sigma}_0$ [138]. Such contours are used in [93, 125, 138], all of which are of the form

$$z = z(\ell), \quad -\infty < \ell < \infty,$$

with the property that $\operatorname{Re} z \to -\infty$ as $\ell \to \pm\infty$.

The efficiency of the Talbot approach depends on the choice of the contour, as well as the number of functions evaluation in the trapezoidal rule. Simpler contours such as hyperbolas and parabolas are proposed in [93, 138]. These contours display a better convergence rate of order $\mathcal{O}(10^{-N})$ than the original cotangent contour used by Talbot [137]. In this chapter, we consider the hyperbola as the integration contour defined by



$$z = \widetilde{\mu}\left(1 + \sin\left(i\ell - \alpha\right)\right), \quad \ell \in \mathbb{R}, \tag{1.2.5}$$

where the real parameters $\widetilde{\mu} > 0$ and $0 < \alpha < \pi/2$ determine the geometry of the contour. The positive parameter $\widetilde{\mu}$ controls the width of the contour while $\alpha$ determines its geometric shape, i.e., the asymptotic angle. On the contour (1.2.5) the inversion formula (1.2.2) can be rewritten as

$$f(t) = \frac{1}{2\pi i}\int_{-\infty}^{\infty} e^{z(\ell)t} F\left(z(\ell)\right) z'(\ell) d\ell, \tag{1.2.6}$$

where

$$z'(\ell) = \widetilde{\mu} i \cos\left(i\ell - \alpha\right).$$

For $h > 0$ such that $\ell_k = kh$, where $k$ is an integer, the trapezoidal rule can then

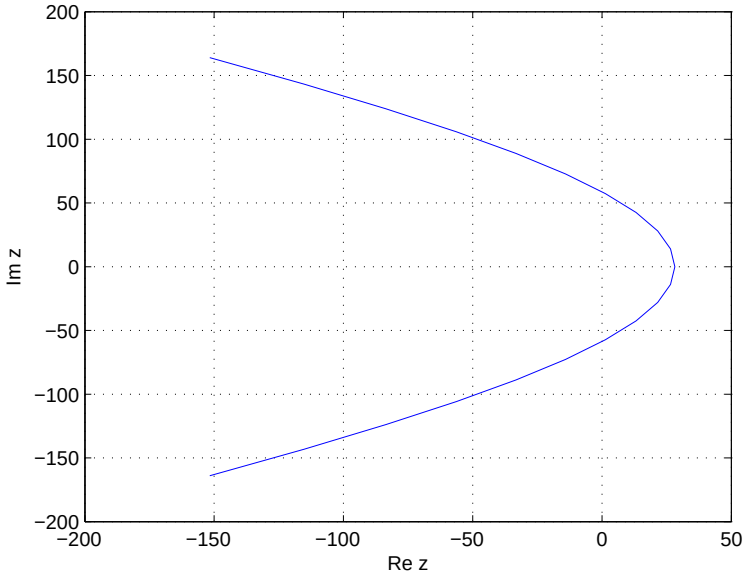


Figure 1.2.1: Talbot contour of hyperbolic type.



be expressed by

$$\tilde{f}(t) \approx \frac{h}{2\pi i} \sum_{k=-\infty}^{\infty} e^{z(\ell_k)t} F\left(z(\ell_k)\right) z'(\ell_k), \tag{1.2.7}$$

where $h$ is the step-size. In practice, the infinite sum has to be truncated at a finite integer $M$, in which case one commits a truncation error as discussed below. Note that, because of the symmetry of the contour (1.2.5), we can re-written (1.2.7) as

$$\tilde{f}_M(t) \approx \mathrm{Re}\left\{ \frac{h}{\pi i} \sum_{k=0}^{M} {}^{\circ} e^{z(\ell_k)t} F\left(z(\ell_k)\right) z'(\ell_k) \right\}, \tag{1.2.8}$$

where $^{\circ}$ indicates that the first term is divided by 2. The benefit of using (1.2.8) is that it reduces by half the summation (1.2.7) and subsequently the number of linear system to be evaluated in (2.4.17) (see page 38), (3.4.6) (see page 57) and (5.4.6) (see page 94).

In the following sections, we analyze the overall error that occur during the approximation of the solution using this integration method in time.

## 1.3 Error analysis of the Laplace transform approach for solving parabolic PDEs

In this section, we analyze the overall error associated with the use of Laplace transform for integration in the time direction. To this end, first we note that the application of the trapezoidal rule (1.2.7) to the unbounded integral (1.2.6) introduces discretization error. Secondly, a truncation of the infinite series (1.2.7) at a finite integer $M$ (for practical implementation) produces a truncation error as one would expects. Furthermore, since the evaluation of (1.2.7) is done in floating point environment, a roundoff (conditioning) error is also introduced at each evaluation there. This roundoff error may increase dramatically and affect the accuracy of the numerical solution due to the exponential factor involved in (1.2.8) as we will discuss below. The total error occurred due to the use of the Laplace transform is therefore the sum of the discretization, truncation and conditioning errors.



### Discretization error

The discretization error in this case is the difference between the continuous formula (1.2.6) and the corresponding trapezoidal formula (1.2.7), i.e.,

$$\begin{aligned} E_d &= f(t) - \tilde{f}(t) \\ &= \int_{-\infty}^{\infty} e^{z(\ell)t} F\left(z(\ell)\right) z'(\ell) d\ell - \frac{h}{2\pi i} \sum_{k=-\infty}^{\infty} e^{z(\ell_k)t} F\left(z(\ell_k)\right) z'(\ell_k). \end{aligned} \tag{1.3.1}$$

To estimate the discrete error (1.3.1), the idea is to use the contour integral to represent $E_d$. This approach is based on the Cauchy's residue theorem in complex analysis was originally developed by Martensen [96] for an analytic function $f(t)$ defined on $(-\infty, \infty)$. In that paper, the author showed that for an analytic function, the trapezoidal rule (1.2.7) converges exponentially as illustrated in the following theorem.

**Theorem 1.3.1** ([96]) *Let $f : \mathbb{R} \to \mathbb{R}$ be an analytic function. Then there exists a strip $\mathbb{R} \times (-d, d)$ in the complex plane with $d > 0$ such that $f$ can be extended to a complex analytic function $f : \mathbb{R} \times (-d, d) \to \mathbb{C}$. Furthermore, the error for the trapezoidal rule indicated in (1.3.1), is given by*

$$E_d = Re\left\{\int_{-\infty+i\theta}^{\infty+i\theta}\left(1 - i\cot\frac{\pi z}{h}\right) f(z)dz\right\},$$

*where $0 < \theta < d$. Moreover, it is bounded by*

$$|E_d| \leq \frac{2C}{e^{2\pi d/h} - 1},$$

*where $C$ is a constant such that*

$$\int_{-\infty+i\theta}^{\infty+i\theta} |f(z)|dz \leq C.$$

*Proof.* See [96].

From the above theorem it is clear that

$$|E_d| \leq \frac{2e^{-2\pi d/h}C}{1 - e^{-2\pi d/h}} \to 0 \qquad \text{as} \qquad h \to 0. \tag{1.3.2}$$

## Truncation error

The truncation error is the error made by ignoring the remaining terms in (1.2.7) after truncating the series at a finite number $M$, and is given by

$$\begin{aligned} E_t &= \frac{h}{2\pi i}\sum_{k=-\infty}^{\infty} e^{z(\ell_k)t}F\left(z(\ell_k)\right)z'(\ell_k) - \frac{h}{2\pi i}\sum_{k=-N}^{N} e^{z(\ell_k)t}F\left(z(\ell_k)\right)z'(\ell_k) \\ &= \frac{h}{2\pi i}\left(\sum_{k=-\infty}^{N-1} e^{z(\ell_k)t}F\left(z(\ell_k)\right)z'(\ell_k) + \sum_{k=N+1}^{\infty} e^{z(\ell_k)t}F\left(z(\ell_k)\right)z'(\ell_k)\right). \end{aligned} \tag{1.3.3}$$

Note that we have $\overline{F\left(z(\ell_k)\right)} = F\left(\overline{z(\ell_k)}\right)$ and $\overline{z(\ell_k)} = z(\ell_{-k})$; and since the contour is symmetric, (1.3.1) becomes

$$E_t = \frac{h}{\pi i} \sum_{k=N+1}^{\infty} e^{z(\ell_k)t} F\left(z(\ell_k)\right) z'(\ell_k). \tag{1.3.4}$$

Because of the exponential factor $e^{z(\ell_k)t}$, the terms in the sum decrease exponentially as $k \to \infty$ and therefore in this case one commits only an exponentially small error whose contribution can be neglected.

## Conditioning error

To study the conditioning error in the application of the Laplace transform, recall that in (1.2.7), the approximation $\tilde{f}(t)$ requires the evaluation of the transformed $F(z_k) = F(z(\ell_k))$, for $-M, -M+1, ..., M-1, M$. In reality these evaluations are affected by round-off errors which means that the actual approximation that takes place is



$$\tilde{F}(z_k) = F(z_k) + \rho_k, \qquad k = -M, -M+1, ..., M-1, M,$$

where $\rho_k > 0$ is a small value such that $|\rho_k| \leq \epsilon$, with $\epsilon$ given by the machine precision. As a result, in (1.2.7) what one really gets is

$$\begin{aligned} \check{f}_M(t) &= \frac{h}{2\pi i} \sum_{k=-M}^{M} e^{z_k t} \Big( F(z_k) + \rho_k \Big) z'_k \\ &= \tilde{f}_M(t) + \frac{h}{2\pi i} \sum_{k=-M}^{M} e^{z_k t} \rho_k z'_k. \end{aligned}$$

We set

$$f_\rho(t) = \frac{h}{2\pi i} \sum_{k=-M}^{M} e^{z_k t} \rho_k z'_k.$$

To see how the conditioning error affects the numerical results, we need to estimate

$||f_\rho(t)||$. Before we proceed, we state the following lemma [93]. Let

$$L(x) = 1 + |\ln(1 - e^{-x})|, \quad x > 0.$$

The function $L$ is such that, $L(x) \to 1$ as $x \to \infty$ and $L(x) \sim |\ln x|$ as $x \to 0^+$. Then function $L$ satisfies the following lemma:

**Lemma 1.3.2** *The function $L$ defined above satisfies the following inequality*

$$\int_0^\infty e^{-\gamma \cosh x} dx \leq L(\gamma), \qquad \gamma > 0.$$

*Proof.* Consider the change of variable $\nu = \cosh x - 1$ so that

$$\int_0^\infty e^{-\gamma \cosh x} dx = e^{-\gamma} \int_0^\infty \frac{e^{-\gamma\nu}}{\sqrt{\nu(2+\nu)}} d\nu.$$

Set $a = \sinh^2(1/2)$, so that

$$\int_0^a \frac{d\nu}{\sqrt{\nu(2+\nu)}} = 1, \quad \text{and} \quad \frac{1}{\sqrt{(k+a)(2+k+a)}} \leq \frac{1}{k+1}, \quad k \geq 0.$$

Thus

$$\begin{aligned} e^{-\gamma} \int_0^\infty \frac{e^{-\gamma\nu}}{\sqrt{\nu(2+\nu)}} d\nu &\leq e^{-\gamma} \left( 1 + \sum_{k=0}^\infty e^{-\gamma k} \int_{a+k}^{a+k+1} \frac{d\nu}{\sqrt{\nu(2+\nu)}} \right) \\ &\leq e^{-\gamma} \left( 1 + \sum_{k=0}^\infty \frac{e^{-\gamma k}}{k+1} \right) = e^{-\gamma} + L(\gamma) - 1, \end{aligned}$$

which concludes the proof.

Now, we note that

$$\begin{aligned} ||f_\rho(t)|| &= \left\| \frac{h}{2\pi i} \sum_{k=-M}^{M} e^{z_k t} \rho_k z_k' \right\| \\ &= \left\| \frac{\widetilde{\mu} e^{\widetilde{\mu} t}}{2\pi} h \sum_{k=-M}^{M} e^{\widetilde{\mu} \sin(i\ell_k - \alpha) t} \rho_k \cos(i\ell - \alpha) \right\|, \quad \alpha \in (\pi/4, \pi/2), \\ &\leq \frac{\widetilde{\mu} e^{\widetilde{\mu} t}}{2\pi} h \sum_{k=-M}^{M} \left\| e^{\widetilde{\mu} \sin(i\ell_k - \alpha) t} \rho_k \cos(i\ell - \alpha) \right\|. \end{aligned} \tag{1.3.5}$$

The following two inequalities are proved in [93]. Here we re-state them in our context. One of them is

$$\left\| e^{\widetilde{\mu} t \sin(i\ell - \alpha)} \rho_k \cos(i\ell - \alpha) \right\| \leq \rho e^{-\widetilde{\mu} t \sin\alpha \cosh\ell} \cos(i\ell - \alpha),$$

whereas the other one is

$$e^{-\widetilde{\mu} t \sin\alpha \cosh\ell} \cos(i\ell - \alpha) \leq \frac{1}{e\widetilde{\mu}\varrho \sin\alpha t} e^{-(1-\varrho)\widetilde{\mu} t \sin\alpha \cosh\ell}, \quad \varrho \in (0,1). \tag{1.3.6}$$



From (1.3.5) and (1.3.6), we deduce that

$$\begin{aligned} \|f_\rho(t)\| &\leq \frac{e^{\widetilde{\mu} t} \rho}{2\pi e \varrho \sin\alpha} \frac{h}{t} \sum_{k=-M}^{M} e^{-(1-\varrho)\widetilde{\mu} t \sin\alpha \cosh\ell_k}, \\ &\leq \frac{e^{\widetilde{\mu} t} \rho}{\pi e \varrho \sin\alpha} \frac{h}{t} \sum_{k=0}^{\infty} e^{-(1-\varrho)\widetilde{\mu} t \sin\alpha \cosh\ell_k}, \\ &\leq \frac{e^{\widetilde{\mu} t}}{\pi e \varrho \sin\alpha} \frac{\rho}{t} \int_0^{\infty} e^{-(1-\varrho)\widetilde{\mu} t \sin\alpha \cosh\ell}. \end{aligned}$$

Using Lemma 1.3.2, we obtain

$$\|f_\rho(t)\| \leq \frac{e^{\widetilde{\mu} t}}{\pi e \varrho \sin\alpha} \frac{\rho}{t} \left[ L\left( (1-\varrho)\widetilde{\mu} t \sin\alpha \right) \right]. \tag{1.3.7}$$

We note that (1.3.7) is independent of $F$ and propagates moderately with respect to $\widetilde{\mu} t$.

In summary, (1.3.2), the argument mentioned just after (1.3.4) and (1.3.7) imply that the total error is fully controllable as long as we choose the optimal values of the associated contour parameters. The derivation of these parameters is described below.

## Derivation of the optimal contour parameters

In this subsection, we present the derivation of the contour parameters. The basic idea is taken from [138]. In that paper, the authors derived the following convergence estimate for a family of hyperbolic contours (1.2.5):

$$E_d = \mathcal{O}(e^{-2\pi(\pi/2-\alpha)/h}), \quad E_{-d} = \mathcal{O}(e^{\widetilde{\mu}t-2\pi\alpha/h}), \quad h \to 0. \tag{1.3.8}$$

Therefore, the total discretization error on the strip $(-d, d)$, denoted by $E_r$, is given by

$$E_r = E_d + E_{-d}.$$

Moreover, the truncation error that we found satisfies



$$E_t = \mathcal{O}(e^{\widetilde{\mu}t(1-\sin\alpha\cosh(hM))}), \quad M \to \infty. \tag{1.3.9}$$

To estimate the optimal parameters of the contour, an asymptotic balance of the three errors, i.e., $E_t$, $E_d$, $E_{-d}$ is required. To this end, we set

$$E_d = E_{-d} = E_t, \tag{1.3.10}$$

so that

$$\frac{-2\left(\frac{\pi}{2}-\alpha\right)}{h} = \widetilde{\mu}t - \frac{2\pi\alpha}{h} = \widetilde{\mu}t\left(1-\sin\alpha\cosh(hM)\right). \tag{1.3.11}$$

We solve these equations for $h$, $\widetilde{\mu}$ and $\alpha \in (\pi/4, \pi/2)$. From the first equation in (1.3.11), we deduce that

$$\widetilde{\mu}t = \pi\frac{4\alpha-\pi}{h}, \tag{1.3.12}$$

and

$$\cosh(hM) = \frac{2\alpha}{(4\alpha - \pi)\sin\alpha}. \tag{1.3.13}$$

Denoting $hM$ by $A(\alpha)$, we obtain from (1.3.13)

$$A(\alpha) = hM = \cosh^{-1}\left(\frac{2\alpha}{(4\alpha - \pi)\sin\alpha}\right). \tag{1.3.14}$$

Finally, (1.3.12) and (1.3.14) give

$$\widetilde{\mu} = \frac{4\pi\alpha - \pi^2}{A(\alpha)}\frac{M}{t}, \quad \text{and} \quad h = \frac{A(\alpha)}{M}. \tag{1.3.15}$$

The corresponding convergence estimate can now be derived from $h$ and $\widetilde{\mu}$ in (1.3.15) as

$$E_M = \mathcal{O}(e^{-B(\alpha)M}), \qquad \text{where} \qquad B(\alpha) = \frac{\pi^2 - 2\pi\alpha}{A(\alpha)}, \quad M \to \infty. \tag{1.3.16}$$

To derive the optimal contour's parameters, note that as $B(\alpha)$ increases, $E_M$ decreases exponentially. Thus $E_M$ attains its optimum value at the maximum of $B(\alpha)$ over the interval $(\pi/4, \pi/2)$. A numerical computation of $B(\alpha)$ shows that the maximum is attained at

$$\alpha_\star = 1.1721. \tag{1.3.17}$$

With the optimal value of $\alpha$ given by $\alpha_\star$ above, we can now compute optimal value of $\widetilde{\mu}$ and $h$ from (1.3.15) and express them as

$$h_\star = \frac{1.0818}{M}, \qquad \text{and} \qquad \widetilde{\mu}_\star = 4.4921\frac{M}{t}. \tag{1.3.18}$$

The optimal contour is therefore given by

$$z = 4.4921\frac{M}{t}\Big(1 + \sin(i\ell - 1.1721)\Big), \qquad \ell \in \mathbb{R}, \tag{1.3.19}$$

and the optimal error as

$$E_M^\star = \mathcal{O}(e^{-2.32M}) = \mathcal{O}(10.2^{-M}), \qquad M \to \infty. \tag{1.3.20}$$

Note from the above that the optimal error while using the Laplace transform will be exponentially small.

In Figure 1.3.1, we show the maximum error (between the exact solution and the numerical solution of the Black-Scholes equation) of the Laplace transform method vs the number of contour points $M$ using parameters $K = 10$; $\sigma = 0.3$; $r = 0.05$; $T = 0.25$.

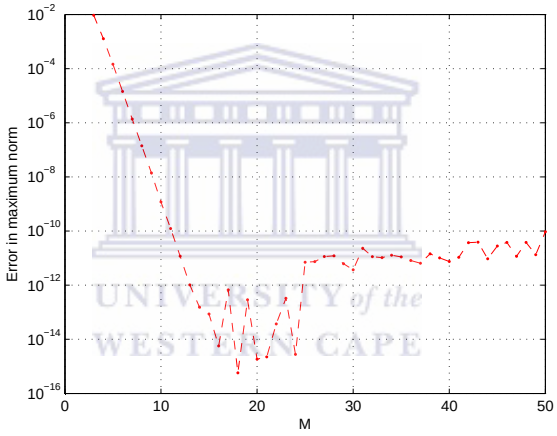


Figure 1.3.1: Convergence error in the maximum norm of the Laplace transform method for the European call option using the parameters $K = 10$; $\sigma = 0.3$; $r = 0.05$; $T = 0.25$; $S_{\max} = 3K$.

Option pricing problems discussed in section 1.1 can be reduced to the semi-discrete problem

$$\dot{V} = AV + b(t), \quad V(0) = V_0, \tag{1.3.21}$$

where $A$ is an $N \times N$ real matrix representing the semi-discrete approximation to an elliptic operator, and $V$, $V_0$ and $b(t)$ are $N \times 1$ vectors representing the semi-discrete solution at time $t$, the initial condition and the boundary conditions, respectively. Note $\dot{V}$ is the derivative w.r.t $t$.

In this thesis, we intend to use numerical methods for inverting the Laplace transform to solve such problems. Below we present some of these approaches which we found in the literature.

## 1.4 Literature review

The creasing interest in option pricing problems has led to the development of numerous numerical methods over the past few years. Elementary introduction to this topic can be found in [89, 141, 142]. Various methods for solving European and American options have been explored in [25, 29, 53, 77, 127]. Besides these, Gesk *et al.* [52], introduced quasi-analytical formula which generates approximative solution of an American option by restricting the early exercise at discrete times. In [16, 17], Brennan and Schwartz introduced finite difference methods for solving American options. They proposed a finite difference scheme for solving partial integro differential equations. In their approach the difference operator is splitted into local and non-local parts. Then the local term is treated using an implicit time step integration method and the nonlocal term using an explicit time step integration method. This idea, previously used for non-linear PDEs in [4], allowed an efficient numerical implementation of option prices.



In [122], the approach was to approximate the solution of the Black-Scholes equation by applying a quadrature formula. Like the method of eigenfunctions expansion, this method requires that the matrix operator, resulting from the space discretization, be independent of time and symmetric positive definite.

For European options, Merton [100] derived analytical expressions, however for options under jump-diffusion models no closed-form solutions exist. One has to resort to numerical methods for pricing the resulting partial integro-differential equation (PIDE) that arise. However, the convolution integral involved in these PIDEs adds to the difficulty of finding efficient numerical solutions. Commonly used finite difference methods (FDMs) hardly attain higher order accuracy [3]. Typical quadrature rules such as the trapezoidal and Simpson's rules are of low order as compared to Gaussian quadrature

method. However the later is expensive to implement since it requires the interpolation to match the Chebyshev grid point with those of the FDMs. To reduce the computational cost in solving the convolution integral term, Fast Fourier Transform (FFT) was used in [3, 150].

Tangman *et al.* [126] proposed a different approach. They combined the central difference method and the exponential time differencing (ETD) scheme to solve the PIDE. The ETD method was proved very effective and gave second order accuracy.

In [84], Kim formulated the American option valuation problem in an economical and mathematically meaningfully ways. He examined the properties associated with the optimal exercise boundary and presented a numerical technique to implement the valuation formulas. Kuske and Keller [88] obtained the optimal exercise boundary by using the Green's theorem to convert the boundary value problem for the option into an integral equation for the optimal exercise boundary. Then they used asymptotic methods to solve this integral for small values of the time to expiration. However, these studies were unable to obtain exact solutions of their integral equations.



In [144] integral transform was used to obtained analytic solution of various option pricing problems rather than to develop an efficient numerical scheme. Related to integral transforms there are other methods based on the so-called $H$-matrix approach.

As indicated earlier, the modeling of American options leads to a free boundary problem. To solve this problems numerically, Kwok and Wu [143] considered the transformation of the American option into a fixed domain problem. The fixed boundary facilitates effective discretization of the resultant partial differential equation which was then solved by finite difference methods. The advantage of this method is that no embedded iteration is needed at each time step of the evolution. Moreover it capture the whole optimal exercise boundary.

Han and Wu in [58] introduced a fast numerical method for American option problems. In this approach, the original problem was transformed into a standard forward diffusion equation over an infinite domain. An accurate boundary condition was then obtained as a relation between the function and its partial differential derivatives. Dis-

cretization of the boundary condition combined with finite difference method allowed an efficient valuation of option's prices.

Following the success of Crank-Nicolson method, a Crandall-Douglas [35, 38] scheme was used for pricing European options in [97]. These authors observed the poor convergence rate for high-order schemes due to the non-smoothness nature of the terminal condition. To improve the convergence rate, Oosterlee *et al.* [107] used a grid stretching transformation combined with a fourth order backward differentiation formula. In order to cluster grid point in the neighborhood of the option's exercise price and the initial price, they applied an analytic transformation. Then the transformed equation was discretized by fourth order finite difference in space and time. But for time integration four initial steps were required which brought some complications since only the payoff was available.

To restore the fourth-order convergence, Tangman *et al.* [127] used a method based on grid stretching to improve on the well known second order Crank-Nicolson method for solving these problems. They proposed a method based on a high order compact scheme together with a grid stretching technique for European options. For American option, they used a time grid stretching transformation but solved the linear complementary problem using an efficient procedure for the location of the free boundary. They showed that this strategy gives optimal results compared to those obtained in [23]. However the grid-stretching strategy failed to produce accurate high-order results. To circumvent this, they considered a front-fixing transformation to get a solution which was smooth on the domain.

Toivanen [131] considered numerical method for pricing American options based on partial differential equations and partial integro-differential equations arising from diffusion and jump-diffusion models, respectively, for the underlying asset. In his study, he derived a numerical method based on the free boundary formulation for pricing American options under jump-diffusion models with finite jumps. The front-tracking method used an implicit finite difference discretization on time-dependent nonuniform grids which were refined near the expiry and free boundary. For interpolations be-

tween grids and the construction of finite difference stencils, Lagrange interpolation polynomials were used. This gave an easy way to implement the fourth-order accurate discretization.

To solve the unknown free boundary associated with the American option prices, Brennan and Schwartz [16, 17] used implicit finite difference to account for the early exercise possibility of American options on futures contracts. Macmillan [94] employed a quadratic approximation to value the early exercise. Sevčovič [120] developed an iterative algorithm for evaluating the approximation of the optimal exercise boundary. His idea was to transform the free boundary problem for the early exercise boundary position into a semi-linear parabolic equation defined on the fixed domain. The resulting equation was then solved by the operator splitting method. To further improve this method, he proposed a transformation of the free boundary problem into a semi-linear parabolic equation coupled with a nonlocal algebraic constraint equation for the free boundary position [121]. A full space-time discretization of the problem led to a system of semi-linear algebraic equations which was solved by an iterative procedure at each time level.



In [104], Nielsen *et al.* developed a penalty method to solve American option prices. In this approach the free and moving boundary are removed by adding a small continuous term to the Black-Scholes equation to ensure that the solution stays in the proper state space. To gain insight in the accuracy of the method, they compared the approximations with the analytic solution.

As far as the numerical methods for barrier options valuation are concerned, lattice methods have been used quiet extensively despite their low order of accuracy. However, the implementation of these methods present a computational challenge. Numerous techniques have been developed to improved their computational cost [59], still the improvement is not fully satisfying. Recently, Monte Carlo methods have emerged as a viable alternative to lattice methods.

Finite difference methods appear to be cost effective and flexible, compared to lattice and Monte Carlo methods, for pricing barrier options. In [15], the authors

considered an explicit finite difference approach. They constructed a grid which lies right at the barrier and applied an interpolation to find the values of the option. Following on the same principle, Figlewski *et al.* [45] used an adaptive method to refine the mesh in regions around a barrier and obtained very efficient results.

Phelim *et al.* developed an explicit finite difference approach to price barrier options in [113]. They developed a new strategy for smoothing Crank-Nicolson scheme at each time step when the barrier is applied. This smoothing procedure gave second order convergence.

Besides the classical models as mentioned above, researchers are also interested in expending to some volatility models. In this regard, the Heston's model ([62]) is one of the most popular stochastic volatility models for pricing derivatives. The model leads to a more realistic option price evaluation than the celebrated Black-Scholes constituting its extension to the two-dimensional form [70, 100]. In [62], Heston derived a semi-closed formula for the model, however, its implementation is not a straightforward exercise because of the oscillatory behavior of the complex integrand which comes into play through the Fourier-type inversion formula. This necessitated the use of the numerical methods to approximate these option pricing problems.



Most of numerical methods for evaluating the Heston model are based on the method-of-line approach which consists of two steps. Firstly, the PDE is discretized in space thus generating a system of ordinary differential equation. Secondly, the subsequent semi-discrete problem is solved in time by applying a suitable time integrating method. This is the approach followed in some of the numerical methods we review below.

Recently some researchers have considered the Laplace inversion method as a valuable alternative to the finite difference method for the solution of the parabolic PDEs [40, 125, 138]. This has led to great applications in the financial world. Very recently Ahn *et al.* [2] develop an efficient numerical method for solving the Black-Scholes equation. This method based on the numerical inversion of Laplace transform and finite differences method in space computes European option prices effectively at reduced

cost compared to the more conventional time marching method. They first applied the integral transform on the time domain to eliminate the temporal derivative. Then a finite difference method is applied to the transformed equation on the space domain. The time dependant option prices are recovered by applying an algorithm developed in [110].

Some other works related to the pricing of standard options can be found in [27, 58, 82, 83, 92, 98, 101, 109, 140, 134, 143, 145]. Furthermore, the works which are more specific to the particular models and approaches are reviewed in the individual chapters.

## 1.5 Outline of the thesis

The rest of this thesis is organized as follows:

In Chapter 2, we investigate two efficient numerical methods for solving the Black-Scholes equation for pricing the European options. We use spectral methods to discretize the associated partial differential equation with respect to space and generate a system of ODEs which is then solved by applying two contour integral methods. The first one is the exponential time differencing Runge-Kutta method of order 4. The second one is based on the application of trapezoidal rule to approximate a Bromwich integral. We give a comparative discussion on these two methods and compare the numerical results with conventional methods such as the MATLAB solver ode15s and Crank-Nicholson's method.

In Chapter 3, we investigate a new approach to improve the results obtained in Chapter 2. The approach is based on spectral domain decomposition and the Laplace transform method. The spectral domain decomposition method approximates the solution using piecewise high order rational interpolant on the Chebyshev mesh points within each sub-domain. The boundary domain is placed at the strike price where the discontinuity is located. The resulting system is then solved by applying the inverse Laplace transform method. To assess the accuracy and efficiency of this method,

the solutions obtained by using this approach are compared with those obtained with conventional methods such as Crank-Nicholson and finite difference methods.

Ideas explored in Chapter 2 and 3 are then extended to design a robust numerical method to price American options in Chapter 4. Due to the non-smooth initial condition associated with the American options, we use spectral domain decomposition method to approximate the option price. To avoid the computation of the unknown free boundary associated with the American option, we use an updating procedure. Numerical results of the proposed method are presented for the solution and the Greeks.

In Chapter 5, we consider options with jumps on a single asset. We take advantage of the suitability of the Chebyshev grid point for Gauss-Legendre quadrature to efficiently approximate the convolution integral. The resulting discrete problem is solved by the inverse Laplace transform using the Bromwich contour integral approach. The numerical results obtained are compared with those obtained using Crank-Nicholson and finite difference methods.

In Chapter 6, we solve problems for pricing exotic options. In particular, we solve a single barrier European down-and-out and a double barrier European knock-out option. We compare the results obtained from our approach with those seen in the literature.



To see further the applicability of the methods proposed in previous chapters, in Chapter 7, we apply them to solve the Heston's volatility model. To approximate the associated two-variable PDE, we construct a grid which is the tensor product of the two grids each of which are based on the Chebyshev points in the two spacial directions. The resulting semi-discrete problem is then solved by applying Laplace transform method.

Finally, we present some concluding remarks and indicate the scope for future research in Chapter 8.

# Chapter 2

# Numerical application of the Laplace transform for pricing European options


In this chapter we investigate two efficient numerical methods for solving the Black-Scholes equation for pricing European options. We use spectral methods to discretize the associated partial differential equation with respect to space and generate a system of ordinary differential equations in time. This system is then solved by applying two time integrating methods. The first method is the exponential time differencing Runge-Kutta method of order 4. The second method is based on the application of trapezoidal rule to approximate a Bromwich integral. We give a comparative discussion on these two methods and compare the numerical results with conventional methods such as the MATLAB solver ode15s and Crank-Nicholson.

## 2.1 Introduction

Since its development in the 1970s by F. Black and M. Scholes, the Black-Scholes equation has become a fundamental model for pricing financial derivatives [12]. A derivative security is a financial instrument whose value depends on the values of some

other underlying variables, e.g. stocks, foreign currency. Among the most popular derivatives, options are actively traded on different financial markets over the world. An option gives its holder the right without any obligation to buy (call option) or to sell (put option) the underlying asset by a certain date (maturity date) for a certain price (strike price). The European options can only be exercised at maturity.

The Black-Scholes partial differential equation can be used to model different types of options. However, the exact solution to the corresponding problem does not always exists and we must therefore resort to numerical methods to solve such a PDE. Some of the popular methods used in the past to tackle these type of problems are those based on Monte Carlo simulations [14], binomial trees [32] and finite difference methods [71].

Finite difference methods are classical methods for solving PDEs and have been used extensively to price options since the advent of the financial mathematics. The authors in [107] used a grid stretching in combination with backward difference method of fourth order in time to solve the European options. In [127], Tangman et al. used a method based on the grid stretching to generate a high order compact scheme to improve on the well known second order Crank-Nicolson method for solving these problems. In spite of the popularity of these time marching methods, a critical drawback of these schemes is that they usually require as many time steps as spatial meshes to maintain the stability of the method.



In this chapter, we solve a European option pricing problem in two different ways. Firstly, we use spectral method to discretize the PDE with respect to space, thereby generating a system of ordinary differential equations in time. The main feature of spectral methods is that approximation errors associated with the methods often decay exponentially with increasing numbers of degrees of freedom. In contrast, errors associated with finite difference methods and classical finite element methods decay only algebraically. If the error decays exponentially, then a result that is accurate to, say, 10 digits can be obtained using fewer degrees of freedom. This suggests that spectral methods are often more efficient than finite difference methods and classical finite element methods. Secondly, the resulting system of ODEs is solved by applying

two time integrating methods. The first method is the Exponential time differencing Runge-Kutta method of order 4 (ETDRK4) [33]. The second method is the Talbot's method ([125]) which is based on the application of trapezoidal rule to approximate a Bromwich integral. We compare the results obtained by these methods with other methods such as MATLAB solver *ode15s* which is based on the family of backward differentiation formulas (BDFs) called numerical differentiation formulas (NDFs) [86] and Crank-Nicolson. Some other works related to the European option pricing can be found in [6, 9, 28, 85].

The rest of this chapter is organized as follows. In Section 2.2, we give a full description of the Black-Scholes equation used to model the European put and call options. In Section 2.3, we introduce the spectral discretization method. We developed the time integration method based on ETDRK4 method and apply the Laplace transform method to the European call option in Section 2.4. In Section 2.5, we present comparative numerical results. Finally, a brief summary and some concluding remarks are given in Section 2.6.



## 2.2 Description of the model problem

We consider the following Black-Scholes (BS) equation to price European options

$$\frac{\partial V}{\partial t} + \frac{1}{2}\sigma^2 S^2 \frac{\partial^2 V}{\partial S^2} + rS\frac{\partial V}{\partial S} - rV = 0, \qquad S \in (0, \infty), \quad t \in (0, T). \tag{2.2.1}$$

Final condition is given by

$$V(S,T) = \begin{cases} \max(S-K,0) & \text{for call,} \\ \\ \max(K-S,0) & \text{for put,} \end{cases} \tag{2.2.2}$$

whereas the boundary conditions are

$$\left.\begin{array}{lll} V(0,t) = 0, & V(S,t) \to S - Ke^{-r(T-t)}, & \text{as} \quad S \to \infty \quad \text{for call,} \\ V(0,t) = Ke^{-rt}, & V(S,t) \to 0, & \text{as} \quad S \to \infty \quad \text{for put.} \end{array}\right\} \tag{2.2.3}$$

In the above, $V(S,t)$ is the price of a call/put option for the underlying asset whose price is $S$ at time $t$ up to the expiry date $T$, $r$ is the interest rate, $\sigma$ is the volatility of the underlying asset and $K$ is the strike price.

We set $\tau = T - t$ to transform the backward formulation (2.2.1) – (2.2.3) to the following forward equation

$$\frac{\partial V}{\partial \tau} - \frac{1}{2}\sigma^2 S^2 \frac{\partial^2 V}{\partial S^2} - rS\frac{\partial V}{\partial S} + rV = 0. \tag{2.2.4}$$

The initial condition is given by the terminal payoff

$$V(S,0) = \begin{cases} \max(S-K,0) & \text{for call,} \\ \max(K-S,0) & \text{for put} \end{cases} \tag{2.2.5}$$



and the boundary conditions are given by

$$\left.\begin{array}{lll} V(0,\tau) = 0, & V(S,\tau) \to S - Ke^{-r\tau}, & \text{as} \quad S \to \infty \quad \text{for call,} \\ V(0,\tau) = Ke^{-r\tau}, & V(S,\tau) \to 0, & \text{as} \quad S \to \infty \quad \text{for put.} \end{array}\right\} \tag{2.2.6}$$

For a European option (call and put), the analytical solution exists and is given by

$$V(S,\tau) = \begin{cases} S\mathcal{N}(d_1) - Ke^{-r\tau}\mathcal{N}(d_2) & \text{for call,} \\ Ke^{-r\tau}\mathcal{N}(-d_2) - S\mathcal{N}(-d_1) & \text{for put.} \end{cases} \tag{2.2.7}$$

where $\mathcal{N}(.)$ is the normal distribution function defined by

$$\mathcal{N}(x) = \int_{-\infty}^{x} e^{-\frac{s^2}{2}} ds,$$

and the expressions for $d_1$ and $d_2$ are given by

$$d_1 = \frac{\log(S/K) + \left(r + \frac{1}{2}\sigma^2\right)\tau}{\sigma\sqrt{\tau}},$$

$$d_2 = \frac{\log(S/K) + \left(r - \frac{1}{2}\sigma^2\right)\tau}{\sigma\sqrt{\tau}}.$$

A typical representation of (2.2.7) can be seen from Figure 2.2.1 (for a call option)

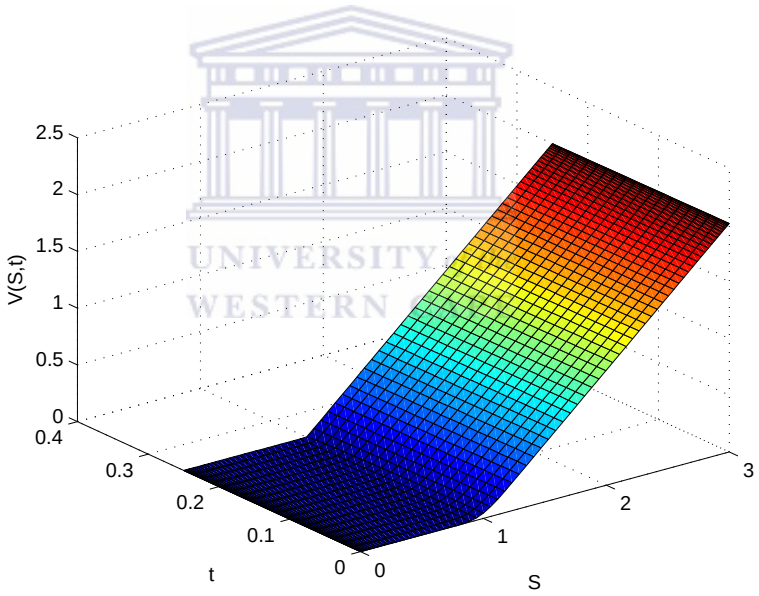


Figure 2.2.1: Exact solution given by (2.2.7) for $r = 0.05$, $T = 0.25$, $\sigma = 0.3$, $K = 1$, $S \in (0, 3)$.

Here we note that, even though the analytical solution of European options exist, for practical application as well as due to the aim of solving more complicated option pricing problems which fundamentally originate from these type of basic options, one has to resort to numerical methods. Because once the model gets complicated it would

be difficult if not impossible to solve it analytically. To this end, in the next sections we develop a numerical approach based on spectral method and inversion of the Laplace transform method. Our intention here is to develop a method that will be used for more complicated problems whose analytical solutions do not exist or are hard to implement directly.

## 2.3 Spectral discretization

To semi-discretize the PDE (2.2.1), we consider a spectral method. The basic idea behind the spectral methods is as follows. For a given set of points, we interpolate the unknown solution and differentiate the interpolating polynomial at these grid points. This discretization process leads to a system of equations which can then be solved using any state-of-the-art solvers.

The discretization using spectral method (in this chapter) is based on the Chebyshev polynomial interpolation [132]. Methods such as finite elements or finite differences divide the domain into sub-domains and use local polynomials of low degree. By contrast, spectral methods use global representations of high degree over the entire domain.



The implementation of spectral methods can be divided into three categories, namely, the Galerkin, tau and the collocation (or pseudo-spectral) methods. The first two of these methods use the expansion coefficients of the global approximation and the latter can be viewed as a method of finding numerical approximations to derivatives at collocations points. In a manner similar to finite difference or finite element methods, the equation to be solved is satisfied in space at the collocations points. In this chapter, we use the third one, i.e., the spectral collocation method.

### 2.3.1 Polynomial interpolation

The spectral process involves seeking the solution to a differential equation by polynomial interpolation. In order to review the concept of polynomial interpolation, we

consider interpolating an arbitrary function $f(x)$ at $N+1$ distinct nodes $\{x_k\}_{k=0}^{N}$ in $[-1,1]$.

**Definition 2.3.1** *Given a set of grid points $\{x_j\}_{j=0}^{N}$, an interpolating approximation to a function $f(x)$ is a polynomial $f_N(x)$ of degree $N$, determined by the requirement that the interpolant agrees with $f(x)$ at the set of interpolation points $\{x_j\}_{j=0}^{N}$, i.e.,*

$$f_N(x_i) = f(x_i), \qquad i = 0, 1, ..., N.$$

We define by $L_k(x)$, the Lagrange polynomial of degree $N$,

$$L_k(x) = \prod_{\substack{j=0 \\ j\neq k}}^{N} \frac{x - x_j}{x_k - x_j}, \qquad k = 0, 1, ..., N.$$

Note that $L_k(x)$ satisfies $L_j(x_k) = \delta_{jk}$, where $\delta_{jk}$ is the Kronecker delta function. The interpolation polynomial $f_N(x)$ is then given by



$$f_N(x) = \sum_{k=0}^{N} f(x_k) L_k(x). \tag{2.3.1}$$

The grid points $\{x_k\}_0^N$ are the roots of the Jacobi polynomials; they have a nonuniform distribution [135] in the interval $[-1,1]$ with a node density (per unit length) of

$$\mu \approx \frac{N}{\sqrt{1-x^2}} \qquad \text{as} \qquad N \to \infty.$$

In this chapter, we use the Chebyshev points as the grid points. These are given by

Chebyshev zeros: $x_j = \cos\left(\frac{2j+1}{2(N+1)}\pi\right), \qquad j = 0, ..., N,$

and

Chebyshev extrema: $x_j = \cos\left(\frac{j\pi}{N}\right), \qquad j = 0, ..., N.$

The Chebyshev points are often defined as the projection onto the interval $[-1,1]$

of the roots of unity along the unit circle $|z| = 1$ in the complex plane [132]. For European options, since the payoff is non smooth, a direct application of the chebyshev points for discretization leads to low order approximation. To regain a high order accuracy an alternative is proposed by Tangman [126, 149]. The basic idea is to modify the Chebyshev points as follows

$$x = [x_k, x_\ell]^T, \tag{2.3.2}$$

where

$$x_k = S_{min} + \left(\frac{K - S_{min}}{2}\right)\left(1 - \cos\left(\frac{2\pi k}{N}\right)\right), \quad k = 0, 1, ..., \frac{N}{2}, \tag{2.3.3}$$

$$x_\ell = K + \left(\frac{S_{max} - K}{2}\right)\left(1 - \cos\left(\frac{2\pi l}{N}\right)\right), \quad \ell = 1, 2, ..., \frac{N}{2}. \tag{2.3.4}$$

for $N$ even. This discretization clusters grid nodes at the boundaries located at $S_{min}$ and $S_{max}$ as well as at the strick price $K$ where the discontinuity of the payoff occurs. As we show in Section 2.5, it follows that local grid refinement improve accuracy of the spectral method at the payoff. Another advantage of this strategy is that it applies directly to the equation (2.2.4) without the need for transforming into the interval $[-1, 1]$.



### 2.3.2 Differentiation matrices

The concept of collocation derivatives is associated with the interpolation polynomial $f_N(x)$ described above. These are the derivatives of $f_N(x)$ at the collocation points $\{x_k\}_{k=0}^N$. Using (2.3.1), we can see that the $m$-th order collocation derivative of $f_N(x)$ is given by

$$\frac{d^m f_N(x)}{dx^m} = \sum_{k=0}^{N} f(x_k) \frac{d^m L_k(x)}{dx^m}. \tag{2.3.5}$$

Nodal representation yields

$$\frac{d^m f_N(x_j)}{dx^m} = \sum_{k=0}^{N} f(x_k) \frac{d^m L_k(x_j)}{dx^m}, \qquad j = 0, ..., N, \tag{2.3.6}$$

which can be expressed by the matrix formula

$$f^{(m)}{}_N = D_N^{(m)} f_N, \tag{2.3.7}$$

where

$$f_N = \begin{bmatrix} f_N(x_0) \\ \vdots \\ f_N(x_N) \end{bmatrix}, \quad f^{(m)}{}_N = \begin{bmatrix} f_N^{(m)}(x_0) \\ \vdots \\ f_N^{(m)}(x_N) \end{bmatrix},$$

and $D_N^{(m)}$ is the $(N+1) \times (N+1)$ differentiation matrix of order $m$ with entries

$$(D_N^{(m)})_{j,k} = L_k^{(m)}(x_j), \qquad j, k = 0, ..., N. \tag{2.3.8}$$



The computation of these differentiation matrices for an arbitrary order $m$ has been considered in [69, 132, 136]. Following the approach in [139], Weideman and Reddy [136] developed a MATLAB algorithm that computes the Chebyshev grid points as well as the differentiation matrices of an arbitrary order. This algorithm is implemented in the DMSUITE package [136] which contains a function `chebdif` that computes the extreme points of the Chebyshev polynomial $T_N(x)$ and the differentiation matrix $D_N^{(m)}$. The code takes as input the size of the differentiation matrix $N$ and the highest derivative order $m$ and produces matrices $D_N^{(\ell)}$ of order $\ell = 1, 2, ..., m$.

The next theorem gives the formulas for the computation of the entries of $D_N^{(1)}$.

**Theorem 2.3.2** [132] *For any $N \geq 1$, let $i, j = 0, 1, ...N$. Then the entries of $D_N^{(1)}$*

*are given by*

$$\left.\begin{array}{lll} \left(D_N^{(1)}\right)_{00} = \dfrac{2N^2+1}{6}, & & \left(D_N^{(1)}\right)_{NN} = \dfrac{2N^2+1}{6}, \\ \left(D_N^{(1)}\right)_{jj} = \dfrac{-x_j}{2(1-x_j^2)}, & & j = 1, ..., N-1, \\ \left(D_N^{(1)}\right)_{ij} = \dfrac{c_i}{c_j}\dfrac{(-1)^{i+j}}{(x_i - x_j)}, & & i \neq j, \quad i, j = 0, ..., N, \end{array}\right\} \tag{2.3.9}$$

*where*

$$c_i = \begin{cases} 2, & i = 0 \text{ or } N \\ 1, & \text{otherwise.} \end{cases}$$

*Proof.* See [132].

Higher order derivatives are evaluated by recursions at a cost of $\mathcal{O}(N^2)$ operations [136, 139]. This turns out to be cost effective as compared to $\mathcal{O}(N^3)$ if higher derivatives are obtained by taking powers of the first derivative [136].

Using the differentiation matrices described above, we can rewrite (2.2.4) in matrix form as

$$\dot{V} - \frac{1}{2}\sigma^2 P D^{(2)} V - rQD^{(1)}V + rV = 0, \tag{2.3.10}$$

where $P$ and $Q$ are the diagonal matrices with entries on the main diagonals as $(x_k+1)^2$ and $(x_k+1)$, respectively, for $k = 0, 1, ..., N$.

In next the section, we discuss a time discretization method to solve (2.3.10).

## 2.4 Time discretization

### 2.4.1 Exponential Time Differencing Runge-Kutta Method

The Exponential Time Differentiating (ETD) schemes are time integration methods especially suited for semi-linear problems which can be splitted into a linear part and non-linear part. The linear part which is very often stiff is solved exactly by a matrix exponential whereas the non-linear part which varies more slowly is solved recursively.

In recent years, numerous authors have shown an interest in ETD methods, see, e.g., [33, 65, 66] and some of the references therein.

In order to elaborate the approach, let us consider the following semi-linear partial differential equation

$$\frac{\partial u}{\partial t} = \mathcal{A}u + \mathcal{L}(u,t), \tag{2.4.1}$$

where $\mathcal{A}$ is the semi-discrete spectral linear operator containing higher-order spatial derivatives than those contained in the non-linear operator $\mathcal{L}(u,t)$ and is the responsible for stiffness. After discretizing by Chebyshev collocation method, we obtain the following system of ODEs

$$\frac{\partial u}{\partial t} = Au + L(u,t), \tag{2.4.2}$$

where $A$ and $L$ represents the discrete analogue of the continuous operators $\mathcal{A}$ and $\mathcal{L}$, respectively.

Various ETD methods exist for the evaluation of (2.4.2) and it is not the purpose of this work to give a complete classification of the ETD methods. From these, we focus on Exponential Time Differencing Runge-Kutta method of order 4 (ETDRK4) given by



$$\begin{aligned} u_{n+1} &= e^{Ah}u_n + h^{-2}A^{-3}\{[-4 - Ah + e^{Ah}(4 - 3Ah + (Ah)^2)]L(u_n, t_n) \\ &\quad +2[2 + Ah + e^{Ah}(-2 + Ah)](L(a_n, t_n + h/2) + L(b_n, t_n + h/2)) \\ &\quad [-4 - 3Ah - (Ah)^2 + e^{Ah}(4 - Ah)]L(c_n, t_n + h)\}, \end{aligned} \tag{2.4.3}$$

where

$$\begin{aligned} a_n &= e^{Ah/2}u_n + A^{-1}(e^{Ah/2} - I)L(u_n, t_n), \\ b_n &= e^{Ah/2}u_n + A^{-1}(e^{Ah/2} - I)L(a_n, t_n + h/2), \\ c_n &= e^{Ah/2}a_n + A^{-1}(e^{Ah/2} - I)(2L(b_n, t_n + h/2) - L(u_n, t_n)). \end{aligned} \tag{2.4.4}$$

Here $h$ is the time step $h$ and $I$ the identity matrix. The terms $a_n$ and $b_n$ approximate

the values of $u$ at $t_n + h/2$ and the term $c_n$ approximates the value of $u$ at $t_n + h$. For detailed derivation of this method, interested readers are referred to [33]. Note that the direct application of this formula suffers from numerical instability for eigenvalues of $A$ close to zero [66]. To see this, let us first consider the scalar problem and define the function

$$g(z) = \frac{e^z - 1}{z}. \tag{2.4.5}$$

The function $g(z)$ is analytic with a removable singularity at $z = 0$. Moreover the limiting form of $g(z)$ as $z \to 0^{\pm}$ should result in 1. In practice however, it does not happen. The expression does not approach 1 as $z$ gets close to 0. In [63], Higham explains this situation by the fact that for small values of $z$, the terms in the expression do not cancel precisely and therefore leads to small errors. The small errors, occurring due to cancelations, play significant role as we are dividing the result by a number approaching zero. The situation gets worse for higher order version of $g(z)$ given by

$$g_\ell(z) = \frac{e^z - G_\ell(z)}{z^\ell}, \quad \ell = 1, 2, ..., s, \tag{2.4.6}$$



where

$$G_\ell(z) = \sum_{j=0}^{\ell-1} \frac{z^j}{j!},$$

are the first $\ell$ terms in the Taylor series approximation to $g(z)$. The analogy between the coefficient function $a_n, b_n$ and $c_n$ of (2.4.3) with the function $g_\ell(z)$ (here $s = 4$) is apparent. The cancelation error observed in the numerical application of $g(z)$ for small values of $z$ constitute a major challenge in numerical analysis and as a consequence makes the application of the ETDRK4 unstable for small values of $z$.

To overcome the numerical instability in the evaluation of $g(z)$ for $z \to 0$, Kassam and Trefethen [81] proposed a method based on contour integrals over a complex plan that encloses the $z$. This method is based on Cauchy integral formula defined by

$$g(z) = \frac{1}{2\pi i} \int_\Gamma \frac{g(s)}{s - z} ds, \tag{2.4.7}$$

where $\Gamma$ represent the contour of integration that encloses the point $z$. Unlike the Laplace transform approach where we use a hyperbola as a contour, here (for its simplicity) we will consider a circular contour with radius $r$ centered at $z_0$ defined by

$$\Gamma = \{z_0 + re^{i\theta} : 0 \leq \theta \leq 2\pi\}. \tag{2.4.8}$$

The Cauchy integral formula (2.4.7) becomes

$$g(z) = \frac{1}{2\pi}\int_0^{2\pi} \frac{g(z_0 + re^{i\theta})}{s(\theta) - z}(re^{i\theta})d\theta. \tag{2.4.9}$$

Formula (2.4.9) is approximated by the Trapezoidal rule truncated at $N$ as

$$g(z) \approx \frac{1}{N}\sum_{j=1}^{N} \frac{g(z_0 + re^{i\theta})}{s(\theta) - z}(re^{i\theta}). \tag{2.4.10}$$

For matrix problem (2.4.2), the scalar $z$ becomes $A$, and the analogous Cauchy integral formula will be

$$g(A) = \frac{1}{2\pi i}\int_\Gamma g(s)(sI - A)^{-1}ds. \tag{2.4.11}$$



Again the Trapezoidal rule is applied in a manner similar to the scalar case (2.4.10). Moreover the convergence of the method is guaranteed by Theorem 1.3.1.

We apply this approach to the European call and put option problems (2.2.4)-(2.2.6) in the next section.

### 2.4.2 Application of the Laplace transform method

Applying the Laplace transform to equation (2.2.4), the following transformed equation is obtained

$$z\widehat{V} - \frac{1}{2}\sigma^2 S^2 \frac{\partial^2 \widehat{V}}{\partial S^2} - rS\frac{\partial \widehat{V}}{\partial S} + r\widehat{V} = V_0. \tag{2.4.12}$$

The boundary conditions are given by

$$\left.\begin{array}{lll} \widehat{V}(0,z) = 0, & \widehat{V}(S,z) = \frac{S_{max}}{z} - \frac{K}{(z+r)}, & \text{for call,} \\ \widehat{V}(0,z) = \frac{K}{(z+r)}, & \widehat{V}(S,z) = 0, & \text{for put.} \end{array}\right\} \tag{2.4.13}$$

The equation (2.3.10) therefore becomes

$$z\widehat{V} - \frac{1}{2}\sigma^2 PD_N^{(2)}\widehat{V} + rQD_N^{(1)}\widehat{V} - r\widehat{V} = V_0,$$

$$\left(z_k I - \frac{1}{2}\sigma^2 PD_N^{(2)} + rQD_N^{(1)} - rI\right)\widehat{V}_k = V_0, \qquad k = 0, 1, ..., N-1. \tag{2.4.14}$$

A straight forward application of the inversion formula (1.2.6) yields

$$V(t) = \frac{h}{2\pi i}\int_{-\infty}^{\infty} e^{z(\ell)t}\widehat{V}z'(\ell)d\ell. \tag{2.4.15}$$

Using the symmetry of the contour (1.2.5), the trapezoidal rule (1.2.7) gives

$$V_M(t) = \frac{h}{\pi}\sum_{k=0}^{M-1} e^{z_k t}\widehat{V}_k z'_k, \tag{2.4.16}$$

where

$$\widehat{V}_k = (z_k I - A)^{-1} V_0, \quad k = 0, 1, ..., N-1, \tag{2.4.17}$$

and

$$A = \frac{1}{2}\sigma^2 PD_N^{(2)} - rQD_N^{(1)} + rI. \tag{2.4.18}$$

Now since the differentiation matrices $D_N^{(1)}$ and $D_N^{(2)}$ are not sparse, the equation (2.4.17) indicates the bulk of the computation in the trapezoidal rules (2.4.16). To speed up this computation, an Hessenberg decomposition can be computed once at the beginning as follows

$$A = MHM^T, \tag{2.4.19}$$

where $H = (h_{ij})$ is an upper Hessenberg matrix, i.e., $h_{ij} = 0$, $i > j + 1$, and $M$ an orthogonal matrix. Then for each $z_k$, $k = 0, 1, ..., M-1$, the equation (2.4.17) becomes

$$(z_k I - MHM^T)V_k = V_0. \quad k = 0, 1, ..., N-1.$$

From this we have

$$(z_k I - H)U_k = M^T V_0 \quad k = 0, 1, ..., N-1, \tag{2.4.20}$$

where $U_k = M^T V_k$, so that

$$V_k = MU_k, \quad k = 0, 1..., N-1. \tag{2.4.21}$$

The solution $V_k$ for each $z_k$, is obtained by the computation of an almost triangular system (2.4.20) and combining the result in (2.4.21) at only $O(N^2)$ operations [54]. During this process, the Hessenberg reduction (2.4.19) is only computed once, beforehand.

In the next section, we present the numerical results obtained from our Laplace transform, the ETDRK4, the well-known MATLAB solver *ode15s* and the Cranck-Nicolson methods.



## 2.5 Numerical results

In this section, we present some results of the numerical experiments that we have performed to test our method for pricing European options. Even though an analytical solution of the Black-Scholes equation for European options exists, our aim is to compare the results obtained by using our Laplace transform and ETDRK4 methods with more conventional time marching methods such as Crank-Nicholson's methods (with the time step-size 0.00025) and the well-known MATLAB solver *ode15s*. This is done in Table 2.5.1. For the numerical simulations, we fix spatial variable $S$ at $S_{max} = 3K$ to reduce the domain truncation error. Other parameters are chosen as follow: $K = 15$,

$\sigma = 0.2$, $r = 0.05$, $T = 0.25$.

Maximum absolute errors are calculated using the formula

$$\text{error} = \max_{t\in[0,T]} |V(t) - V_M(t)|, \tag{2.5.1}$$

where $V(t)$ is the analytical solution and $V_M(t)$ is the numerical solution obtained by any of the three methods as indicated in Table 2.5.1.

Table 2.5.1: Comparison of the errors defined by (2.5.1), for the Crank-Nicolson's (CN) method, ETDRK4 and the Inverse Laplace Transform (ILT) approach

| | ode15s | | CN | | ETDRK4 | | ILT | |
|---|---|---|---|---|---|---|---|---|
| N | Time(s) | Error | Time(s) | Error | Time(s) | Error | Time(s) | Error |
| 20 | 0.125 | 8.20E-2 | 0.060 | 7.10E-3 | 0.052 | 7.40E-3 | 0.0010 | 7.40E-3 |
| 30 | 0.148 | 6.97E-4 | 0.044 | 1.30E-3 | 0.540 | 1.00E-3 | 0.0050 | 1.00E-3 |
| 40 | 0.193 | 6.59E-5 | 0.109 | 1.93E-4 | 0.075 | 1.22E-4 | 0.0070 | 1.18E-4 |
| 50 | 0.223 | 7.86E-6 | 0.133 | 9.67E-5 | 0.095 | 4.85E-5 | 0.0090 | 1.07E-5 |
| 60 | 0.242 | 4.63E-6 | 0.163 | 9.73E-5 | 0.126 | 4.86E-5 | 0.0095 | 3.52E-6 |
| 80 | 0.310 | 1.86E-5 | 0.261 | 9.80E-5 | 0.218 | 4.89E-5 | 0.0097 | 5.80E-7 |



## 2.6 Summary and discussions

In this chapter, we have investigated two numerical methods for solving the Black-Scholes equation for pricing of European options. Using the spectral method, we obtained a system of ordinary differential equations which we then solve by MATLAB solver *ode15s* and by Laplace transform method. These results are also compared with those obtained by the classical Crank-Nicolson's method and we found that the proposed method outperforms the other three methods.

It is worth mentioning here that even though in practice, the use of spectral methods for boundary value problems may be troublesome because the presence of boundaries often introduces stability conditions that are both highly restrictive and often difficult to analyze, one should note that for smooth solutions the results using spectral methods

are of a degree of accuracy that local approximation methods cannot produce. For such solutions spectral methods can often achieve an exponential convergence rate as compared to the algebraic convergence rate displayed by finite difference or finite element methods.

One may also think that the matrices in spectral methods are neither sparse nor symmetric, in contrast to the situation in finite differences or finite elements where the sparsity structure of the matrices simplifies the computation. However, the number of discretization points required to achieve the expected accuracy using the spectral method is much more less than those required in finite difference or finite element methods, and therefore the spectral method is still very efficient as compared to these other two methods.

Finally, we would like to mention that we have omitted the mathematical details about the Crank-Nicholson's method and the MATLAB solver because the main emphasis of this chapter is on the use of the Laplace transform approach and ETDRK4 to solve the option pricing problems.



The method presented in this chapter gives only fourth order accuracy. The non-smooth payoff downgrades the performance of the spectral methods. In the next chapter, we develop a decomposition method to regain the exponential accuracy of these methods. Furthermore, as contour integral method, we shall only consider the Laplace transform method for its superior accuracy and efficiency as we see in this chapter.

# Chapter 3

# Improved Laplace transform method for the numerical solution of European option pricing problems



In this chapter, we investigate an efficient numerical method for solving the Black-Scholes equation for pricing European options. Our approach is based on spectral domain decomposition and the Laplace transform method. The spectral domain decomposition method approximates the solution using piecewise high order rational interpolant on the Chebyshev mesh points within each sub-domain with the boundary domain placed at the strike price where the discontinuity is located. To ensure the continuity of the solution and that of its derivatives across the boundary, two matching conditions are imposed. The resulting system is then solved by applying Laplace transform method based on Talbot's idea of deformation of contour integral [125]. The accuracy and efficiency of the solutions obtained by using this approach are compared to those obtained with conventional methods such as Crank-Nicholson and finite difference methods. The new approach exhibits spectrally accurate results for the solution and the Greeks.

## 3.1 Introduction

It is well known that the spectral method leads to low order accuracy when applied to problems having non smooth solutions. To regain the spectral accuracy, Zhu [148] used the weak form of spectral element method to compute European option prices. His results display exponential accuracy and were computationally faster than those obtain from finite difference method.

The authors in [107] used a grid stretching in combination with backward difference method of fourth order in time to solve the European options. In [127], Tangman *et al.* used a method based on the grid stretching to generate a high order compact scheme to improve on the well known second order Crank-Nicolson method for solving these problems. In spite of the popularity of these time marching methods, a critical drawback of these schemes is that they usually require as many time steps as spatial meshes to maintain the stability of the method.

In this chapter, we will consider the spectral domain decomposition method to discretize the option pricing PDE with respect to space. As already mentioned above, a direct application of the spectral methods to solve the European option pricing problems leads to low order of accuracy comparable to results obtained by finite difference methods. This poor result is due to the non-smooth payoff function or initial condition. Since the initial condition is smooth only on both side of the strick price, and we aim to retain the higher order accuracy on the whole domain, we will consider the spectral method combined with the domain decomposition approach.

The principle idea behind the use of spectral methods with domain decomposition method, is to divide the solution domain in sub-domains (or elements) where the solution is smooth enough. Therefore, rather than using a global polynomial on the entire interval, the multi-domain spectral approximation method collocates the solution within each sub-domain at the Chebyshev points.

After discretization, the resulting system of ODEs is solved by applying the Laplace transform approach. We compare the results obtained by using our approach with those

from a finite difference discretization and Crank-Nicholsons methods.

The rest of this chapter is organized as follows. To keep this chapter self-contained, in Section 3.2, we re-describe the Black-Scholes equation which is used to model the European call and put options. Application of the Laplace transform is carried out in Section 3.4. In Section 3.3, we introduce the domain decomposition method. In Section 3.5 we present comparative numerical results. Finally a brief summary and some concluding remarks are given in Section 3.6.

## 3.2 Description of the model problem

To keep this chapter self-contained and direct liking of subsequent equations, we rewrite the model presented in the previous chapter. We consider the following PDE to price European options

$$\frac{\partial V}{\partial t} + \frac{1}{2}\sigma^2 S^2 \frac{\partial^2 V}{\partial S^2} + rS\frac{\partial V}{\partial S} - rV = 0, \qquad S \in (0,\infty), \quad t \in (0,T). \tag{3.2.1}$$



Final and boundary conditions are given by

$$V(S,T) = \begin{cases} \max(S-K,0) & \text{for call,} \\ \\ \max(K-S,0) & \text{for put,} \end{cases} \tag{3.2.2}$$

and

$$\left.\begin{array}{lll} V(0,t) = 0, & V(S,t) \to S - Ke^{-r(T-t)}, \quad \text{as} \quad S \to \infty & \text{for call,} \\ \\ V(0,t) = Ke^{-rt}, & V(S,t) \to 0, \quad \text{as} \quad S \to \infty & \text{for put.} \end{array}\right\} \tag{3.2.3}$$

In the above, $V(S,t)$ is the price of a call/put option for the underlying asset whose price is $S$ at time $t$ up to the expiry date $T$, $r$ is the interest rate, $\sigma$ is the volatility of the underlying asset and $K$ is the strike price.

We set $\tau = T - t$ to transform the backward formulation $(3.2.1) - (3.2.3)$ to the following forward equation

$$\frac{\partial V}{\partial \tau} - \frac{1}{2}\sigma^2 S^2 \frac{\partial^2 V}{\partial S^2} - rS\frac{\partial V}{\partial S} + rV = 0, \tag{3.2.4}$$

The initial condition is given by the terminal payoff

$$V(S,0) = \begin{cases} \max(S-K,0) & \text{for call,} \\ \\ \max(K-S,0) & \text{for put,} \end{cases} \tag{3.2.5}$$

and the boundary conditions are given by

$$\left.\begin{array}{lll} V(0,\tau) = 0, & V(S,\tau) \to S - Ke^{-r\tau} & \text{as} \quad S \to \infty \quad \text{for call} \\ \\ V(0,\tau) = Ke^{-r\tau}, & V(S,\tau) \to 0, & \text{as} \quad S \to \infty \quad \text{for put.} \end{array}\right\} \tag{3.2.6}$$



## 3.3 Spectral discretization

Spectral methods are a class of numerical methods that approximate the solution of unknown PDEs/ODEs by a global expansion polynomial over the entire domain. Unlike piecewise interpolation methods such as finite elements or finite differences that approximate solutions over subintervals of the domain. The popularity of spectral methods results mainly from the so-called exponential (i.e. geometric) convergence rate. Indeed for these methods, the decay in the convergence rate of the error associated with them decreases exponentially with increasing degree of freedom (i.e., the order of the expansion polynomial basis). This exponential convergence contrasts with the algebraic convergence rate observed for finite difference methods. At this point, a mathematical definition of algebraic and geometric convergence is in order and given below.

**Definition 3.3.1** [13]. *Let $u_N$ be an approximation to a function $u$. Then $u_N$ is said to convergence algebraically to $u$ if its order of convergence is of the form $\mathcal{O}(N^{-C})$, with $N$ being the number of interpolation points and $C$ some positive constant.*

**Definition 3.3.2** [13]. *Let $u_N$ be an approximation to a function $u$. Then $u_N$ is said to convergence exponentially to $u$ if the convergence rate is asymptotically of order $\mathcal{O}(e^{-CN})$, with $N$ being the number of interpolation points and $C$ some positive constant.*

Spectral methods rose to prominence as numerical methods for PDEs in the 1970s. Their use is now widespread. Based on the choice of the basis functions, they can be divided into two main categories, namely, the fourier and the polynomial spectral methods. Typically writes

$$u_N(\xi, t) = \sum_{k=0}^{N} a_k(t)\phi_k(\xi), \tag{3.3.1}$$

where $\phi_k,\ k = 0, 1, ..., N$ are the basis polynomials and $a_k,\ k = 0, 1, ..., N$ are the unknown coefficients to be determined. The choice of $\phi_k,\ k = 0, 1, ..., N$ depends on the nature of the problem at hand. For periodic boundary value problems, $\phi_k$, $k = 0, 1, ..., N$ are chosen to be trigonometric polynomials. For non-periodic boundary problems, the most convenient choice for the basis functions is the Chebyshev polynomials: $\phi_k = T_k(\xi)$, and the Legendre polynomials: $\phi_k = L_k(\xi)$.

Spectral methods based on algebraic polynomial expansion can be divided into three categories, the Galerkin, tau and the collocation (also known as the pseudo-spectral) methods. One difference between these methods is the error distribution principle, that is, the means of making the residual function

$$R_N(\xi, t) = \frac{\partial u_N}{\partial t} - Hu_N(\xi, t), \tag{3.3.2}$$

small, where $H$ is the associated differential operator. In the Galerkin method, the residual, $R_N(x, t)$ is required to be orthogonal to the span of $\phi_k(\xi)$, $k = 0, 1, ..., N$. The

tau method works similarly to the Galerkin method but unlike the Galerkin method which requires each $\phi_k(\xi)$ to satisfy the boundary conditions, it only requires that the approximation $u_N(\xi, t)$ satisfies the boundary conditions. The Galerkin and Tau methods involved a projection of the residual onto some polynomials space to be zero. For a thorough discussion on these two methods, interested readers are referred to [13, 61].

The method which we shall focus on in this work is the collocation method, often referred to as pseudo-spectral method. In contrast to the Galerkin and Tau methods, spectral collocation method requires that the residual $R_N(x, t)$ vanishes at a set of collocation points, making it easy to apply to variable coefficients and non-linear problems.

### 3.3.1 Chebyshev collocation methods

The basic idea behind spectral methods is to approximate the unknown solution of a differential equation by a global interpolant, and requires the interpolant to satisfy the differential equation exactly at predefined collocation points. Usually, each spectral method is named after choosing a function class for the basis functions. Since we use Chebyshev grid points in this case, the method is known as the Chebyshev collocation method.



In Chebyshev spectral method, the spectral process involves seeking the solution to a differential equation by polynomial interpolation. In order to review the formulas of polynomial interpolation, we consider interpolating an arbitrary function $u(\xi)$ at $N+1$ distinct nodes $\xi_k$, $k = 0, 1, ..., N$, in $[-1, 1]$.

**Definition 3.3.3** *Given a set of grid points $\xi_j$, $j = 0, 1, ..., N$, an interpolating approximation to a function $u(\xi)$ is a polynomial $u_N(\xi)$ of degree $N$, determined by the requirement that the interpolant agrees with $f(\xi)$ at the set of interpolation points $\xi_j$, $j = 0, 1..., N$, i.e.,*

$$u_N(\xi_i) = u(\xi_i), \qquad i = 0, 1, ..., N.$$

We define $L_k(\xi)$ as the Lagrange polynomial of degree $N$,

$$L_k(\xi) = \prod_{\substack{j=0 \\ j\neq k}}^{N} \frac{\xi - \xi_j}{\xi_k - \xi_j}, \qquad k = 0, 1, ..., N.$$

Note that at the discrete points $\xi_k$, $k = 0, 1..., N$, $L_k(\xi)$ satisfies

$$L_j(\xi_k) = \delta_{jk} = \begin{cases} 1 & \text{if } j = k \\ \\ 0 & \text{otherwise} \end{cases}$$

where $\delta_{jk}$ is the Kronecker delta function. The interpolation polynomial, $f_N(\xi)$ is then given by

$$u_N(\xi) = \sum_{k=0}^{N} u(\xi_k) L_k(\xi). \tag{3.3.3}$$

The grid points $\xi_k$, $k = 0, 1, ..., N$ are the roots of the Jacobi polynomials; they have a nonuniform distribution [47, 132] in the interval $[-1, 1]$ with a node density per unit length of

$$\mu \approx \frac{N}{\sqrt{1 - \xi^2}} \qquad \text{as} \qquad N \to \infty.$$

In this chapter, we use the Chebyshev points as the grid points. These are given by

$$\xi_j = \cos\left(\frac{j\pi}{N}\right), \qquad j = 0, 1, ..., N.$$

The Chebyshev points are often defined as the projection onto the interval $[-1, 1]$ of the roots of unity along the unit circle $|z| = 1$ in the complex plane [132]. One should note that the Chebyshev points are defined on the canonical interval $[-1, 1]$, therefore any problem posed on an arbitrary interval $[a, b]$ should be converted to $[-1, 1]$ through the linear transformation $\xi \longleftrightarrow (1/2)((b - a)\xi + (b + a))$.

The Chebyshev collocation methods are renowned for their exponential accuracy as illustrated in the following theorem [57] for an analytic function.

**Theorem 3.3.4** [57] *Let $u_N$ be the polynomial of degree at most $N$ that interpolates a function $u$ at Chebyshev points $\xi_k = \cos k\pi/N$, $k = 0, ..., N$. If $u$ is analytic in the closed ellipse with foci $\pm 1$ and semi-axis lengths that sum to $\rho$, then*

$$\max_{\xi\in[-1,1]} |u_N - u| \leq \mathcal{O}(\rho^{-N}), \quad as \quad N \to \infty.$$

*Proof.* See [57].

In the following, we discuss the concept of collocation derivative associated with the interpolation polynomial $u_N(\xi)$ described above.

### Differentiation matrices

Using (3.3.3), the $m$-th order derivative of $u_N(\xi)$ at the collocation points $\xi_k$, $k = 0, 1, ..., N$, is given by

$$u_N^{(m)} = \frac{d^m u_N(\xi)}{d\xi^m} \tag{3.3.4}$$

$$= \sum_{k=0}^{N} u(\xi_k) \frac{d^m L_k(\xi)}{d\xi^m}. \tag{3.3.5}$$



Nodal representation yields

$$\frac{d^m u_N(\xi_j)}{d\xi^m} = \sum_{k=0}^{N} u(\xi_k) \frac{d^m L_k(\xi_j)}{d\xi^m}, \qquad j = 0, 1, ..., N, \tag{3.3.6}$$

which can be represented by the matrix formula

$$\boldsymbol{u}_N^{(\boldsymbol{m})} = D_N^{(m)} \boldsymbol{u}_N, \tag{3.3.7}$$

where

$$\boldsymbol{u}_N = \begin{bmatrix} u_N(\xi_0) \\ \vdots \\ u_N(\xi_N) \end{bmatrix}, \quad \boldsymbol{u}_N^{(\boldsymbol{m})} = \begin{bmatrix} u_N^{(m)}(\xi_0) \\ \vdots \\ u_N^{(m)}(\xi_N) \end{bmatrix},$$

and $D_N^{(m)}$ is the $(N+1)\times(N+1)$ differentiation matrix of order $m$ with entries

$$(D_N^{(m)})_{j,k} = L_k^{(m)}(\xi_j), \qquad j,k = 0,1,...,N. \tag{3.3.8}$$

The computation of these differentiation matrices for an arbitrary order $m$ has been considered in [136]. Moreover as for the Theorem 3.3.4, the following theorem shows that the approximation of the $m^{th}$ order derivative $u_N^{(m)}$ of $u$ converges exponentially.

**Theorem 3.3.5** *[57] Let $u_N$ be the polynomial of degree at most $N$ that interpolates a function $u$ at Chebyshev points $\xi_k = \cos k\pi/N$, $k = 0,...,N$. If $u$ is analytic in the closed ellipse with foci $\pm 1$ and semi-axis lengths that sum to $\rho$, then the error in the approximation of the $m^{th}$ order derivative $u_N^{(m)}$ of $u$ is given by*

$$\max_{\xi\in[-1,1]} |u_N^{(m)} - u^{(m)}| \leq \mathcal{O}(\rho^{-N}), \quad as \quad N\to\infty.$$

*for any integers $m > 0$.*

*Proof.* See [57].



As we noted earlier, the exponential convergence rate of spectral methods is strictly dependent on the smoothness of the unknown function. However option pricing PDEs have the interesting feature that the initial conditions are not smooth. Therefore direct application of a spectral method to the solution of the Black-Scholes equation will lead to a low order, slowly convergent approximation. To illustrate this fact, we consider the following European call option

$$\frac{\partial V}{\partial \tau} - \frac{1}{2}\sigma^2 S^2 \frac{\partial^2 V}{\partial S^2} - rS\frac{\partial V}{\partial S} + rV = 0, \qquad S\in[0,S_{\max}], \quad \tau\in(0,T), \tag{3.3.9}$$

with initial and boundary conditions

$$\left.\begin{aligned} V(S,0) &= \max(S-K,0),\\ V(0,\tau) &= 0,\\ V(S_{\max},\tau) &= S_{\max} - Ke^{-r\tau}. \end{aligned}\right\} \tag{3.3.10}$$

After discretization, (3.3.9) can be expressed as

$$\frac{\partial V}{\partial t} - \frac{1}{2}\sigma^2(\xi+1)^2 D^{(2)}V - r(\xi+1)D^{(1)}V + rV = 0, \tag{3.3.11}$$

where $\dot{V}$ denotes the differentiation with respect to $\tau$; $D^{(1)}$ and $D^{(2)}$ represent the first and second order matrices, respectively, and $\xi$ are the Chebyshev points. The equation (3.3.11) can be integrated in time by any one of a number of time stepping schemes. However, we consider a method based on the application of the Laplace transform as described in the next section. The poor performance of the direct application of the spectral method is presented in Figure 3.5.2 (page 61) where only a second order convergence rate is observed as expected.

To remedy this, we propose the spectral domain decomposition method (SDDM). In the spectral domain decomposition approach, the domain $S \in [0, S_{\max}]$ is divided into sub-domains. For the problem at hand, we need to divide the domain into two sub-domains, with the transition point as the strike price. To represent the solution in each sub-domains, we choose to approximate the solution by a linear rational interpolant for their improved stability properties compared to the polynomial interpolant [5, 11, 130].

### 3.3.2 Domain decomposition based on rational interpolant

Instead of the general spectral methods, we shall consider spectral methods based on rational interpolants which are more convenient for the problems at hand. The rational approximation of a function $u$ at the Chebyshev points $\xi_k$, for $k = 0, 1, ..., N$, is given by

$$u_N(\xi) = \frac{\displaystyle\sum_{k=0}^{N} \frac{w_k}{\xi - \xi_k} u(\xi_k)}{\displaystyle\sum_{k=0}^{N} \frac{w_k}{\xi - \xi_k}}, \tag{3.3.12}$$

where $w_k$, $k = 0, 1, ..., N$ are the barycentric weights defined by $w_0 = 1/2$, $w_N = (-1)^N/2$, and $w_k = (-1)^k$, $k = 1, ..., N-1$. For the spectral polynomial method,

the $m^{th}$ order differentiation matrix associated with the rational interpolant (3.3.12) is given by

$$u_N^{(m)}(\xi_k) = \sum_{k=0}^{N} \frac{d^m}{d\xi^m} \left( \frac{\sum_{k=0}^{N} \frac{w_k}{\xi - \xi_k} u(\xi_k)}{\sum_{k=0}^{N} \frac{w_k}{\xi - \xi_k}} \right), \tag{3.3.13}$$

$$= \sum_{k=0}^{N} D_{jk}^{(m)} u(\xi_k), \tag{3.3.14}$$

where the $D_{jk}^{(m)}$ are the entries of the differentiation matrix of order $m$. Formula to construct $D_N^{(m)}$ are given by Schneider and Werner in [119] for $m = 1$ and $m = 2$ and latter generalized for any order by Tee in [130]. The first and second order differentiation matrices are given by the following formulas

$$D_{jk}^{(1)} = \begin{cases} \frac{w_k}{w_j(\xi_j - \xi_k)}, & j \neq k, \\ -\sum_{i \neq k} D_{ji}^{(1)}, & j = k, \end{cases} \tag{3.3.15}$$



and

$$D_{jk}^{(2)} = \begin{cases} 2D_{jk}^{(1)} \left( D_{jj}^{(1)} - \frac{1}{\xi_j - \xi_k} \right), & j \neq k, \\ -\sum_{i \neq k} D_{ji}^{(2)}, & j = k, \end{cases} \tag{3.3.16}$$

The above expression will be used when we approximate first and second derivative term in (3.2.1).

**Domain decomposition method combined with spectral approximation**

From our earlier discussion in this section, we know that the direct application of spectral method to the Black-Scholes problem leads to low order convergence results. The

poor convergence is attributed due to the non-smoothness of the initial condition at the strike price. To recover spectral accuracy, we consider using the domain decomposition approach which we discuss here. We split the domain at the point of discontinuity, and apply the Chebyshev spatial discretization to reduce the problem to a set of coupled ordinary differential equations in time. Since the function is smooth on each subinterval including the point of discontinuity (strike $K$), a spectral accuracy can be obtained provided that appropriate matching conditions are set across the point of discontinuity.

To begin with this, we consider the domain decomposition approach for the Black-Scholes European call option (3.3.9)-(3.3.10). Since the initial condition is non-smooth at the strike price, we split the interval $[0, S_{\max}]$ at that point into two subintervals, $\vartheta = [0, K]$ and $\chi = [K, S_{\max}]$ of lengths $d^{\vartheta} = K$ and $d^{\chi} = S_{\max} - K$, respectively. To apply the Chebyshev discretization we map each element to the reference element $[-1, 1]$ by the linear transformation:

$$S^{\vartheta,\chi}(\xi) = \begin{cases} \frac{d^{\vartheta}}{2}(\xi + 1), & S \in [0, K], \\ \frac{d^{\chi}}{2}(\xi + 1) + K, & S \in [K, S_{\max}]. \end{cases} \tag{3.3.17}$$



The linear transformation to the derivative leads

$$dS^{\vartheta,\chi}(\xi) = \begin{cases} \frac{d^{\vartheta}}{2} d\xi, & S \in [0, K], \\ \\ \frac{d^{\chi}}{2} d\xi, & S \in [K, S_{\max}], \end{cases} \tag{3.3.18}$$

which implies that

$$\frac{\partial}{\partial S} \equiv \frac{\partial}{\partial \xi}\frac{\partial \xi}{\partial S} \equiv \begin{cases} \frac{2}{d^{\vartheta}}\frac{\partial}{\partial \xi}, & S \in [0, K], \\ \\ \frac{2}{d^{\chi}}\frac{\partial}{\partial \xi}, & S \in [K, S_{\max}]. \end{cases} \tag{3.3.19}$$

From equations (3.3.18)-(3.3.19) we can write Black-Scholes equation (3.3.9) into each

sub-domain as follows

$$\frac{\partial V^{\vartheta}}{\partial \tau} = \frac{2}{(d^{\vartheta})^2}\sigma^2 S^{\vartheta}(\xi)^2 \frac{\partial^2 V^{\vartheta}}{\partial \xi^2} + \frac{2r}{d^{\vartheta}} S^{\vartheta}(\xi)\frac{\partial V^{\vartheta}}{\partial \xi} - rV^{\vartheta}, \tag{3.3.20}$$

and

$$\frac{\partial V^{\chi}}{\partial \tau} = \frac{2}{(d^{\chi})^2}\sigma^2 S^{\chi}(\xi)^2 \frac{\partial^2 V^{\chi}}{\partial \xi^2} + \frac{2r}{d^{\chi}} S^{\chi}(\xi)\frac{\partial V^{\chi}}{\partial \xi} - rV^{\chi}. \tag{3.3.21}$$

Using matrix notations, we have

$$\dot{V}^{\vartheta} = \frac{\sigma^2}{2}(W^{\vartheta})^2 D^{(2)} V^{\vartheta} + rW^{\vartheta} D^{(1)} V^{\vartheta} - rV^{\vartheta}, \tag{3.3.22}$$

and

$$\dot{V}^{\chi} = \frac{\sigma^2}{2}(W^{\chi})^2 D^{(2)} V^{\chi} + rW^{\chi} D^{(1)} V^{\chi} - rV^{\chi}. \tag{3.3.23}$$

Here $W^{\vartheta,\chi}$ are the diagonal matrices $W^{\vartheta,\chi} = diag\left((2/d^{\vartheta,\chi})S(\xi)\right)$ and $\dot{V}^{\vartheta,\chi}$, are the derivatives with respect to $\tau$. Defining



$$B^{\vartheta,\chi} := \frac{\sigma^2}{2}(W^{\vartheta,\chi})^2 D^{(2)}, \tag{3.3.24}$$

and

$$C^{\vartheta,\chi} := rW^{\vartheta,\chi} D^{(1)}, \tag{3.3.25}$$

we obtain from (3.3.22)-(3.3.23),

$$\dot{V}^{\vartheta} = (B^{\vartheta} V^{\vartheta}) + (C^{\vartheta} V^{\vartheta}) - rV^{\vartheta}, \tag{3.3.26}$$

and

$$\dot{V}^{\chi} = (B^{\chi}V^{\chi}) + (C^{\chi}V^{\chi}) - rV^{\chi}. \tag{3.3.27}$$

To impose the boundary conditions, we replace the first and last equations from the first and second sub-domains, respectively, by the boundary conditions (3.3.10). Furthermore, to ensure the continuity of the solution and that of its first derivatives at the interface, we impose matching conditions across the point of discontinuity, i.e., at the strike price $K$. Defining

$$V^* = V_N^{\vartheta} = V_0^{\chi}, \tag{3.3.28}$$

and

$$\frac{\partial V_N^{\vartheta}}{\partial \xi} = \frac{\partial V_0^{\chi}}{\partial \xi}, \tag{3.3.29}$$

we see that equation (3.3.28) implies

$$2\dot{V}^* = \left(\left(B^{\vartheta} + C^{\vartheta} - rI^{\vartheta}\right)V^{\vartheta}\right)_N + \left(\left(B^{\chi} + C^{\chi} - rI^{\chi}\right)V^{\chi}\right)_0. \tag{3.3.30}$$



Here $I^{\vartheta}$ and $I^{\chi}$ are identity matrices on $\vartheta$ and $\chi$ respectively. From (3.3.29) we have

$$\frac{2}{d^{\vartheta}}(D^{(1)}V^{\vartheta})_N - \frac{2}{d^{\chi}}(D^{(2)}V^{\chi})_0 = 0. \tag{3.3.31}$$

The solution vector $V$ of (3.3.9)-(3.3.10) is obtained from the system of $2N+2$ equations from (3.3.26), (3.3.30), (3.3.31) and the boundary conditions. We combine the approximations from the two sub-domains with boundary and matching conditions included into a global system with the governing equation

$$\dot{V} = AV - rV. \tag{3.3.32}$$

Here $V$ is the vector

$$V = \left(V_0^{\vartheta}, \ldots, V_N^{\vartheta}, V_0^{\chi}, \ldots, V_N^{\chi}\right),$$

and

$$A = B + C,$$

where $B$ and $C$ are block diagonal matrices of $B^{\vartheta,\chi}$ and $C^{\vartheta,\chi}$, respectively. After the discretization, the resulting ODE is solved using Laplace method as discussed in the next section.

## 3.4 Practical implementation of the Laplace transform method to solve the discrete problem

We apply the Laplace transform to (3.3.32) which yields

$$z\widehat{V} = A\widehat{V} - r\widehat{V} + V_0, \tag{3.4.1}$$

where $\widehat{V}$ is the unknown solution in this domain. The boundary conditions becomes

$$\left.\begin{array}{lll} \widehat{V}(-1,z) = 0, \quad \widehat{V}(1,z) = \frac{S_{\max}}{z} - \frac{K}{z+r}, & \text{for call,} \\ \widehat{V}(-1,z) = \frac{K}{(z+r)}, \quad \widehat{V}(1,z) = 0, & \text{for put.} \end{array}\right\} \tag{3.4.2}$$



For each $z_k$ on the contour (1.2.5), the equation (3.4.1) in matrix form is solved as

$$(z_k I - (A + rI))\,\widehat{V}_k = V_0, \qquad k = 0, 1, ..., M. \tag{3.4.3}$$

A straight forward application of the inversion formula (1.2.6) yields

$$V(t) = \frac{h}{2\pi i}\int_{-\infty}^{\infty} e^{z(\ell)t}\widehat{V}z'(\ell)d\ell. \tag{3.4.4}$$

We approximate the integral (3.4.4) using the trapezoidal rule truncated at $M$, and taking advantage of the symmetry of the contour (1.2.5), we obtain

$$V_M(t) = \mathrm{Re}\left\{\frac{h}{\pi i}\sum_{k=0}^{M} e^{z_k t}\widehat{V}_k z_k'\right\}, \tag{3.4.5}$$

where

$$\widehat{V}_k = (z_k I - (A + rI))^{-1} V_0, \quad k = 0, 1, ..., M. \tag{3.4.6}$$

In the next section, we present some numerical results illustrating the performance of the proposed method.

## 3.5 Numerical results

In this section, we present some results of numerical experiments we performed to test our method for pricing European call options. Even though an analytical solution of the Black-Scholes equation for European option exists, for practical application numerical results is often needed. The efficiency and accuracy of the numerical method assist us in determining the suitability of the proposed approach while tackling more challenging problems. To this end, our aim is to compare the results obtained by finite difference method and those obtained by the spectral decomposition method on one hand, and the Laplace transform approach with the conventional time marching methods such as Crank-Nicholson on the other hand. The truncated value $S_{\max}$ of the stock price interval, is chosen sufficiently large to reduce the truncation error.

The spectral domain decomposition method has the flexibility in the choice of the number of sub-domains depending on the complexity of the computational interval. For the problem at hand, however, we divide the interval $[0, S_{\max}]$ into two sub-domains. One sub-domain is to the left of the strike price with length $K$ and the other one is on the right of the stock price and is of length $S_{\max} - K$. Subsequently, we match both sub-domains to the standard interval $[-1, 1]$ for spectral discretization as described in

Section 1.3.

In the implementation of the inverse Laplace transform, the number of terms in the summation (3.4.5) depends on the number of points $z_k$, $k = 0, ..., M$. From section 1.3, we know that the conditioning error increases moderately and depends on $M$, therefore above a certain threshold number of points $z_k$ on the contour, the error starts to increase and eventually may become large enough to hinder the exponential accuracy one would normally observe. Though the optimal number of contour points may vary with the problem at hand, for the European options, we carry out different simulations by keeping the number grid points $N$ fixed and varying the number of these contour points $z_k$. For different values of $N$, we find that the optimal number of contour grid points vary from 20 to 30.

For numerical comparisons, we compute the maximum absolute errors using the formula

$$\max_{t\in[0,T]} |V(t) - V_M(t)|, \tag{3.5.1}$$

where $V(t)$ is the analytical solution and $V_M(t)$ is the numerical solution obtained by the two methods as indicated in tables 3.5.1 and 3.5.2. To compare the order of convergence for the finite difference and the spectral decomposition methods, we compute the solution for a set of typical parameter values: $K = 10$; $\sigma = 0.3$; $r = 0.05$; $T = 0.25$ and $S_{\max} = 3K$. Also $M$ is the number of point on the contour, $N$ indicates the total number of grid points use in the discretization and time refers to computational time in seconds.

For simplicity, we use the following abbreviations in tables and graphs below. SDDM means the spectral domain decomposition method, FDM refers to the finite difference method, ILT refers to the Inverse Laplace transform whereas CN stands for Crank-Nicholson method.

Tables 3.5.1 and 3.5.2 show the convergence rate and computational time of the ILT and CN method for both SDDM and FDM methods. The computation are performed on the same set of parameters for comparison purposes. As expected, the ILT method

has a higher convergence rate than the CN. In both tables, we observe that 20 contour points $z_k$ with the ILT method are sufficient to obtain higher accuracy than what we can achieve with CN.

From tables 3.5.1 and 3.5.2, we can also observe that SDDM method converges much faster than the FDM. In fact, the SDDM converges exponentially. Combination of ILT and SDDM methods allow even more accurate results. For example, to attain the error less than $10^{-5}$, only 40 grid points in each sub-domain is required using SDDM whereas FDM requires 700 grid points.

In Figure 3.5.2, we highlight the superiority of the SDDM method over FDM and the spectral method without the decomposition. The SDDM displays a spectral convergence, whereas FDM and the direct spectral method (without decomposition) both display only second order accuracy. In Figure 3.5.3, we compare the convergence of the proposed approach with the FDM and CN. This figure confirms the superior accuracy of our approach.

To further corroborate the reliability of the ILT and SDDM method, we computed the Greeks $\Delta$ and $\Gamma$. In figures 3.5.4 (left) and 3.5.5 (left), we see that the numerical valuation of both $\Delta$ and $\Gamma$ is in agreement with their exact counterparts. This observation is demonstrated in figures 3.5.4 (right) and 3.5.5 (right) which show the spectral accuracy obtained with the ILT method in the computation of these quantities.



## 3.6 Summary and discussions

We have investigated the use of the spectral domain decomposition method for the discretization in asset direction (space) and the Inversion of the Laplace transform for time integration for numerically solving the European option pricing problem.

For time integration of the discrete problem, we have investigated a numerical method for inverting the Laplace transform based on the trapezoidal rule that approximates the Bromwich integral. This approximation is based on the deformation of the contour suggested by Talbot. For the problem in this chapter, we have used a parabolic

contour.

We compared our approach with the conventional finite difference and Crank-Nicholson methods. In all experiments, the Inverse Laplace transform method and spectral domain decomposition approach displayed better results, whereas the finite difference and Crank-Nicholson methods were only second order accurate. The same observation was made for the approximation of the Greeks, $\Delta$ and $\Gamma$.

In the next chapter, we extent the approach developed here to more complex problem of pricing options, namely, American.

Table 3.5.1: Numerical results obtained by using Crank-Nicholson and Inverse Laplace transform method for time and standard finite difference method for the spatial (asset) discretization using the parameters $K = 10$; $\sigma = 0.3$; $r = 0.05$; $T = 0.25$; $S_{\max} = 3K$.

| CN and FDM | | | | ILT and FDM | | | |
|---|---|---|---|---|---|---|---|
| $N$ | Time steps | Error | Time (s) | $N$ | M | Error | Time (s) |
| 10 | 100 | 4.13E-2 | 0.001 | 10 | 20 | 4.51E-2 | 0.004 |
| 70 | 200 | 2.00E-3 | 0.008 | 70 | 20 | 1.30E-3 | 0.006 |
| 250 | 280 | 1.72E-4 | 0.110 | 250 | 20 | 1.06E-4 | 0.022 |
| 400 | 400 | 1.22E-4 | 0.650 | 400 | 20 | 4.17E-5 | 0.109 |
| 700 | 600 | 8.20E-5 | 3.580 | 700 | 20 | 1.37E-5 | 0.262 |
| 1000 | 1000 | 4.94E-5 | 13.890 | 1000 | 20 | 6.73E-6 | 0.606 |

Table 3.5.2: Numerical results obtained by using Crank-Nicholson and Inverse Laplace transform method for time and Spectral domain decomposition method for the spatial (asset) discretization with two sub-domains and the parameters $K = 10$; $\sigma = 0.3$; $r = 0.05$; $T = 0.25$; $S_{\max} = 3K$.

| CN and SDDM | | | | ILT and SDDM | | | |
|---|---|---|---|---|---|---|---|
| $N$ | Time steps | Error | Time (s) | $N$ | M | Error | Time (s) |
| 10 | 50 | 1.27E-2 | 0.002 | 10 | 20 | 1.27E-2 | 0.004 |
| 20 | 100 | 1.20E-3 | 0.042 | 20 | 20 | 1.27E-2 | 0.004 |
| 40 | 200 | 6.17E-4 | 0.059 | 40 | 20 | 1.23E-5 | 0.005 |
| 50 | 400 | 3.09E-4 | 0.142 | 50 | 20 | 3.00E-7 | 0.007 |
| 60 | 800 | 1.54E-4 | 0.362 | 60 | 20 | 1.42E-8 | 0.009 |
| 80 | 1500 | 8.23E-5 | 1.062 | 80 | 20 | 2.64E-11 | 0.015 |

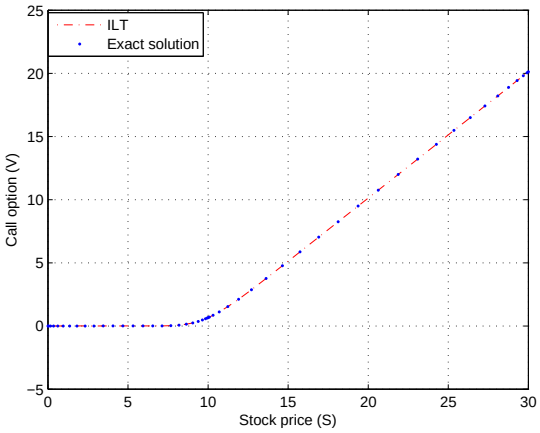


Figure 3.5.1: Valuation of the European option using SDDM and ILT method using parameters $K = 10$; $\sigma = 0.3$; $r = 0.05$; $T = 0.25$; $S_{\max} = 3K$; and $N = 40$ in each of the two sub-domains.



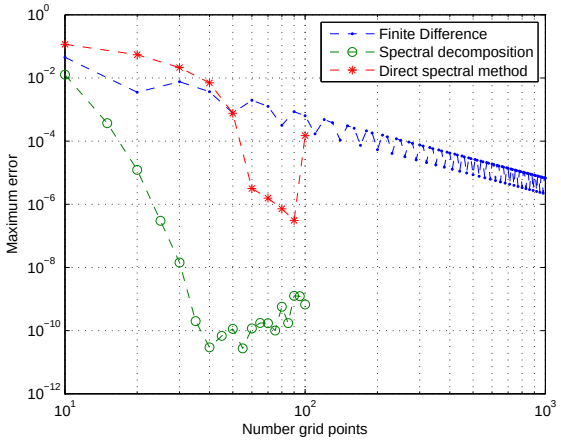


Figure 3.5.2: Comparison of finite difference, standard spectral and spectral method based on the domain decomposition using the parameters $K = 10$; $\sigma = 0.3$; $r = 0.05$; $T = 0.25$; $S_{\max} = 3K$.

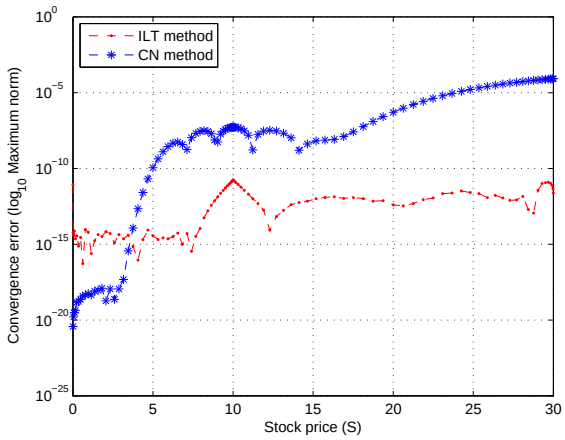


Figure 3.5.3: Comparison of the ILT and CN methods with SDDM method for pricing European options using the parameters $K = 10$; $\sigma = 0.3$; $r = 0.05$; $T = 0.25$; $S_{\max} = 3K$; and $N = 40$ in each sub-domain.



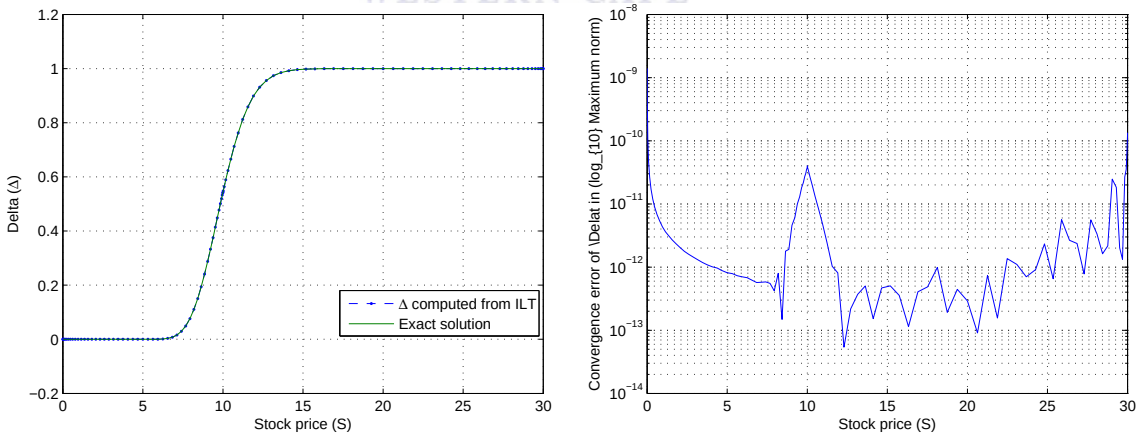


Figure 3.5.4: Left figure: results for $\Delta$ obtained by using the Inverse Laplace transform (ILT) and the exact formula; Right figure: maximum errors occurred during the computation of the $\Delta$. Computing parameters were taken as $K = 10$; $\sigma = 0.3$; $r = 0.05$; $T = 0.25$; $S_{\max} = 3K$; and $N = 40$ in each sub-domain.

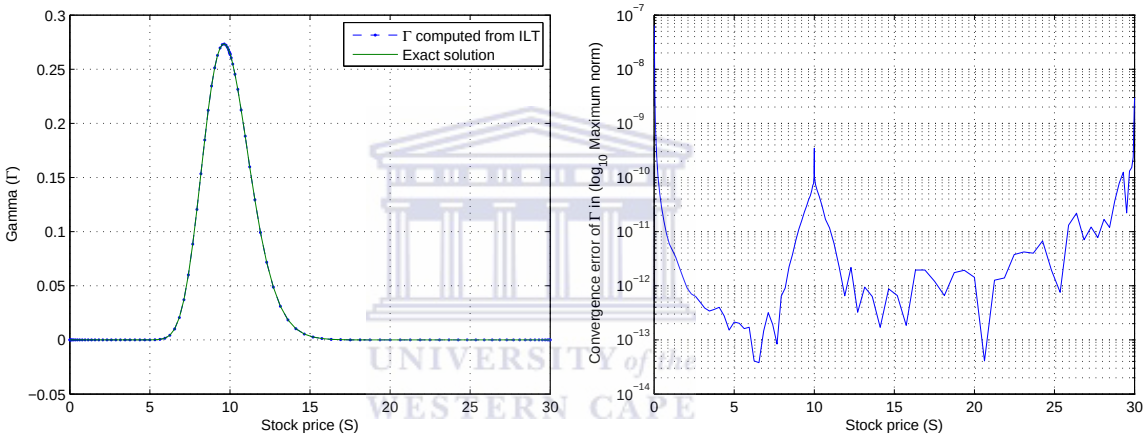


Figure 3.5.5: Left figure: results for $\Gamma$ obtained by using the Inverse Laplace transform (ILT) and the exact formula; Right figure: maximum errors occurred during the computation of $\Gamma$. Computing parameters were taken as $K = 10$; $\sigma = 0.3$; $r = 0.05$; $T = 0.25$; $S_{\max} = 3K$; and $N = 40$ in each sub-domain.

# Chapter 4

# A robust Laplace transformed method for pricing American options



In this chapter, we present a robust numerical method to price American options based on the spectral method approximation of the solution and its derivatives in the asset (space) direction and the application of the Laplace transform for the discretization in time direction. Due to the non-smooth initial condition associated with the American options, we use spectral domain decomposition method to approximate the option price which is represented pointwise on a Chebyshev grid within each sub-domain. Furthermore, it is known that the early exercise associated with the American options leads to a free boundary problem. To avoid the computation of this unknown free boundary, we first solve the corresponding European put option and then use an updating procedure to evaluate the American put option. Our numerical results show that the proposed method is very competitive for the solution and the Greeks.

## 4.1 Introduction

Among the most popular derivatives, both standard and non-standard options are actively traded on different financial markets worldwide. Depending on the exercise possibility, the standard (plain vanilla) options can be classified into two main cate-

gories: the European and American options. European options can only be exercised at the expiration of the contract whereas the American options can be exercised at any time between the start date and the expiry date. This added freedom of exercise makes American options more attractive to investors than their European counterparts. However, this apparent freedom of exercise also adds the difficulty in pricing these type of options. Now, the option holder is faced with the dilemma of deciding when to exercise the option to ensure an optimal gain. For example, if at a specific time before the maturity date, the option is out-of-the money then the owner will not exercise. However, if the option is in-the-money, it may be beneficial for him/her to hold the option until a later time when the payoff might be bigger.

Like European options, American options can also be modeled by the Black-Scholes equation. However, the possibility of an early exercise for the American options translates the corresponding Black-Scholes PDE into a free (moving) boundary problem. On one side of the free boundary (known as the continuation region) it is optimal to hold the option. On the other side of the free boundary (known as the stoping region), it is optimal to exercise it. For a put (call) option, the stoping region is located on the left (right) of the free boundary whereas the continuation region is on the right (left). Therefore, determining the free boundary becomes a crucial part when one wishes to solve a problem of pricing American options.



Many researchers have attempted to solve these options analytically. Gesk *et al.* [52] introduced a quasi-analytical solution which generates an approximative solution by restricting the early exercise at discrete times. Kwok and Wu [143] considered the transformation of the American option into a fixed boundary problem. The fixed boundary facilitates effective discretization of the resultant partial differential equation which was then solved by linear difference methods. The advantage of this method is that no embedded iteration is needed at each time step.

In his quest to solve the American options analytically, Zhu derived an exact and explicit solution of these options in [146]. However, the implementation of his approach is a complicated exercise. Firstly, the solution is written in a Taylor's series

expansion form which converges slowly. Secondly, each term involves multiple integrals which must be solved numerically. This renders the evaluation of the exact solution impractical in most applications.

Due to the lack of reliable analytical solutions, the problem of pricing American options needs to be solved numerically. This has been the subject of intensive research in the last two decades. Brennan and Schwartz [16, 17] and Cox [31] were among the first to use numerical methods for solving these options. The former introduced implicit finite difference methods to account for the early exercise possibility of American options whereas the latter introduced binomial methods. Han and Wu in [58] introduced a fast numerical method based on finite difference approximations. Their idea was to transform the original problem into a standard forward diffusion equation over an infinite domain. The discretization of the boundary condition combined with finite difference methods allowed them to accurately value the options.

Another popular method for pricing American options is the front-fixing method of Nielsen *et al.* [104]. It consists of transforming the free boundary problem into a non-linear problem with fixed boundary. Similar to the front-fixing method is the front-tracking method which was also applied to the free boundary problem associated with American options as discussed in [68].



In [129], Tangman *et al.* considered a high order compact finite difference scheme. They used a grid stretching transformation in time combined with a modified Thomas algorithm based on the location of the free boundary. They showed that this strategy gives optimal results compared to those obtained in [23]. However, the grid-stretching strategy failed to produce high-order results. To circumvent this, they considered a front-fixing transformation to fix the boundary.

In [48, 104, 150], the authors developed a new approach known as the penalty method. In this approach, the free boundary problem is replaced by a fix boundary problem by adding a penalty term. The non-linear equation thus obtained is solved by some iterative solvers.

A pioneered work by Mallier and Alobaidi [95] gives an analysis of the application of

the method based on Laplace transform to price the European and American options. In this work, they proposed a redefinition of the Laplace transform formula to allow its application to American options. However, they failed to give a corresponding inversion formula to evaluate the solution after transforming the problem into the Laplace transform space.

In this chapter, we propose the use of a multi-domain spectral method for space discretization and the Laplace transform for time integration. The multi-domain spectral methods uses the spectral method, based on rational interpolants, directly in each sub-domain to approximate the unknown solution. Matching conditions are imposed across the sub-domain to ensure the continuity of the solution and that of its first derivative. After the spatial discretization, the resulting semi-discrete problem is solved by the Laplace transform approach. To recover the solution, an inversion of the Laplace transform is performed with an updating procedure to obtain American option prices. Some other works related to the pricing of American options can be found in [6, 7, 20, 26, 43, 46, 85].



The rest of this chapter is organized as follows. In Section 4.2, we give a description of the model. Section 4.3 deals with the application of the Laplace transform to solve the semi-discrete problem. We also discuss the error analysis related to this approximation in this section. Numerical results are given in Section 4.4. Section 4.5 deals with summary and conclusion.

## 4.2 Description of the model problem

In this section, we formulate the American option problem known as a free boundary problem due to the possibility of an early exercise that characterizes this type of option.

Let $S$ be the underlying asset, $t$ the time, and $S_f$ the free boundary. As mentioned earlier, $S_f$ divides the region $(S, t)$ into two parts, the continuation region

$$\{(S,t) \in \mathbb{R}_+ \times [0,T] : V(S,t) > \max(K - S, 0)\},$$

which is the region where the option is suppose to be alive, and the stopping region which is the region where early exercise is advisable, and defined as

$$\{(S,t) \in \mathbb{R}_+ \times [0,T] : V(S,t) = \max(K-S,0)\}.$$

The price of an American put option $V(S,t)$ satisfies the following free boundary problem

$$\frac{\partial V}{\partial t} + \frac{1}{2}\sigma^2 S^2 \frac{\partial^2 V}{\partial S^2} + rS\frac{\partial V}{\partial S} - rV = 0, \qquad S > S_f(t), \quad 0 \leq t < T. \tag{4.2.1}$$

The final condition is given by

$$V(S,T) = \max(K-S,0), \qquad 0 \leq S \leq S_f(T) = S_0.$$

On the free boundary $S_f$, we have

$$V(S_f(t),t) = K - S_f(t).$$



To complete the system, we need the following additional conditions

$$\left.\begin{array}{ll} \frac{\partial V}{\partial S}(S_f(t),t) = -1, & 0 \leq t \leq T, \\ \lim_{S\to\infty} V(S,t) \to 0, & 0 \leq t \leq T, \\ V(S,t) = E - S, & 0 \leq S \leq S_f(t), \\ S_f(T) = E. & \end{array}\right\} \tag{4.2.2}$$

The case when the asset pays a dividend with the rate $\widetilde{\delta}$, the analogous of (4.2.1) will

be

$$\frac{\partial V}{\partial t} + \frac{1}{2}\sigma^2 S^2 \frac{\partial^2 V}{\partial S^2} + \left(r - \widetilde{\delta}\right) S\frac{\partial V}{\partial S} - rV = 0, \qquad S > S_f(t), \quad 0 \leq t < T. \tag{4.2.3}$$

In the above, $T$ is the maturity (expiry) date of the option, $r$ is the interest rate, $\sigma$ is the volatility of the underlying asset and $K$ is the strike price. For a put option, the PDE satisfies the additional condition

$$V(S,t) \geq \max(K - S_f(t), 0), \qquad \text{for all } 0 \leq t \leq T, \quad S \geq 0.$$

This additional inequality follows from an arbitrage argument and the early exercise possibility of the option. For numerical applications, we set $\tau = T - t$ to transform the backward formulation (4.2.1)-(4.2.2) to a forward equation formulation. In other words, we reformulate the final boundary value problem as an initial boundary value problem.

Having already applied the spectral decomposition method to the Black-Scholes equation in Chapter 3, we consider the discretization from section 3.3 for solving problem (4.2.1)-(4.2.2). To this end, we consider the semi-discrete equation

$$\dot{V} = AV, \tag{4.2.4}$$

where $V$ is the vector

$$V = \left(V_0^{\vartheta}, \ldots, V_N^{\vartheta}, V_0^{\chi}, \ldots, V_N^{\chi}\right),$$

and

$$A = B + C - rI,$$

where $I$ is the identity, $B$ and $C$ are block diagonal matrices of $B^{\vartheta,\chi}$ and $C^{\vartheta,\chi}$, respectively obtained in section 3.3. After the discretization, the resulting ODE is solved using Laplace method as discussed in the next section.

## 4.3 Application of Laplace transform method to solve the semi-discrete problem

In this section, we consider the Laplace transform for integrating the parabolic problem (4.2.4) with an initial condition $V_0$ and where $A$ represents a parabolic operator with its eigenvalues located in a region $\Sigma_\delta = \{z \in \mathbb{C} : |\arg(z)| < \delta, z \neq 0\}$, for some $\delta \in (0, \pi/2)$. Furthermore, the resolvent $(zI - A)^{-1}$ of $A$ satisfies

$$\|(zI - A)^{-1}\| \leq \frac{C}{1 + |z|}, \quad \text{for } z \in \mathbb{C} \setminus \Sigma_\delta,$$

for some constant $C > 0$ independent of $z$. Note that, this implies that the function $V$ admits an holomorphic and bounded extension to a region containing $t \geq 0$, a familiar situation arising for example in the context of parabolic problems.

A direct application of the Laplace transform to (4.2.4) leads to

$$(zI - A)\widehat{V} = V_0, \tag{4.3.1}$$



where $I$ is the identity matrix and $\widehat{V}$ the Laplace transform of $V(\cdot, t)$ defined by

$$\widehat{V}(\cdot, z) = \int_0^\infty V(\cdot, t) e^{-zt} dt. \tag{4.3.2}$$

The inverse is evaluated on a contour $\Gamma$ known as the Bromwich contour and is given by

$$V(\cdot, t) = \frac{1}{2\pi i} \int_\Gamma e^{zt} \widehat{V}(\cdot, z) dz, \quad t > 0. \tag{4.3.3}$$

The contour $\Gamma$ is chosen such that it encloses all the singularities of $\widehat{V}(., z)$.

Our numerical methods for inverting the Laplace transform is based on the method developed by Talbot [125] and uses the deformation of the Bromwich contour. The integral is then evaluated using the trapezoidal rule. Talbot's idea was to deform the Bromwich line into a contour which starts and ends in the left half-plane. Such a

deformation of the contour is possible by the Cauchy's integral theorem [123]. This theorem is applicable provided that all singularities of the transformed function $\widehat{V}(\cdot, z)$ are contained in the interior of the new contour and that $\left|\widehat{V}(\cdot, z)\right| \to 0$ as $|z| \to \infty$ in the half-plane [138]. Such contours are used in [93, 125, 138] all of which are of the form

$$z = z(\ell), \quad -\infty < \ell < \infty,$$

with the property that $\operatorname{Re} z \to -\infty$ as $\ell \to \pm\infty$.

The efficiency of the Talbot approach depends on the choice of the contour, as well as the number of function evaluations in the trapezoidal rule. Simpler contours such as hyperbolas and parabolas are proposed in [93, 138]. These contours display better convergence rate than the original cotangent contour used by Talbot. In this chapter, we consider the hyperbola as the integration contour defined by

$$z(\ell) = \widetilde{\mu}\left(1 + \sin\left(i\ell - \alpha\right)\right), \quad \ell \in \mathbb{R}, \tag{4.3.4}$$



where the real parameters $\widetilde{\mu} > 0$ and $0 < \alpha < \pi/2$ determine the geometry of the contour. The positive parameter $\widetilde{\mu}$ controls the width of the contour while $\alpha$ determines its geometric shape, i.e., the asymptotic angle. On the contour (4.3.4) the inversion formula (4.3.3) can be rewritten as

$$V(\cdot, t) = \frac{1}{2\pi i}\int_{-\infty}^{\infty} e^{z(\ell)t}\widehat{V}\left(\cdot, z(\ell)\right) z'(\ell) d\ell, \tag{4.3.5}$$

where

$$z'(\ell) = \widetilde{\mu} i \cos\left(i\ell - \alpha\right).$$

For $h > 0$ such that $\ell_k = kh$, where $k$ is an integer, the trapezoidal rule yields

$$V(\cdot, t) \approx \frac{h}{2\pi i}\sum_{k=-\infty}^{\infty} e^{z(\ell_k)t}\widehat{V}\left(\cdot, z(\ell_k)\right) z'(\ell_k). \tag{4.3.6}$$

In practice, the infinite sum has to be truncated at a finite integer $M$, in which case one

commits a truncation error as discussed below. Note that, because of the symmetry of the contour (4.3.4), (4.3.6) can be rewritten as

$$V_M(\cdot,t) \approx \mathrm{Re}\left\{ \frac{h}{\pi i} \sum_{k=0}^{M} {}^{\circ} e^{z(\ell_k)t} \widehat{V}\left(\cdot, z(\ell_k)\right) z'(\ell_k) \right\}, \tag{4.3.7}$$

where $^{\circ}$ indicates that the first term is divided by 2. The benefit of using (4.3.7) is that it reduces by half the summation (4.3.6) and subsequently the number of linear system to be evaluated in (4.3.1).

From (1.3.19), we observe that the optimal contour parameter depends on time $t$. This means the evaluation of $V(\cdot,t)$ in (4.3.7) is carried out on different contour for each $t$ [138, 93]. For instance, to compute $V(\cdot,t)$ for each $t_j$, a new set of transforms $\widehat{V}(\cdot,z_\ell)$, for $\ell = 0,1,...,M$ in (4.3.1) is computed on different contours. This in turn involve significant amount of work and there solving of matrix problem such as (4.3.7) can be inefficient and computationally expensive. To overcome this drawback, note that the same evaluation of $\widehat{V}(\cdot,z_\ell)$ for $\ell = 0,1,..,M$ can be used in (4.3.7) at different $t$. The transform $\widehat{V}(\cdot,z_\ell)$ can be computed once for the set of nodes for $z_\ell$, $\ell = 0,1,...,M$ and then they are used to reconstruct the solution $V(\cdot,t)$ for any $t_1 \le t \le t_\ell$. In view of the problem that we are solving in this chapter, we discuss this topic in the next subsection.



### 4.3.1 Derivation of the optimal contour parameters

In this subsection we derive optimal parameters of the contour (4.3.4) when solving the American option pricing problem. To this end, we note that the computational effort in the evaluation of $V_M(\cdot,t)$ in (4.3.6) comes from the evaluation of the Laplace transform in (4.3.1) for each $z(\ell_k)$. Furthermore, we note that the evaluation of $\widehat{V}(\cdot,t)$ in (4.3.1) is independent of time $t$ and thus can be carried out once and subsequently use the same evaluation to approximate $V_M(\cdot,t)$ at different time level over an interval $[t_0, \Lambda t_0]$ for an integer $\Lambda$. Note that, various methods for finding an optimal contour

were developed in [93, 138]. In [138], the following convergence estimate for the family of hyperbolic contours (4.3.4) were derived

$$E_d = \mathcal{O}(e^{-2\pi(\pi/2-\alpha)/h}), \quad E_{-d} = \mathcal{O}(e^{\widetilde{\mu}t-2\pi\alpha/h}), \quad h \to 0. \tag{4.3.8}$$

Therefore, the total discretization error on the strip $(-d, d)$, denoted by $E_r$, is given by

$$E_r = E_d + E_{-d}.$$

Moreover, the truncation error that we found satisfies

$$E_t = \mathcal{O}(e^{\widetilde{\mu}t(1-\sin\alpha\cosh(hM))}), \quad M \to \infty. \tag{4.3.9}$$

To obtain an optimal contour parameter, we argue as follows: first note that only the second equation in (4.3.8) and the equation (4.3.9) are time dependent. On one hand, the error $E_t$ decreases when $t$ increases and thus is maximum at $t_0$. To see this, we consider $\alpha \in (\pi/4, \pi/2)$ which implies that the inequality $1/\sqrt{2} < \sin\alpha < 1$ holds. For $M \to \infty$, multiplication of both side of the inequality by $\cosh(hM)$ yields

$$\frac{\cosh(hM)}{\sqrt{2}} < \sin\alpha\cosh(hM) < \cosh(hM).$$

Since $\cosh(hM)/\sqrt{2} > 1$ for sufficiently large $M$, we get

$$1 - \sin\alpha\cosh(hM) < 0 \quad \text{for a fixed } h \neq 0 \quad \text{and} \quad M \to \infty.$$

On the other hand, the discretization error $E_{-d}$ increases with $t$, and attains its maximum at $t = \Lambda t_0$.

To estimate the optimal parameters on the contour $[t_0, \Lambda t_0]$, an asymptotic balance of the three errors at their maximum, i.e., $E_t$, $E_d$, $E_{-d}$ is required. To this end, we set

$$-2\pi\left(\pi/2-\alpha\right)/h = \widetilde{\mu}\Lambda t_0 - 2\pi\alpha/h = \widetilde{\mu}t_0\left(1-\sin\alpha\cosh(hM)\right). \tag{4.3.10}$$

We solve these equations for $\widetilde{\mu}$ and $h$. From the first equation we have

$$\widetilde{\mu}h = \frac{4\alpha\pi - \pi^2}{\Lambda t_0}. \tag{4.3.11}$$

The last equation in (4.3.10) together with (4.3.11) yields

$$\cosh(hM) = \frac{(\pi - 2\alpha)\,\Lambda - \pi + 4\alpha}{(4\alpha - \pi)\sin\alpha},$$

From this it follows that

$$A(\alpha) = hM = \cosh^{-1}\left(\frac{(\pi - 2\alpha)\,\Lambda - \pi + 4\alpha}{(4\alpha - \pi)\sin\alpha}\right). \tag{4.3.12}$$

Therefore, we obtain

$$h = \frac{A(\alpha)}{M} \tag{4.3.13}$$

and

$$\widetilde{\mu} = \frac{4\alpha\pi - \pi^2}{h\Lambda t_0} = \frac{4\alpha\pi - \pi^2}{A(\alpha)}\frac{M}{\Lambda t_0}. \tag{4.3.14}$$



The contour parameters (4.3.13) and (4.3.14) are fixed and time independent. As a result, the corresponding contour (4.3.4) is also fixed over the interval $[t_0, \Lambda t_0]$. From the parameters derived above, the error is

$$E_M = \mathcal{O}(e^{-B(\alpha)M}), \tag{4.3.15}$$

where

$$B(\alpha) = \frac{\pi^2 - 2\pi\alpha}{\cosh^{-1}\left(\frac{(\pi-2\alpha)\Lambda+4\alpha-\pi}{(4\alpha-\pi)\sin\alpha}\right)}. \tag{4.3.16}$$

The optimal error is obtained when $B(\alpha)$ attains its maximum for each value of $\Lambda$. In our computations, we choose $\Lambda = 50$ and obtained optimal parameters as listed in Table 4.3.1. To obtain the solution for the American option pricing problem, we use the updating procedure which we discuss below.

Table 4.3.1: Optimal parameters of the contour (4.3.4) for $\Lambda = 50$.

| $\Lambda$ | $\alpha$ | $A(\alpha)$ | $\mu\Lambda t_0/M$ | $B(\alpha)$ |
|---|---|---|---|---|
| 50 | 0.9381 | 5.5582 | 0.3452 | 0.7152 |

## Updating procedure for American options

In this section we describe the updating procedure to compute the American option from its European counterpart. We know that American options valuation can be treated as a moving boundary value problem and require solving the unknown free boundary $S_f$ simultaneously with the option $V(S,\tau)$. In this chapter we follow on the work from [67], where instead of solving the free boundary problem, the valuation of the American put options is carried out using the updating procedure. To this end, the authors in [67] solved the following problem

$$\left.\begin{aligned} \frac{\partial V}{\partial \tau} &= \frac{1}{2}\sigma^2 S^2 \frac{\partial^2 V}{\partial S^2} + rS\frac{\partial V}{\partial S} - rV, && S > S_f(\tau), \\ V(S,\tau) &= \max\{V(S,\tau), V(S,0)\}, && S < S_f(\tau). \end{aligned}\right\} \tag{4.3.17}$$

The region $S < S_f(\tau)$ corresponds to where the American options need to be exercised to attain an optimal value $V(S,\tau)$. The difficulty associated with solving (4.3.17) is related to the location of the unknown free boundary $S_f(\tau)$. However, to satisfy this early optimal exercise for the valuation of the American put option, we simply update the solution of the corresponding European put option at each time level as

$$V = \max\{V, K - S\}. \tag{4.3.18}$$

This makes the valuation of the American options relatively simple. Note that from the physical point of view, the difference between pricing the American options and the European options is that the propagation process has an effect of moving the unknown free boundary $S_f(\tau)$. This places an additional restriction at any time $\tau$ on the solution

that its value must be at least $V(S,0) = K - S$.

## 4.4 Numerical results

In this section, we illustrate the performance of the inverse Laplace transform with updating (ILTU) procedure and the spectral domain decomposition method (SDDM) for solving the American option pricing problem (4.2.1)-(4.2.2). We also evaluate the $\Delta$ and $\Gamma$ of this option.

To apply the SDDM, we split the domain into two sub-domains consisting of equal number of grid points, with the domain boundary placed at the strike price $K$ where the initial condition is non-smooth. For numerical illustration of our approach, as a reference solution of the American option pricing, we use the fast and rapidly convergent Fast Fourier transform method for Lévy process (FFT) [78] using a very large number of point. In Tables 4.4.1 and 4.4.2, we present the values of the American put option obtained by using our ILTU approach and those obtained in [129] by using the operator splitting method (OS), and the optimal compact algorithm (OCA). The first column gives the values of the asset price $S$, whereas the second column contains the reference solution. In Table 4.4.1, we present the results for American options on a non-dividend paying asset whereas those obtained on a dividend paying assets (with dividend rate $\widetilde{\delta}$ as 0.05) are presented in Table 4.4.2. The other parameters used in the simulations are $T = 0.25$; $K = 100$; $r = 0.05$; $\sigma = 0.20$; $S_{\max} = 3K$.



For numerical comparison, we compute the maximum absolute errors using the formula

$$\max_{\tau\in[0,T]} |V(\cdot,\tau) - V_M(\cdot,\tau)|, \tag{4.4.1}$$

where $V(\cdot,\tau)$ and $V_M(\cdot,\tau)$ represent the reference solution and the numerical solution, respectively, at time $\tau$. Here we consider the parameters: $T = 0.25$; $K = 100$; $r = 0.05$; $\sigma = 0.3$; $S_{\max} = 3K$. We show the performance of our method in Figure 4.4.1. In Figure 4.4.1 (left), we can observe the good agreement between the reference solution and the

numerical solution obtained by using our approach. This is further confirmed in Figure 4.4.1 (right) where we display the error on the log scale. From this figure, we observe that the error reaches its maximum around the strike price.

Note that the payoff given by

$$V(S,0) = \max(K - S, 0),$$

for put option, is an indicator to the option holder as to when he/she can potentially exercise the option. The option will be in-the-money if the payoff is greater than zero, that is if $K > S$. In Figure 4.4.1, the option is clearly in-the-money for all the values of $S$ from 1 to 100. As the option holder will never desire to lose money by exercising, an option will never have a value less than zero. If the option is out-of-money, the holder can only lose at most the premium. The more an option will be in-the-money, the greater will be the gain. If $S = K$, the option is at-the-money and if $K < S$, the option is out-of-the-money that is the case for values of $S$ after 100 up to $S_{\max}$.

To further corroborate the applicability of our approach, we also calculate the Greeks $\Delta$ and $\Gamma$ of the option. The Greeks measure the sensitivity of the option to its dependent parameters and variation in asset prices. The $\Delta$ is the ratio comparing the change in the underlying asset to the corresponding change in the price of the option, and $\Gamma$ measures the rate of change of $\Delta$ with respect to the asset price $S$.

In each sub-domain the $\Delta$ and $\Gamma$ are computed as

$$\left.\begin{aligned} \Delta^{\vartheta,\chi} &= \frac{2}{d^{\vartheta,\chi}} DV^{\vartheta,\chi}, \\ \Gamma^{\vartheta,\chi} &= \frac{2}{d^{\vartheta,\chi}} D\Delta^{\vartheta,\chi}. \end{aligned}\right\} \tag{4.4.2}$$

Figures 4.4.2 (left) and (right) show the values of $\Delta$ and $\Gamma$, respectively. We see that the $\Delta$ of the put is always negative, therefore the value of the put decreases when the asset price $S$ increases. Moreover, $\Gamma$ is positive and becomes zero when it is away from

$K$, but become more and more peaked at $K$ as is expected theoretically.

Table 4.4.1: Values of the American put options on a non-dividend paying asset using the OS (Operator Splitting), OCA (Optimal Compact Algorithm), and our ILTU approach.

| $S$ | Reference Solution | OS [129] | OCA [129] | ILTU |
|---|---|---|---|---|
| 80 | 20.0000 | 20.000 | 20.0000 | 20.0000 |
| 90 | 10.6660 | 10.6656 | 10.6660 | 10.6658 |
| 100 | 4.6556 | 4.6548 | 4.6555 | 4.6554 |
| 110 | 1.6680 | 1.6674 | 1.6679 | 1.6679 |
| 120 | 0.4976 | 0.4974 | 0.4975 | 0.4976 |

Table 4.4.2: Values of the American put options on a dividend paying asset using the OS (Operator Splitting), OCA (Optimal Compact Algorithm), and our ILTU approach.

| $S$ | Reference Solution | OS [129] | OCA [129] | ILTU |
|---|---|---|---|---|
| 80 | 20.2577 | 20.2579 | 20.2578 | 20.2576 |
| 90 | 12.5979 | 12.5977 | 12.5979 | 12.5981 |
| 100 | 7.2770 | 7.2766 | 7.2769 | 7.27690 |
| 110 | 3.9229 | 3.9225 | 3.9228 | 3.9231 |
| 120 | 1.9907 | 1.9904 | 1.9906 | 1.9901 |



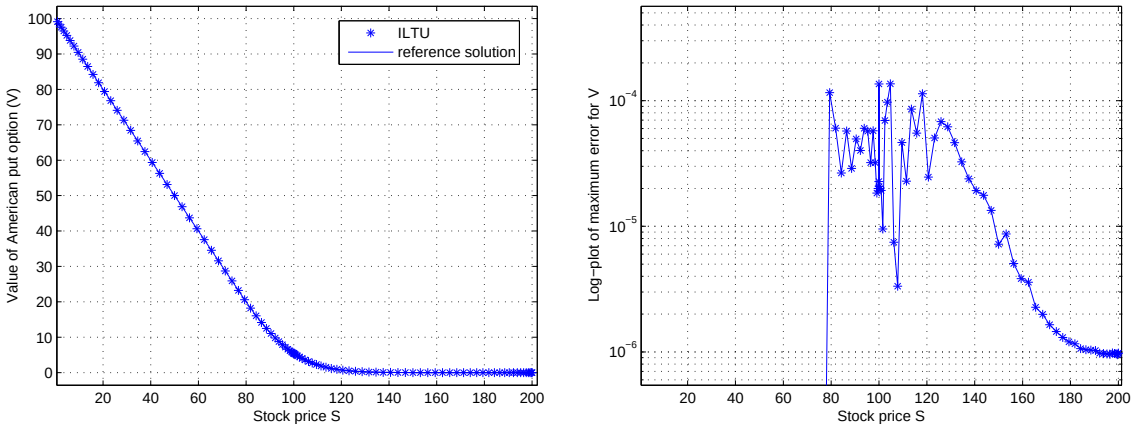


Figure 4.4.1: Left figure: Values of the American put option; Right figure: maximum errors using our ILTU approach using parameters $K = 100$; $\sigma = 0.3$; $r = 0.05$; $T = 0.25$; $S_{\max} = 3K$; and $N = 50$ in each of the two sub-domains.

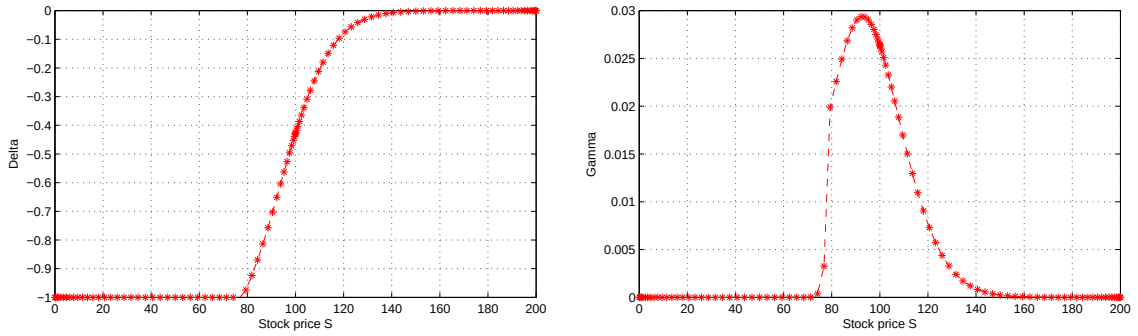


Figure 4.4.2: Results for $\Delta$ (left figure) and $\Gamma$ (right figure) obtained by using our ILTU approach using the parameters $K = 100$; $\sigma = 0.3$; $r = 0.05$; $T = 0.25$; $S_{\max} = 3K$; and $N = 50$ in each of the two sub-domains.

## 4.5 Summary and discussions

In this chapter, we have presented a new approach to price American options on a single asset. Our approach consisted of the spectral domain decomposition method (SDDM) as a spatial discretization method and the inverse Laplace transform with an updating procedure (ILTU) method as a time integrator.

The free boundary condition in the evaluation of the American option usually constitutes the major difficulty for solving this type of options. To avoid the computation of this unknown free boundary, we first solved the European put option using the Laplace transform method and then used an updating procedure to evaluate the American option. This makes the valuation of the American option easy to implement. As can be seen from Figures 4.4.1 and 4.4.2, the proposed approach gave very accurate results of the solution and that of the Greeks $\Delta$ and $\Gamma$. We also noticed that the SDDM gave very accurate results and therefore in next chapter, we extend this approach to solve a jump-diffusion model for pricing European options.

# Chapter 5

# Contour integral method for pricing European options with jumps



In this chapter, we develop an efficient method for pricing European options with jump on a single asset. Our approach is based on the combination of two powerful numerical methods, the spectral domain decomposition method and the Laplace transform method. The domain decomposition method, divides the original domain into sub-domains where the solution is approximated by using piecewise high order rational interpolants on a Chebyshev grid points. This set of points are suitable for the approximation of the convolution integral using Gauss-Legendre quadrature method. The resulting discrete problem is solved by the numerical inverse Laplace transform using the Bromwich contour integral approach. Through rigorous error analysis, we determine the optimal contour on which the integral is evaluated. The numerical results obtained are compared with those obtained from conventional methods such as Crank-Nicholson and finite difference. The new approach exhibits spectrally accurate results for the evaluation of options and associated Greeks. The proposed method is very efficient in the sense that we can achieve higher order accuracy on a coarse grid, whereas traditional methods would required significantly more time-steps and large number of grid points.

## 5.1 Introduction

In a general framework of the Black-Scholes model, the underlying stock price asset follows a geometric Brownian motion process and has a continuous sample path defined by

$$\frac{dS}{S} = \mu dt + \sigma dW_t. \tag{5.1.1}$$

Here $S$ represents the underlying stock price at time $t$. It is assumed that the associated sample path is continuous. The constants $\mu$ and $\sigma$ represent the expected return on the stock and the volatility of the return respectively; $dW_t$ is the standard Brownian motion or a Wiener process. The Black-Scholes model predicts that the stock price $S$ follows a log-normal distribution at any future time $t$, i.e.,

$$S(t) = S_0 e^{\left(\left(\mu - \frac{\sigma^2}{2}\right)t + \sigma W_t\right)}.$$

The continuity of the sample path indicates that the stock price can only change by a small amount in a short interval. However, the reality on the stock market is different. Jumps are regularly observed in the discrete movement of the stock price $S(t)$. This movement cannot be capture by the log-normal distribution characteristic of the stock price in the Black-Scholes setting and therefore an alternative model which addresses this shortcoming is necessary.

A number of models have been proposed in the literature that more appropriately describe the movement of the stock price in the market. Among these, the jump-diffusion model proposed in [100] by Merton is one of the most widely used model. In this framework, the Brownian motion observed in the Black-Scholes model is combined with a poisson distribution which model the jump discontinuities that normally occur on the market place. For the jump-diffusion model, the movement of the stock price is therefore modeled by the following stochastic differential equation (SDE)

$$\frac{dS}{S} = (\mu - \lambda\kappa)dt + \sigma dW_t + dq. \tag{5.1.2}$$

As in the previous model, $\sigma$ represents the volatility, $\mu$ is the instantaneous expected return on the stock, and $\lambda$ is the intensity of the poisson precess (or the jump arrival rate), $dW_t$ is the increment of the Brownian motion process, $\kappa = E(\eta - 1)$, where $E$ is the expectation and $\eta - 1$ is the impulse producing the jump from $S$ to $S\eta$ if a Poisson event occurs and $dq$ is the independent Poisson process defined by

$$dq = \begin{cases} 0 & \text{with probability} \quad 1 - \lambda dt, \\ 1 & \text{with probability} \quad \lambda dt. \end{cases}$$

Using the Itô formula, we rewrite the SDE (5.1.2) as the following partial integro-differential equation (PIDE):

$$\frac{\partial V}{\partial t} = \frac{1}{2}\sigma^2 S^2 \frac{\partial^2 V}{\partial S^2} + (r - \lambda\kappa)S\frac{\partial V}{\partial S} - (r + \lambda)V + \lambda \int_0^\infty V(S\eta)\psi(\eta)d\eta. \tag{5.1.3}$$

In the above, $V(S, t)$ is the value of the option depending on the underlying stock price $S$ at any given time $t$, $T$ is the expiry date, $r$ is the risk-free interest rate ($r \geq 0$), $\lambda$ is the intensity of the Poisson process ($\lambda > 0$), $\kappa$ is the expected jump size, $t$ is the current time, $\psi(\eta)$ is the probability function of the jump amplitude $\eta$, where $\psi(\eta) \geq 0$, for all $\eta$, and is defined by

$$\psi(\eta) = \frac{e^{-\frac{(\log\eta - \mu)^2}{2\gamma^2}}}{\sqrt{2\pi}\gamma\eta}. \tag{5.1.4}$$

Note that $\int_0^\infty \psi(\eta)d\eta = 1$, and when $\lambda = 0$ in (5.1.3), we recover the standard Black-Scholes partial differential equation.

For European options, Merton [100] derived formula for European call and put but for most exotic options under jump-diffusion models, no closed-form solutions exist and one needs to find numerical solutions for the partial integro-differential equations that arise. However, the convolution integral in (5.1.3) add to the difficulty of finding efficient numerical solutions. Commonly used finite difference methods (FDMs) hardly attain higher order accuracy [3]. Typical quadrature rules such as the trapezoidal and Simpson's rules are of low order accurate as compared to Gaussian quadrature method.

However, the later is expensive to implement since it requires the interpolation to match the Chebyshev grid point with those of the FDMs. To reduce the computational cost in solving the convolution integral term, Fast Fourier Transform (FFT) was used in [3, 150].

Tangman *et al.* [126] proposed a different approach in combining the central difference method and the exponential time differencing (ETD) scheme to solve (5.1.3). The ETD method was proved as very effective and gave second order accuracy.

Spectral method are attractive for their exponential convergence rate. This presents an advantage for a direct computation of the convolution integral by a high order Gauss quadrature method. However the high rate of convergence of the spectral method is only guaranteed for smooth solution, a condition which is not fulfilled for the jump-diffusion model (5.1.3) which has a non-smooth initial condition.

To overcome this situation, one might consider using a spectral element approach. This is the approach followed in [148] where the PIDE (5.1.3) is solved and the resulting discrete ODE is integrated in time by the Crank-Nicholson method. This resulted in spectrally accurate results in space and second order accuracy in time. The exponential results are partly due to the successful approximation of the integral term by Gauss quadrature rule. However, the application of the spectral element involved successive approximation of different integrals generated by the weak form and hence computationally expensive.



In this chapter, we propose the use of a multi-domain spectral method. This method uses the spectral method directly in each sub-domains. Matching conditions are imposed to ensure the continuity of the solution and that of its first derivative. After this spatial discretization, the resulting system of ODEs is solved by the Laplace transformation. To recover the solution, an inversion of the Laplace transform solution is then performed using the Talbot's method [125] which is based on the application of trapezoidal rule to approximate a Bromwich integral.

The rest of this chapter is organized as follows. In Section 5.2, we give a description of the jump-diffusion model and derive formula for the resolution of the convolution

integral. In Section 5.3, we describe the spectral domain decomposition method for the differential part as well as the integral part. The later is computed by the Gauss-Legendre quadrature. Section 5.4 deals with the application of the Laplace transform to solve the semi-discrete problem. Section 5.5 contains the numerical results of our approach with more conventional methods such as Crank-Nicholson for time integration and finite difference for space discretization. Summary and conclusion are given in Section 5.6.

## 5.2 Description of the model problem

We consider the PIDE (5.1.3) and apply the change of the variable $s = \log(S/K)$ and $\eta = e^y$. This gives

$$\frac{\partial V}{\partial t} = \frac{1}{2}\sigma^2\frac{\partial^2 V}{\partial s^2} + \left(r - \lambda\kappa - \frac{\sigma^2}{2}\right)\frac{\partial V}{\partial s} - (r+\lambda)V + \lambda\int_{-\infty}^{\infty} V(s+y)\widetilde{\psi}(y)dy. \quad (5.2.1)$$

In the above, $V(s+y) \equiv V(t, s+y)$, i.e., $V$ is a function of $t$ and variables $s$ and $y$, with $s \in (-\infty, \infty)$ and $\sigma > 0$ is the volatility, $r \geq 0$ is the risk-free interest rate, $\lambda > 0$ is the intensity of the Poisson process (or the jump). The jump probability density function is

$$\widetilde{\psi}(y) = \frac{e^{-\frac{(y-\mu)^2}{2\gamma^2}}}{\sqrt{2\pi}\gamma},$$

while the expected jump size $\kappa$ is

$$\kappa = e^{\mu+\frac{\gamma^2}{2}} - 1.$$

Let $\Omega = [s_{\min}, s_{\max}]$ be the truncated interval and $\Omega^c = \mathbb{R}\backslash[s_{\min}, s_{\max}]$ its complement in $\mathbb{R}$. To facilitate the computation of the integral part, we note that

$$\begin{aligned}\int_{-\infty}^{\infty} V(y)\widetilde{\psi}(y-s)dy &= \int_{-\infty}^{\infty} V(s+y)\widetilde{\psi}(y)dy,\\ &= \int_{-s_{\min}}^{s_{\max}} V(s+y)\widetilde{\psi}(y)dy + \int_{\Omega^c} V(s+y)\widetilde{\psi}(y)dy,\end{aligned}$$

where

$$\int_{\Omega^c} V(s+y)\widetilde{\psi}(y)dy = \int_{-\infty}^{s_{\min}} V(s+y)\widetilde{\psi}(y)dy + \int_{s_{\max}}^{\infty} V(s+y)\widetilde{\psi}(y)dy. \tag{5.2.2}$$

For a European style put option, the boundary condition

$$V(0,t) = Ke^{-rt} \quad \text{is changed to} \quad V(s,t) = Ke^{-rt}, \quad s \to -\infty, \tag{5.2.3}$$

and

$$V(S,t) = 0, \quad S \to \infty \quad \text{becomes} \quad V(s,t) = 0, \qquad s \to \infty. \tag{5.2.4}$$



Using these boundary conditions, and setting $w = (y - s - \mu)/\sigma$ so that $dw = dy/\sigma$, we obtain the following outer integral from (5.2.2):

$$\begin{aligned}\int_{\Omega^c} V(s+y)\widetilde{\psi}(y)dy &= \int_{-\infty}^{s_{\min}} V(s+y)\widetilde{\psi}(y)dy\\ &= Ke^{-rt}\int_{-\infty}^{s_{\min}} \frac{e^{-\frac{(y-s-\mu)^2}{2\sigma^2}}}{\sqrt{2\pi}\sigma}dy\\ &= Ke^{-rt}\int_{-\infty}^{\frac{s_{\min}-s-\mu}{\sigma}} \frac{e^{-\frac{w}{2}}}{\sqrt{2\pi}}dw\\ &= Ke^{-rt}\Phi\left(\frac{s_{\min}-s-\mu}{\sigma}\right),\end{aligned}$$

where $\Phi(\cdot)$ is the normal cumulative distribution function.

For a European style call option, we observe that boundary condition

$$V(0,t) = 0 \quad \text{is changed to} \quad V(s,t) = 0, \quad s \to -\infty, \tag{5.2.5}$$

and

$$V(S,t) \to S - Ke^{-rt}, \quad S \to \infty \quad \text{becomes} \quad V(s,t) \to Ke^{s} - Ke^{-rt}, \quad s \to \infty. \tag{5.2.6}$$

Again setting $w = (y - s - \mu)/\sigma$ and $dw = dy/\sigma$, the outer integral in (5.2.2) leads to

$$\begin{aligned}
\int_{\Omega^c} V(s+y)\widetilde{\psi}(y)dy &= K\int_{s_{\max}}^{\infty} e^{y}\widetilde{\psi}(y-s)dy - Ke^{-rt}\int_{s_{\max}}^{\infty}\widetilde{\psi}(y-s)dy \\
&= K\int_{s_{\max}}^{\infty} e^{y}\frac{e^{-\frac{(y-s-\mu)^2}{2\sigma^2}}}{\sigma\sqrt{2\pi}}dy - Ke^{-rt}\int_{s_{\max}}^{\infty}\frac{e^{-\frac{(y-s-\mu)^2}{2\sigma^2}}}{\sigma\sqrt{2\pi}}dy \\
&= K\frac{e^{s+\mu}}{\sqrt{2\pi}}\int_{\frac{s_{\max}-s-\mu}{\sigma}}^{\infty} e^{-\frac{1}{2}(w-\sigma)^2+\frac{\sigma^2}{2}}dw - \frac{Ke^{-rt}}{\sqrt{2\pi}}\int_{\frac{s_{\max}-s-\mu}{\sigma}}^{\infty} e^{-\frac{w^2}{2}}dw \\
&= K\frac{e^{s+\mu+\frac{\sigma^2}{2}}}{\sqrt{2\pi}}\int_{\frac{s_{\max}-s-\mu}{\sigma}-\sigma}^{\infty} e^{-\frac{w^2}{2}}dw - \frac{Ke^{-rt}}{\sqrt{2\pi}}\int_{\frac{s_{\max}-s-\mu}{\sigma}}^{\infty} e^{-\frac{w^2}{2}}dw \\
&= K\frac{e^{s+\mu+\frac{\sigma^2}{2}}}{\sqrt{2\pi}}\int_{-\infty}^{\frac{s-s_{\max}+\mu+\sigma^2}{\sigma}} e^{-\frac{w^2}{2}}dw - \frac{Ke^{-rt}}{\sqrt{2\pi}}\int_{-\infty}^{\frac{s-s_{\max}+\mu}{\sigma}} e^{-\frac{w^2}{2}}dw \\
&= Ke^{s+\mu+\frac{\sigma^2}{2}}\Phi\left(\frac{s-s_{\max}+\mu+\sigma^2}{\sigma}\right) - Ke^{-rt}\Phi\left(\frac{s-s_{\max}+\mu}{\sigma}\right).
\end{aligned}$$

In the next section, we use the spectral domain decomposition method (SDDM) to discretize the jump-diffusion model (5.1.3).

## 5.3 Spectral discretization

As mentioned earlier, the spectral methods are often more efficient than finite difference and classical finite element methods. However, the exponential convergence rate of spectral method is strictly dependent on the smoothness of the unknown function. Option pricing problems involve PDEs with initial conditions that are non-smooth. Therefore, direct application of a spectral method to the solution of such equations usually lead to a low order approximation.

To resolved this problem, we propose the spectral domain decomposition method (SDDM). In the spectral domain decomposition approach, the domain $s \in [s_{\min}, s_{\max}]$ is divided into sub-domains. For the problem at hand, we need to divide the domain in two sub-domains, with the transition point as the strike price. To represent the solution in each sub-domain, we choose to approximate the solution by a linear rational interpolants for their improved stability properties compared to the polynomial interpolant [11, 130].



### 5.3.1 Spectral domain decomposition method based on rational interpolants

Domain decomposition is a discretization technique for solving differential equations whereby the computational domain is divided into a number of smaller sub-domains. The equation is then solved on each sub-domain with matching conditions enforced at the interface (or transition point $K$) to ensure the continuity of the solution and that of it first derivative across the sub-domains. In the context of spectral methods on an interval, this means that rather than using a single global polynomial on the entire domain, polynomials of different order may be used on each subinterval. However in this work, rather than using polynomial interpolants for spectral methods, we will consider the more stable linear rational interpolants. For further discussion on these types of interpolants, readers are referred to [11, 130].

**Rational interpolants**

Rational interpolants are more convenient for the problem at hands. The rational approximation of a function $u(\xi)$ at the Chebyshev points $\xi$, for $k = 0, 1, ..., N$, is given by

$$u_N(\xi) = \frac{\sum_{k=0}^{N} \frac{w_k}{\xi - \xi_k} u(\xi_k)}{\sum_{k=0}^{N} \frac{w_k}{\xi - \xi_k}}, \tag{5.3.1}$$

where $w_k$, for $k = 0, 1, ..., N$, are the barycentric weights defined as $w_0 = 1/2$, $w_N = (-1)^N/2$, and $w_k = (-1)^k$, $k = 1, ..., N-1$. The Chebyshev points are define as

$$\xi_k = \cos\left(\frac{k\pi}{N}\right), \qquad k = 0, 1, ..., N.$$

As for the spectral polynomial method, the $m^{th}$ order differentiation matrix associated with the rational interpolant (5.3.1) is given by



$$u_N^{(m)}(\xi_k) = \sum_{k=0}^{N} \frac{d^m}{d\xi^m} \left( \frac{\sum_{k=0}^{N} \frac{w_k}{\xi - \xi_k} u(\xi_k)}{\sum_{k=0}^{N} \frac{w_k}{\xi - \xi_k}} \right) \tag{5.3.2}$$

$$= \sum_{k=0}^{N} D_{jk}^{(m)} u(\xi_k), \tag{5.3.3}$$

where $D_{jk}^{(m)}$ are the entries of the differentiation matrix of order $m$. Formulae of the first and second order are given by (3.3.15) and (3.3.16), respectively.

We apply the rational interpolant along with the domain decomposition method (as described below) to solve the jump-diffusion call option (5.2.1), (5.2.5)-(5.2.6).

**Discretization of the jump-diffusion model**

We split the domain into two sub-domains at the point of discontinuity, and apply Chebyshev spatial discretization to reduce the problem to a set of coupled ordinary differential equations in time. Since the function is smooth on each subinterval including the point of discontinuity, a spectral accuracy can be regained provided that appropriate matching conditions are set across the point of discontinuity.

Since the initial condition is non-smooth at the strike price, we split the interval $[s_{\min}, s_{\max}]$ at 0 into two subintervals: $\vartheta = [s_{\min}, 0]$ and $\chi = [0, s_{\max}]$ of lengths $d^{\vartheta} = s_{\min}$ and $d^{\chi} = s_{\max}$, respectively. To apply the Chebyshev discretization, we map each subdomain to the reference element $[-1, 1]$ by the linear transformation

$$s^{\vartheta,\chi}(\xi) = \begin{cases} \frac{d^{\vartheta}}{2}(1-\xi), & s \in [s_{\min}, 0], \\ \\ \frac{d^{\chi}}{2}(\xi+1), & s \in [0, s_{\max}]. \end{cases} \tag{5.3.4}$$



The linear transformation to its derivative leads to

$$ds^{\vartheta,\chi}(\xi) = \begin{cases} -\frac{d^{\vartheta}}{2}d\xi, & s \in [s_{\min}, 0], \\ \\ \frac{d^{\chi}}{2}d\xi, & s \in [0, s_{\max}]. \end{cases} \tag{5.3.5}$$

Thus

$$\frac{\partial}{\partial s} \equiv \frac{\partial}{\partial \xi}\frac{\partial \xi}{\partial s} \equiv \begin{cases} -\frac{2}{d^{\vartheta}}\frac{\partial}{\partial \xi} & s \in [s_{\min}, 0], \\ \\ \frac{2}{d^{\chi}}\frac{\partial}{\partial \xi}, & s \in [0, s_{\max}]. \end{cases} \tag{5.3.6}$$

In the following, we use the spectral domain decomposition method to the model problem (5.2.1) subject to the boundaries (5.2.5)-(5.2.6). To keep the expressions simple, we first discretize the differential part of (5.2.1) and thereafter the integral part.

On each sub-domains $\vartheta$ and $\chi$, the differential part of (5.1.3) is discretized as

$$\frac{\partial V^{\vartheta}}{\partial \tau} = \frac{2}{(d^{\vartheta})^2}\sigma^2\frac{\partial^2 V^{\vartheta}}{\partial \xi^2} - \frac{2}{d^{\vartheta}}\left(r - \lambda\kappa - \frac{\sigma^2}{2}\right)\frac{\partial V^{\vartheta}}{\partial \xi} - (r+\lambda)V^{\vartheta}, \quad (5.3.7)$$

and

$$\frac{\partial V^{\vartheta}}{\partial \tau} = \frac{2}{(d^{\vartheta})^2}\sigma^2\frac{\partial^2 V^{\vartheta}}{\partial \xi^2} - \frac{2}{d^{\vartheta}}\left(r - \lambda\kappa - \frac{\sigma^2}{2}\right)\frac{\partial V^{\vartheta}}{\partial \xi} - (r+\lambda)V^{\vartheta}. \quad (5.3.8)$$

In matrix form, we have

$$\dot{V}^{\vartheta} = \frac{2}{(d^{\vartheta})^2}\sigma^2 D^{(2)}V^{\vartheta} - \frac{2}{d^{\vartheta}}\left(r - \lambda\kappa - \frac{\sigma^2}{2}\right)D^{(1)}V^{\vartheta} - (r+\lambda)\,V^{\vartheta}, \quad (5.3.9)$$

and

$$\dot{V}^{\chi} = \frac{2}{(d^{\chi})^2}\sigma^2 D^{(2)}V^{\chi} - \frac{2}{d^{\chi}}\left(r - \lambda\kappa - \frac{\sigma^2}{2}\right)D^{(2)}V^{\chi} - (r+\lambda)\,V^{\chi}. \quad (5.3.10)$$

Here $\dot{V}^{\vartheta,\chi}$ is the derivative of $V$ with respect to $\tau$ in the sub-domains $\vartheta$ and $\chi$, respectively. Note that the derivatives of the same order from both sub-domains would be different if rational interpolants of different order are chosen in each sub-domain.

The above equations imply

$$\dot{V}^{\vartheta,\chi} = B^{\vartheta,\chi}V^{\vartheta,\chi}, \quad (5.3.11)$$

where

$$B^{\vartheta,\chi} = \frac{2}{(d^{\vartheta,\chi})^2}\sigma^2 D^{(2)} - \frac{2}{d^{\vartheta,\chi}}\left(r - \lambda\kappa - \frac{\sigma^2}{2}\right)D^{(1)} - (r+\lambda)\,I^{\vartheta,\chi},$$

and $I^{\vartheta,\chi}$ is the $(N+1)\times(N+1)$ identity matrix.

Now we consider the approximation of the integral part in (5.1.3). We know that

for a call option the indefinite integral gives

$$\int_{-\infty}^{\infty} V(s+y)\widetilde{\psi}(y)dy = \int_{s_{\min}}^{s_{\max}} V(y)\widetilde{\psi}(y-s)dy + Ke^{s+\mu+\frac{\sigma^2}{2}}\Phi\left(\frac{s-s_{\max}+\mu+\sigma^2}{\sigma}\right)$$

$$-Ke^{-rt}\Phi\left(\frac{s-s_{\max}+\mu}{\sigma}\right). \tag{5.3.12}$$

Hence we need only to discretize the integral on the right of the equation. For simplicity, we consider the same number of grid points in each sub-domains $\vartheta$ and $\chi$. This gives

$$\int_{s_{\min}}^{s_{\max}} V(z)\widetilde{\psi}(z-s)dz = \int_{s_{\min}}^{0} V(z^{\vartheta})\widetilde{\psi}^{\vartheta}(z^{\vartheta}-s)dz + \int_{0}^{s_{\max}} V(z^{\chi})\widetilde{\psi}^{\chi}(z^{\chi}-s)dz$$

$$= H^{\vartheta} + H^{\chi}. \tag{5.3.13}$$

Mapping the two intervals $[S_{\min}, 0]$ and $[0, S_{\max}]$ to the standard element $[-1, 1]$ by the linear transformation



$$z^{\vartheta,\chi}(\xi) = \begin{cases} \frac{d^{\vartheta}}{2}(1-\xi), & z^{\vartheta} \in [s_{\min}, 0], \\ \\ \frac{d^{\chi}}{2}(\xi+1), & z^{\chi} \in [0, s_{\max}], \end{cases}$$

we obtain

$$H^{\vartheta} = -\frac{s_{\min}}{2}\int_{-1}^{1} V(z^{\vartheta})\widetilde{\psi}^{\vartheta}(z^{\vartheta}-s)dz^{\vartheta}, \tag{5.3.14}$$

and

$$H^{\chi} = \frac{s_{\max}}{2}\int_{-1}^{1} V(z^{\chi})\widetilde{\psi}^{\chi}(z^{\chi}-s)dz^{\chi}. \tag{5.3.15}$$

Finally since the grid points are Chebyshev, a well suited approximation method to evaluate integrals $H^{\vartheta}$ and $H^{\chi}$ is the Gauss-Legendre quadrature rule, which converges

geometrically ([132]). Making use of this rule in each sub-domain, the two terms on the right hand side of (5.3.13) given by (5.3.14) and (5.3.15) are approximated as

$$H^{\vartheta} = -\frac{s_{\min}}{2}\sum_{k=0}^{N} V(z^{\vartheta})\widetilde{\psi}^{\vartheta}(z^{\vartheta}-s)\varpi_k, \tag{5.3.16}$$

and

$$H^{\chi} = \frac{s_{\max}}{2}\sum_{k=0}^{N} V(z^{\chi})\widetilde{\psi}^{\chi}(z^{\chi}-s)\varpi_k, \tag{5.3.17}$$

where $\varpi_k$, for $k = 0, 1, ..., N$ denotes the Gauss-Legendre quadrature weights.

On the sub-domain $\vartheta$, the discretization of the differential and integral parts yields

$$\begin{aligned}\dot{V}^{\vartheta} &= \frac{2}{(d^{\vartheta})^2}\sigma^2 D^{(2)}V^{\vartheta} + \frac{2}{d^{\vartheta}}\left(r - \lambda\kappa - \frac{\sigma^2}{2}\right)D^{(1)}V^{\vartheta} \\ &\quad - (r+\lambda)V^{\vartheta} - \frac{s_{\min}}{2}\sum_{k=0}^{N} V(z^{\vartheta})\widetilde{\psi}^{\vartheta}(z^{\vartheta}-s)\varpi_k,\end{aligned} \tag{5.3.18}$$



whereas on the sub-domain $\chi$ we have

$$\begin{aligned}\dot{V}^{\chi} &= \frac{2}{(d^{\chi})^2}\sigma^2 D^{(2)}V^{\chi} - \frac{2}{d^{\chi}}\left(r - \lambda\kappa - \frac{\sigma^2}{2}\right)D^{(1)}V^{\chi} \\ &\quad - (r+\lambda)V^{\chi} + \frac{s_{\max}}{2}\sum_{k=0}^{N} V(z^{\chi})\widetilde{\psi}^{\chi}(z^{\chi}-s)\varpi_k.\end{aligned} \tag{5.3.19}$$

Upon simplification, (5.3.18) and (5.3.19) give

$$\dot{V}^{\vartheta} = B^{\vartheta}V^{\vartheta} + \lambda H^{\vartheta}V^{\vartheta}, \quad \text{and} \quad \dot{V}^{\chi} = B^{\chi}V^{\chi} + \lambda H^{\chi}V^{\chi}. \tag{5.3.20}$$

To impose the boundary conditions, we substitute the first and last equations from the first and second sub-domains, respectively, by the boundary conditions (5.2.3)-(5.2.4). Furthermore, to ensure the continuity of the solution and that of its first derivatives at the interface, we impose matching conditions across the point of discontinuity, i.e.,

at $s = 0$,

$$V^* = V_N^\vartheta = V_0^\chi,$$

and

$$\frac{\partial V_N^\vartheta}{\partial \xi} = \frac{\partial V_0^\chi}{\partial \xi}.$$

The first matching condition leads to

$$2\dot{V}^* = \left[\left(B^\vartheta + \lambda H^\vartheta\right) V^\vartheta\right]_N + \left[\left(B^\chi + \lambda H^\chi\right) V^\chi\right]_0. \tag{5.3.21}$$

From the second condition above we have

$$\frac{2}{d^\vartheta}\left(D^{(1)} V^\vartheta\right)_N - \frac{2}{d^\chi}\left(D^{(1)} V^\chi\right)_0 = 0. \tag{5.3.22}$$

Finally, the discrete approximation of the jump-diffusion model (5.2.1) is obtained by combining the approximations from the two sub-domains with boundary and matching conditions included into a global system. This gives



$$\dot{V} = (B + \lambda H)V + \epsilon_1(s) - \epsilon_2(s)e^{-r\tau}, \tag{5.3.23}$$

where $V$ is the vector

$$V = \left[V_0^\vartheta, \ldots, V_N^\vartheta, V_0^\chi, \ldots, V_N^\chi\right],$$

$B$, $H$ are block matrices of $B^{\vartheta,\chi}$ and $H^{\vartheta,\chi}$ respectively; and

$$\epsilon_1(s) = \lambda K e^{s+\mu+\frac{\sigma^2}{2}} \Phi\left(\frac{s - s_{\max} + \mu + \sigma^2}{\sigma}\right),$$

and

$$\epsilon_2(s) = \lambda K e^{-rt} \Phi\left(\frac{s - s_{\max} + \mu}{\sigma}\right).$$

After this discretization, the resulting system of ODEs is solved by using the Laplace transform approach which we discuss in the next section.

## 5.4 Application of Laplace transform method to the jump-diffusion model

In the Laplace domain, equation (5.3.23) becomes

$$z\widehat{V} - V_0 = (B + \lambda H)\widehat{V} + \frac{\epsilon_1(s)}{z} - \frac{\epsilon_2(s)}{z+r}, \tag{5.4.1}$$

where $\widehat{V}$ is the unknown solution in this domain. The boundary conditions are given as

$$\left.\begin{aligned} \widehat{V}(0,z) &= 0, \\ \widehat{V}(s_{\max},z) &= \tfrac{Ke^{s_{\max}}}{z} - \tfrac{K}{z+r}. \end{aligned}\right\} \tag{5.4.2}$$

From (5.4.1), we deduce

$$[zI - (B + \lambda H)]\widehat{V} = V_0 + \frac{\epsilon_1(s)}{z} - \frac{\epsilon_2(s)}{z+r}. \tag{5.4.3}$$



Application of the inversion formula (4.3.5) yields

$$V(t) = \frac{h}{2\pi i}\int_{-\infty}^{\infty} e^{z(\ell)t}\widehat{V}z'(\ell)d\ell. \tag{5.4.4}$$

Using the trapezoidal rule (4.3.6) truncated at $M$ and the symmetry of the contour (1.2.5), we obtain the value of the option as

$$V_M(t) = \mathrm{Re}\left\{\frac{h}{\pi}\sum_{k=0}^{M}{}^{\circ} e^{z_k t}\widehat{V}_k z_k'\right\}, \tag{5.4.5}$$

where $^{\circ}$ indicates that the first term is divided by 2 and the vector $\widehat{V}_k$ is solved for each $k$ as

$$\widehat{V}_k = [z_k I - (B + \lambda H)]^{-1}\left(V_0 + \frac{\epsilon_1(s)}{z_k} - \frac{\epsilon_2(s)}{z_k + r}\right), \quad k = 0, 1, ..., M. \tag{5.4.6}$$

In the next section, we present some numerical results illustrating the proposed method.

## 5.5 Numerical results

In this section we illustrate the performance of our Laplace inversion method (ILT) and the spectral domain decomposition method (SDDM) in solving the European jump-diffusion model. We also evaluate the $\Delta$ and $\Gamma$ of this option.

To apply the SDDM, we split the domain into two sub-domains consisting of equal number of grid points, with the domain boundary placed at 0 where the initial condition is non-smooth. For numerical illustration of our approach, we consider the European jump-diffusion model with the following parameters $K = 10$; $\sigma = 0.2$; $\lambda = 0.1$; $\gamma = 0.3$; $\mu = 0$; $r = 0.02$; $T = 0.25$ and truncated domain $s_{\min} = -3$ and $s_{\max} = 1.5$.

For numerical comparison, we consider the computational time and the maximum absolute errors which is calculated using the formula

$$\max_{t\in[0,T]} |V(t) - V_N(t)|, \tag{5.5.1}$$



where $V(t)$ is the analytical solution and $V_N(t)$ is the numerical solution at time $t$.

Though the number of contour points may vary with the problem at hand, for the European option, we carry out different simulations by keeping the number of grid points $N$ fixed and varying the number of points on the contour. For different value of $N$, we found that the optimal number of contour grid points varies from 20 to 30.

Table 5.5.1 displays the numerical results obtained by using the Crank-Nicholson (CN) and the ILT method for time integration and the Finite difference method (FDM) for spatial discretization. The numerical results obtained by using CN and ILT methods for time integration and SDDM for spatial discretization are presented in Table 5.5.2. The computations are performed for the same set of parameters except that different grids are used for the comparison purpose. The ILT method is clearly more accurate than the CN for both the finite difference and spectral domain decomposition

discretizations. For example, for 180 grid points we get an order of accuracy of $10^{-3}$ in 0.144 second and 150 time step using CN, whereas we obtain an order of accuracy of $10^{-4}$ in 0.061 second and 20 contour points using the ILT method in Table 5.5.1. Table 5.5.2 displays improve results compared to those from Table 5.5.1 for both ILT and CN methods as the number of spatial points is significantly fewer for the SDDM method to get the same level of accuracy than FDM. This illustrates the superiority of the SDDM over FDM.

Tables 5.5.1 and 5.5.2 also show the computational time taken by both approaches. We see that the ILT and SDDM methods are faster than the CN and FDM methods respectively. Furthermore, from Table 5.5.2 we note that despite computing block matrices in the SDDM as opposed to the computation of sparse matrices in the FDM discretization, the advantage of the SDDM is that the number of grid points $N$ is usually smaller to achieve higher order at a faster speed.

In Figure 5.5.1 (left) we have plotted the numerical and exact solution of the European jump-diffusion problem. To illustrate the effect of the jump, we also plotted the solution of the Black-Scholes equation without jump. Figure 5.5.1 (right) shows the graphical accuracy of the numerical solution for $N = 50$ in each sub-domains.



Figures 5.5.2 (left) and 5.5.3 (left) show the numerical values of $\Delta$ and $\Gamma$ respectively with and without jump. We also plot exact values of these Greeks. The convergence error observed in figures 5.5.2 (right) and 5.5.3 (right) demonstrates exponential accuracy of the proposed method.

## 5.6 Summary and discussions

We have presented a new approach to price European options with jump. Our approach consisted of the inverse Laplace transform (ILT) method as a time integrator and the spectral domain decomposition method (SDDM) as a spatial discretization method.

The SDDM uses piecewise high order linear rational interpolants represented pointwise on a Chebyshev grid points in each sub-domain. The choice of the decomposition

Table 5.5.1: Numerical results obtained by using Crank-Nicholson and Inverse Laplace transform method for time and standard finite difference method for the spatial (asset) discretization; M number of points on the contour and using the parameters $K = 10$; $\sigma = 0.2$; $\lambda = 0.1$; $\gamma = 0.3$; $\mu = 0$; $r = 0.02$; $T = 0.25$; $x_{\min} = -2$, $x_{\max} = 1.5$.

| CN and FDM | | | | ILT and FDM | | | |
|---|---|---|---|---|---|---|---|
| $N$ | Time steps | Error | Time(s) | $N$ | M | Error | Time(s) |
| 40 | 50 | 1.40E-2 | 0.013 | 40 | 20 | 1.04E-2 | 0.012 |
| 90 | 60 | 4.60E-3 | 0.027 | 90 | 20 | 2.80E-3 | 0.022 |
| 180 | 150 | 1.50E-3 | 0.144 | 180 | 20 | 6.86E-4 | 0.061 |
| 650 | 340 | 3.14E-4 | 5.240 | 650 | 20 | 1.25E-5 | 1.083 |
| 900 | 650 | 3.60E-4 | 22.355 | 900 | 20 | 2.66E-5 | 2.473 |

Table 5.5.2: Numerical results obtained by using Crank-Nicholson and Inverse Laplace transform method for time and spectral domain decomposition method for the spatial (asset) discretization; M the number of points on the contour and using the parameters $K = 10$; $\sigma = 0.2$; $\lambda = 0.1$; $\gamma = 0.3$; $\mu = 0$; $r = 0.02$; $T = 0.25$; $x_{\min} = -2$, $x_{\max} = 1.5$.

| CN and SDDM | | | | ILT and SDDM | | | |
|---|---|---|---|---|---|---|---|
| $N$ | Time steps | Error | Time(s) | $N$ | M | Error | Time(s) |
| 5 | 200 | 2.490E-1 | 0.049 | 5 | 20 | 6.20E-1 | 0.047 |
| 10 | 200 | 6.300E-2 | 0.050 | 20 | 20 | 1.30E-3 | 0.054 |
| 20 | 300 | 1.300E-3 | 0.076 | 20 | 20 | 1.30E-3 | 0.048 |
| 35 | 380 | 1.310E-4 | 0.120 | 35 | 20 | 1.31E-5 | 0.062 |
| 50 | 400 | 1.240E-4 | 0.177 | 50 | 20 | 2.68E-8 | 0.071 |
| 70 | 650 | 7.650E-5 | 0.315 | 70 | 20 | 3.19E-10 | 0.084 |

method was motivated by the need to obtain high accuracy results since a direct application of spectral method (without decomposition) is not well suited to the non-smooth initial condition of the PIDE. To approximate the convolution integral that represents the jump process, we used the same grid points as for the differential part, i.e., the Chebyshev grid points.

We compared both the ILT and SDD methods with the Crank-Nicholson method and finite difference discretizations. The proposed approach is exponentially convergent in space and time, with the further advantage that it computes the solution at a particular time level directly and thus no time stepping is required. Spectral accuracy is observed not only in the evaluation of the option but also in the valuation of the Greeks

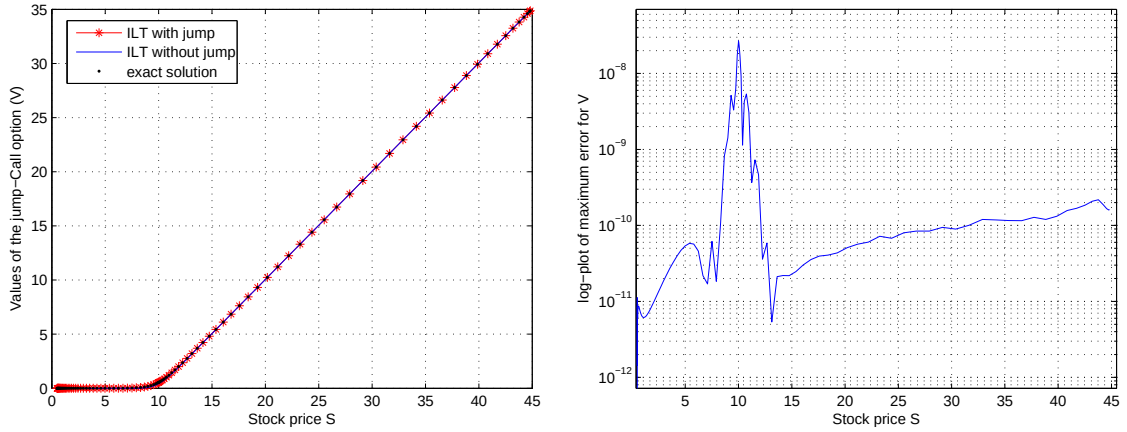


Figure 5.5.1: Left figure: Inverse Laplace transform (ILT) solution of the European call option with jump, without jump and the exact solution; Right figure: maximum errors occurred during the evaluation of the European call option with jump using Inverse Laplace transform (ILT). The domain was divided into two sub-domains, and other computing parameters were taken as $K = 10$; $\sigma = 0.2$; $r = 0.02$; $\gamma = 0.2$; $\lambda = 0.5$, $\mu = 0$; $T = 0.25$; $x_{\max} = 1.5$, $x_{\min} = -3$; $N = 50$ in each sub-domain.

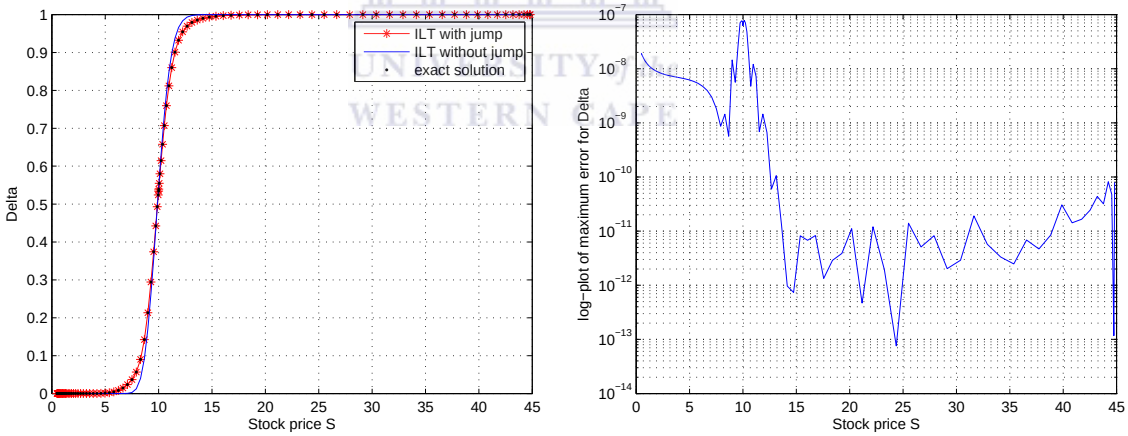


Figure 5.5.2: Left figure: Inverse Laplace transform (ILT) approximation of the $\Delta$ with jump, without jump and the exact solution; Right figure: maximum errors occurred during the computation of $\Delta$. Computing parameters were taken as $K = 10$; $\sigma = 0.2$; $r = 0.02$; $\gamma = 0.2$; $\lambda = 0.5$, $\mu = 0$; $T = 0.25$; $x_{\max} = 1.5$, $x_{\min} = -3$; $N = 50$ in each sub-domain.

$\Delta$ and $\Gamma$. Moreover, the computational time taken by this method is significantly less as compared to the one taken by CN and FDM.

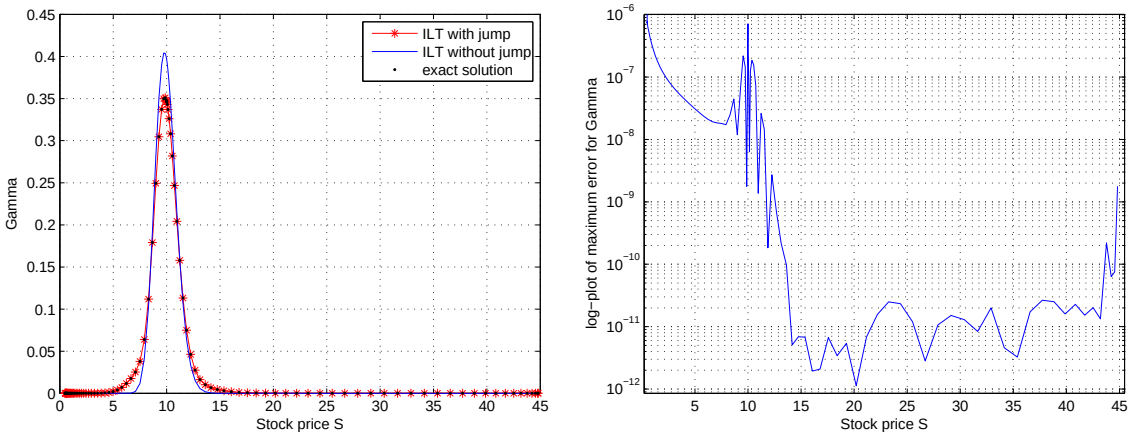


Figure 5.5.3: Left figure: Inverse Laplace transform (ILT) approximation of the $\Gamma$ with jump, without jump and the exact solution; Right figure: maximum errors occurred during the computation of $\Gamma$. Computing parameters were taken as $K = 10$; $\sigma = 0.2$; $r = 0.02$; $\gamma = 0.2$; $\lambda = 0.5$, $\mu = 0$; $T = 0.25$; $x_{\max} = 1.5$, $x_{\min} = -3$; $N = 50$ in each sub-domain.



The numerical results presented here suggest that the spectral domain decomposition method is very robust for pricing financial derivatives. We further extend this approach to solve the problems of pricing barrier options in the next chapter.

# Chapter 6

# Pricing barrier options using a Laplace transform approach



In this chapter, we consider two types of exotic options, namely a single barrier European down-and-out call and a double barrier European knock-out call options. Like some other standard and non-standard options, these barrier options also have non-smooth payoffs at the exercise price. This non-smooth payoff is the main cause of the reduction in accuracy when the classical numerical methods, for example, lattice method, Monte Carlo method or other methods based on finite difference and finite elements are used to solve such problems. In fact, the same happens when one uses the spectral method which are known to be exponentially accurate. In order to retain this high order accuracy, in this chapter we propose a spectral decomposition method which approximates the unknown solution by rational interpolants on each sub-domain. The resulting semi-discrete problem is solve by a contour integral method. Our numerical results affirm that the proposed approach is very robust and gives very reliable results.

## 6.1 Introduction

Barrier options are a class of exotic options that are traded in over-the-counter markets worldwide. These options are particularly attractive for their lower cost compared to

vanilla options and the market for these options has been expanding rapidly over the last two decades [133]. They are characterized by the dependence of their payoffs on the path of the underlying asset throughout their life time. When the asset price reaches a specified barrier level, these options are either exercisable (activated) in which case they are called knock-in options or they expire (extinguish) in which case they are called knock-out options.

Both knock-in and knock-out options are divided into down and up options depending on the level of the asset price compared to the barrier level. On one hand, knock-out options are either up-and-out or down-and-out. The up-and-out options can be exercised unless the asset price reaches the barrier level from below and the down-and-out options are exercisable until the asset price reaches the barrier level from above. Knock-in options are also classified as the up-and-in and down-and-in knock-in-options. The up-and-in options are exercisable if the asset reaches the barrier level from below whereas the down-and-in options can be exercised only if the asset price reaches the barrier from above the barrier level.



An important issue of pricing barrier options is whether the barrier crossing is monitored in continuous time or in discrete time. A continuously monitored option is an option which is monitored constantly between the current and the final time $T$ at maturity of the option. A discretely monitored option is only monitored at discrete time $t \leq t_1 < t_2 <, ..., < t_N < T$. On the market, barrier options are mostly discretely monitored. Analytical solutions of these options are expressed in terms of an $m$-dimensional integral over the $m$-dimensional multivariate normal distribution. However the computation of the multivariate normal distribution is compromised when $m > 5$ (where $m$ is the number of monitored points) [87], and thus one has to resort to numerical methods for practical implementation [18, 44, 87]. We prefer to solve the options that are monitored continuously under the Black-Scholes framework because they give their holders more flexibility in exercising.

In [151], Zvan *et al.* took advantage of the higher order implicit methods to successfully price a variety of barrier option problems. Their approach used a fine grid around

the location of the barrier. Fang and Oosterlee [41] considered the Fourier-based numerical method for American and barrier options. They obtained exponential results. This approach was extended in [42] to Bermudan and Barrier options under the Heston stochastic volatility model. The two-dimensional pricing problem was dealt with by a combination of a Fourier cosine series expansion in one dimension and high-order quadrature rules in the other dimension. Error analysis and experiments confirmed a fast error convergence.

A radial basis approach with Crank-Nicholson discretization in time was proposed in [55] for pricing barrier, European as well as Asian options. Recently a high-order accurate implicit finite-difference method to price various types of barrier options was applied in [103]. This approach was used for both the discretely and continuously monitored options. The scheme was also applied to the analysis of Greeks such as $\Delta$ and $\Gamma$ of the option.

In [103], Ndongmo and Ntwiga used the fourth order $\theta$-method for the continuously and discretely monitored options. To refine grid points in regions of interest, they used a coordinate transformation. The strength of their approach lies on a probability-based optimal determination of the boundary conditions, along with the option values. The authors in [24] developed a robust method for both continuously and discretely monitored barrier options. The method is based on the method-of-line and can evaluate the solution of the option price problem and its Greeks very accurately. Furthermore, this approach efficiently handles standard barrier options and barrier options with early exercise feature.

In this chapter, we propose a multi-domain spectral method and the Laplace transformed method. The multi-domain method uses spectral method directly in each subdomains. Appropriate matching conditions are imposed at the interface of the subdomains to ensure the continuity of the solution and that of its first derivative. After the spatial discretization, the resulting semi-discrete problem is solved by a contour integral method. Some other works related to numerical methods on exotic options pricing can be found in [8, 22, 30, 49, 105, 108, 111, 114, 115, 116, 117, 118].

The remainder of the chapter is structure as follows. Section 6.2 outlines the model problem. In Section 6.3, we describe the application of the Laplace transform to solve the semi-discrete problem. Numerical results are presented in Section 6.4. In Section 6.5, we give summary and conclusion.

## 6.2 Description of the model problem

We assume that the asset satisfies the following stochastic differential equation

$$\frac{dS}{S} = \mu dt + \sigma dW_t, \tag{6.2.1}$$

where $\mu$ is a constant representing the drift rate, $\sigma$ is the volatility of the underlying asset, and $dW_t$ is a Wiener process with mean zero and variance $dt$. Under the Itô process, the following Black-Scholes partial differential equation for the valuation of an option $V$ arises

$$\frac{\partial V}{\partial t} + \frac{1}{2}\sigma^2 S^2 \frac{\partial^2 V}{\partial S^2} + rS\frac{\partial V}{\partial S} - rV = 0. \tag{6.2.2}$$



Here $t$ is the current time at which the option $V(S,t)$ is valued before the expiration of the option at time $T$. For numerical computation, we set $\tau = T - t$ and rewrite (6.2.2) to a convenient form as follows

$$\frac{\partial V}{\partial \tau} = \frac{1}{2}\sigma^2 S^2 \frac{\partial^2 V}{\partial S^2} + rS\frac{\partial V}{\partial S} - rV, \tag{6.2.3}$$

with the boundary, initial and barrier conditions given as follow:

- For single barrier down-and-out call, the boundary conditions are

$$V(0,\tau) = 0, \qquad V(S_{\max},\tau) = S_{\max} - Ke^{-r\tau}, \tag{6.2.4}$$

whereas the barrier constraint is

$$V(S,\tau) = \begin{cases} 0, & S \leq X \quad \text{and} \quad 0 \leq \tau \leq T, \\ \\ V(S,\tau), & \text{otherwise.} \end{cases} \tag{6.2.5}$$

The initial condition is given by

$$V(S,0) = \begin{cases} 0, & S \leq X, \\ \\ S-K, & \text{otherwise.} \end{cases} \tag{6.2.6}$$

Here, $X$ is barrier level, $K$ is the strike price, and $S_{\max}$ is chosen sufficiently large.

- For double barrier knock-out call, the boundary conditions are

$$V(0,\tau) = 0, \qquad V(S_{\max},\tau) = 0, \tag{6.2.7}$$



and barrier constraint are given by

$$V(S,\tau) = \begin{cases} 0, & S \leq X_1 \quad \text{or} \quad S \geq X_2 \quad \text{and} \quad 0 \leq \tau \leq T, \\ \\ V(S,\tau), & \text{otherwise.} \end{cases} \tag{6.2.8}$$

The initial condition is given by

$$V(S,0) = \begin{cases} 0, & S \leq X_1, \\ \\ S-E, & X_1 \leq S \leq X_2, \\ \\ 0, & S \geq X_2. \end{cases} \tag{6.2.9}$$

Here, $X_1$ and $X_2$ represent the lower and upper level barriers respectively, $K$ is the strike price, and $S_{\max}$ is chosen sufficiently large.

We use the spectral approach with the domain decomposition method from section 3.3 for the discretization of (6.2.3). The final ODE system with boundary conditions inclueded is given by the following global system

$$\dot{V} = AV. \tag{6.2.10}$$

Here $V$ is the vector

$$V = \left(V_0^{\vartheta}, \ldots, V_N^{\vartheta}, V_0^{\chi}, \ldots, V_N^{\chi}\right),$$

and

$$A = B + C - rI,$$

where $I$ is the identity, $B$ and $C$ are block diagonal matrices of $B^{\vartheta,\chi}$ and $C^{\vartheta,\chi}$, respectively obtained in section 3.3. After the discretization, the resulting semi-discrete problem is solved using the Laplace method as discussed in the next section.



## 6.3 Application of Laplace transform method to solve the semi-discrete problem

In this section, we consider the Laplace transform for integrating the parabolic problem (6.2.10) with an initial condition $V_0$ and where $A$ is a parabolic operator with its eigenvalues located in a region $\Sigma_\delta = \{z \in \mathbb{C} : |\arg(z)| < \delta, z \neq 0\}$, for some $\delta \in (0, \pi/2)$. Furthermore, the resolvent $(zI - A)^{-1}$ of $A$ satisfies

$$\|(zI - A)^{-1}\| \leq \frac{C}{1 + |z|}, \quad \text{for } z \in \mathbb{C} \setminus \Sigma_\delta,$$

for some constant $C > 0$ independent of $z$. Note that, this implies that the function $V$ admits an holomorphic and bounded extension to a region containing $t \geq 0$, a familiar

situation arising for example in the context of parabolic problems.

A direct application of the Laplace transform to (6.2.10) leads to

$$(zI - A)\widehat{V} = V_0, \tag{6.3.1}$$

where $I$ is the identity matrix and $\widehat{V}$ the Laplace transform of $V(\cdot, t)$ defined by

$$\widehat{V}(\cdot, z) = \int_0^\infty V(\cdot, t)e^{-zt}dt. \tag{6.3.2}$$

The inverse is evaluated on a contour $\Gamma$ known as the Bromwich contour as

$$V(\cdot, t) = \frac{1}{2\pi i}\int_\Gamma e^{zt}\widehat{V}(\cdot, z)dz, \quad t > 0. \tag{6.3.3}$$

The contour $\Gamma$ is chosen such that it encloses all the singularities of $\widehat{V}(., z)$. The integral is then evaluated using the trapezoidal rule. Talbot's idea was to deform the Bromwich line into a contour which starts and ends in the left half-plane. Such a deformation of the contour is possible by the Cauchy's integral theorem [123]. Cauchy's theorem is applicable provided that all singularities of the transformed function $\widehat{V}(\cdot, z)$ are contained in the interior of the new contour and that $\left|\widehat{V}(\cdot, z)\right| \to 0$ as $|z| \to \infty$ in the half-plane [138]. Such contours are used in [93, 125, 138] all of which are of the form

$$z = z(\ell), \quad -\infty < \ell < \infty,$$

with the property that $\mathrm{Re}\, z \to -\infty$ as $\ell \to \pm\infty$.

In this chapter, we consider the hyperbola as the integration contour defined by

$$z(\ell) = \widetilde{\mu}\left(1 + \sin\left(i\ell - \alpha\right)\right), \quad \ell \in \mathbb{R}, \tag{6.3.4}$$

where the real parameters $\widetilde{\mu} > 0$ and $0 < \alpha < \pi/2$ determine the geometry of the contour. The positive parameter $\widetilde{\mu}$ controls the width of the contour while $\alpha$ determines

its geometric shape, i.e., the asymptotic angle. On the contour (6.3.4) the inversion formula (6.3.3) can be rewritten as

$$V(\cdot,t)=\frac{1}{2\pi i}\int_{-\infty}^{\infty}e^{z(\ell)t}\widehat{V}\left(\cdot,z(\ell)\right)z'(\ell)d\ell, \tag{6.3.5}$$

where

$$z'(\ell)=\widehat{\mu}i\cos\left(i\ell-\alpha\right).$$

For $h>0$ such that $\ell_k=kh$, where $k$ is an integer, the trapezoidal rule can then be expressed by

$$V(\cdot,t)\approx\frac{h}{2\pi i}\sum_{k=-\infty}^{\infty}e^{z(\ell_k)t}\widehat{V}\left(\cdot,z(\ell_k)\right)z'(\ell_k). \tag{6.3.6}$$

In practice, the infinite sum has to be truncated at a finite integer $M$, in which case one commits a truncation error as discussed below. Note that because of the symmetry of the contour (6.3.4), (6.3.6) can be rewritten as

$$V_M(\cdot,t)\approx\mathrm{Re}\left\{\frac{h}{\pi i}\sum_{k=0}^{M}{}^{\circ}e^{z(\ell_k)t}\widehat{V}\left(\cdot,z(\ell_k)\right)z'(\ell_k)\right\}. \tag{6.3.7}$$



where '$\circ$' indicates that the first term is divided by 2. The benefit of using (6.3.7) is that it reduces by half the summation (6.3.6) and subsequently the number of linear system to be evaluated in (6.3.1).

Below we discuss the numerical results obtained by using the proposed approach.

## 6.4 Numerical results

In this section, we present some numerical results which show the performance of our approach for single and double barrier options. As an example of a single barrier option, we consider the European down-and-out options whereas for double barrier option, we consider the knock-out call options.

In Table 6.4.1, we present the values of a down-and-out call option obtained by

using the inverse Laplace transform combined with the finite difference method (ILT-FDM); Crank-Nicholson method (CN); and our Laplace transform method combined with spectral decomposition method (ILT-SDDM). Furthermore, we list the errors in the solutions obtained by these three methods. The first column gives the values of the asset whereas the second column contains the values of the exact solution. The next three columns represent the solutions obtained by above three methods and then the remaining columns show the errors. The other parameters used in the simulations are $K = 10$, $\sigma = 0.2$, $r = 0.02$, $\tau = 0.5$ and $X = 9$. We see that the errors obtained by the proposed approach is very small.

Figure 6.4.1 (top) shows the graphs of the exact and numerical solution of the European down-and-out option price and that of the computed solution using the ILT-SDDM. We have also computed the $\Delta$ and $\Gamma$ as shown in the bottom left and bottom right plots of this figure. The convergence results obtained by CN, ILT-FDM and ILT-SDDM methods are presented in Figure 6.4.2 (top). In this figure we also present errors for $\Delta$ (bottom left) and $\Gamma$ (bottom right) obtained by using our ILT-SDDM. We use the same parameters as those used for the results presented in Table 6.4.1.



In Table 6.4.2, we show the results obtained for two barriers $X_1$ and $X_2$. In this experiment we solve the problem for asset price ranging from $S_{\min} = 90$ to $S_{\max} = 115$. The barriers are applied at $X_1 = 95$ and $X_2 = 110$. Other parameters are $K = 100$, $\sigma = 0.25$, $r = 0.05$, $\tau = 0.25$. The table includes results obtained by using our ILT-SDDM, and by using Crank-Nicholson (CN) and Crank-Nicholson improved (CN-improved) presented in [133]. We also list the errors in the solutions obtained by these methods. As reference solutions at the barriers, we use the values 0.0969796 at $X_1$ and 0.081481 at $X_2$ as obtained in [133]. The results confirm that the proposed approach outperforms the other methods mention here.

Figure 6.4.3 shows the graphs that we obtained by using the ILT-SDDM to price double barrier options for the set of parameters used for the computation of results presented in Table 6.4.2. The top figure shows the value of the option where the bottom figures show its $\Delta$ (left) and $\Gamma$ (right).

It is clear from all the tabular results and graphs that the proposed method is very competitive.

Table 6.4.1: Values of the European single barrier down-and-out options using the CN, ILT-FDM and our ILT-SDDM. Parameters values are $K = 10$, $\sigma = 0.2$, $r = 0.02$, $\tau = 0.5$ and $X = 9$.

| $S$ | Exact sol. | CN | ILT-FDM | ILT-SDDM | Error (CN) | Error (ILT-FDM) | Error (ILT-SDDM) |
|---|---|---|---|---|---|---|---|
| 7 | 0.0000 | 0.0000 | 0.0000 | 0.0000 | 0.000 | 0.000 | 0.000 |
| 8 | 0.0000 | 0.0000 | 0.0000 | 0.0000 | 0.000 | 0.000 | 0.000 |
| 9 | 0.0000 | 0.0000 | 0.0000 | 0.0000 | 0.000 | 0.000 | 0.000 |
| 11 | 1.294595 | 1.293735 | 1.294598 | 1.294595 | 8.6E-4 | 1.9E-5 | 2.2E-13 |
| 13 | 3.116046 | 3.116054 | 3.116043 | 3.116046 | 7.0E-5 | 1.8E-5 | 1.8E-13 |
| 15 | 5.100318 | 5.100347 | 5.100310 | 5.100318 | 2.8E-5 | 5.1E-5 | 3.8E-13 |
| 17 | 7.099529 | 7.099532 | 7.099529 | 7.099529 | 3.3E-5 | 5.6E-6 | 6.7E-13 |
| 19 | 9.099502 | 9.099502 | 9.099502 | 9.099502 | 8.8E-5 | 3.3E-7 | 5.8E-13 |

Table 6.4.2: Values of the European double barrier knock-out options using the CN, CN-improved, and our ILT-SDDM. Parameters values are $K = 100$; $\sigma = 0.25$; $r = 0.05$; $T = 0.5$; $X_1 = 95$; and $X_2 = 110$.

| Value at | Reference sol. | CN [133] | CN-improved [133] | ILT-SDDM | Error (CN) | Error (CN-improved) | Error (ILT-SDDM) |
|---|---|---|---|---|---|---|---|
| $X_1$ | 0.096979 | -0.094017 | 0.097002 | 0.096979 | 1.90E-1 | 3.10E-5 | 9.20E-8 |
| $X_2$ | 0.081481 | -0.909154 | 0.081503 | 0.081481 | 9.90E-1 | 2.89E-5 | 8.70E-8 |



## 6.5 Summary and discussions

We described the spectral domain decomposition and the Laplace transform methods for valuing single and double barriers option prices. As can be seen from Tables 6.4.1, 6.4.2 and Figures 6.4.1, 6.4.2, that the proposed approach gave very accurate results for the down-and-out call and the double barrier options. Currently, we are investigating the possibility of extending this approach to solve two-asset barriers options.

In the next chapter, we extend our approach to solve the Heston's volatility model.

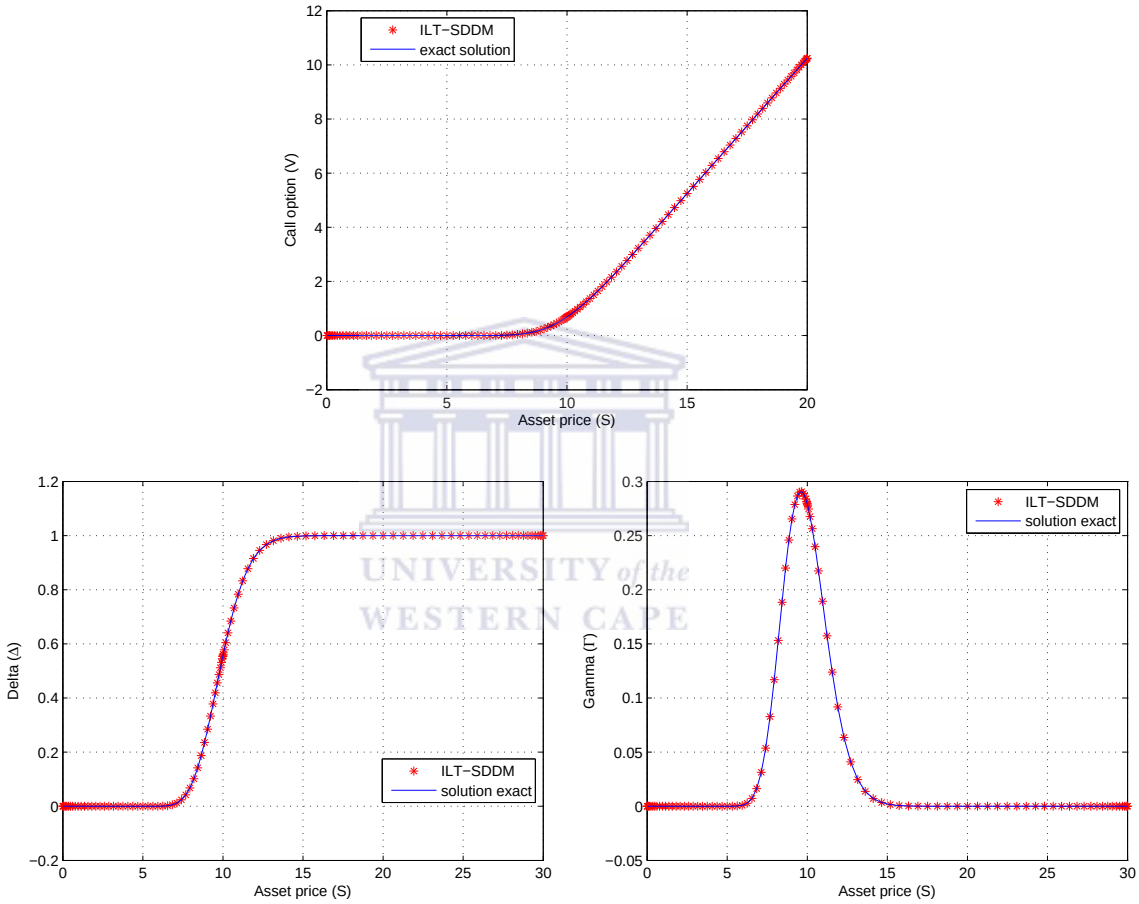




Figure 6.4.1: Values of the European single barrier down-out call option (top) and its $\Delta$ (bottom left) and $\Gamma$ (bottom right); using $K = 10$; $\sigma = 0.20$; $r = 0.05$; $T = 0.50$; $X = 9$.

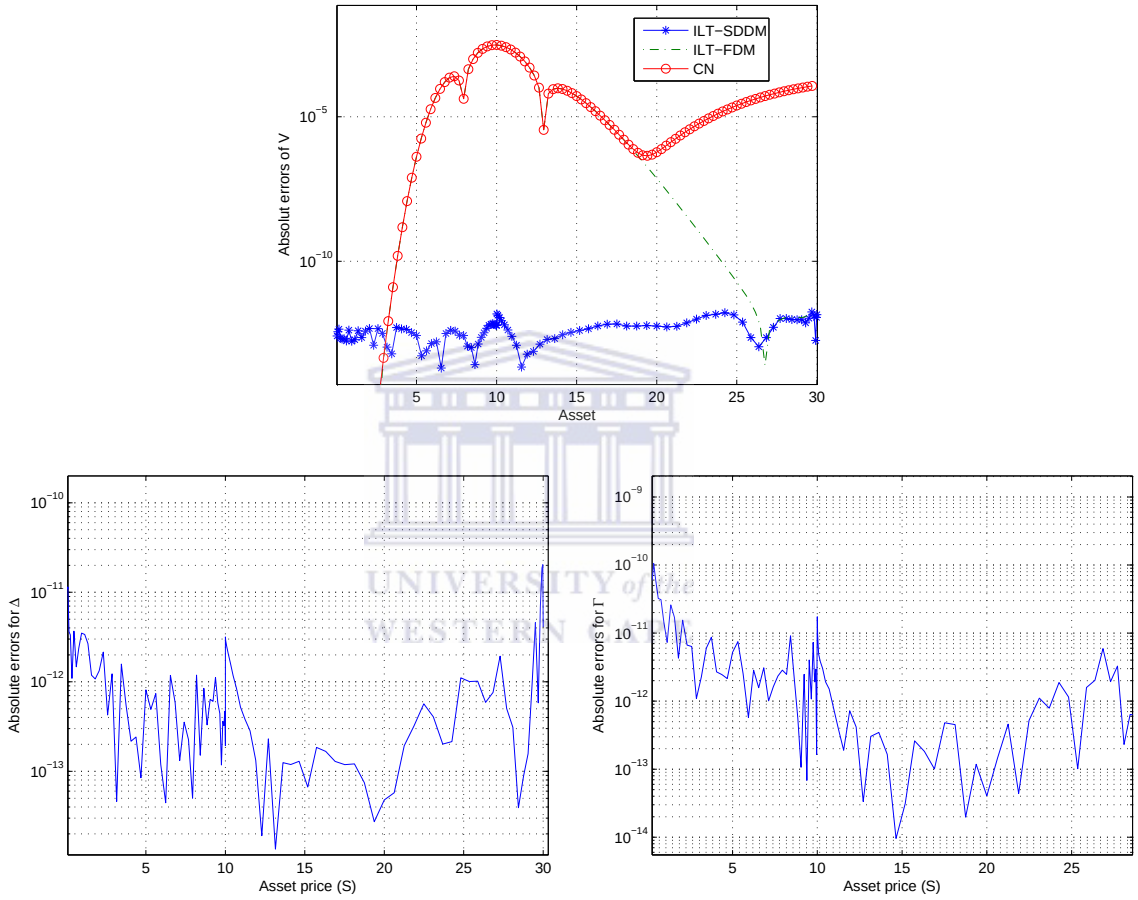


Figure 6.4.2: Convergence of CN, ILT-FDM and ILT-SDDM methods for the European single barrier down-out call options (top), $\Delta$ (bottom left) and $\Gamma$ (bottom right); using $K = 10$; $\sigma = 0.20$; $r = 0.05$; $T = 0.50$; $X = 9$. We took $N = 50$ in each of the two sub-domains.

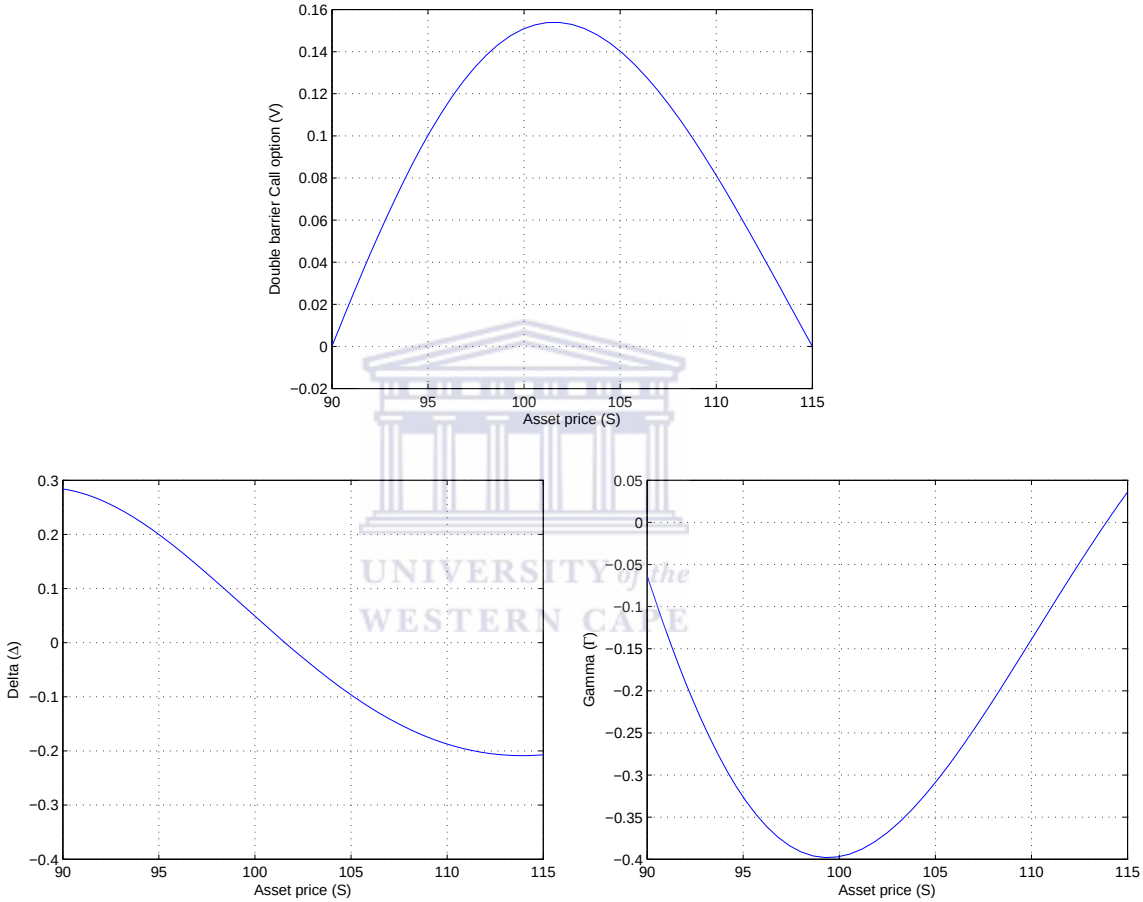




Figure 6.4.3: Values of the European double barrier knock-out call option (top) and its $\Delta$ (bottom left) and $\Gamma$ (bottom right); using $K = 100$; $\sigma = 0.25$; $r = 0.05$; $T = 0.5$; $X_1 = 95$; and $X_2 = 110$.

# Chapter 7

# A contour integral methods for solving Heston's volatility model



In this chapter we consider the Heston's volatility model [62]. We simulate this model using a combination of spectral collocation method and the Laplace transforms method. To approximate the two dimensional PDE, we construct a grid which is the tensor product of the two grids each of which are based on the Chebyshev points in the two spacial directions. The resulting semi-discrete problem is then solved by applying Laplace transform method based on Talbot's idea of deformation of the contour integral.

## 7.1 Introduction

The Heston model is one of the most popular stochastic volatility models for derivatives pricing. The model leads to a more realistic option price evaluation than the celebrated Black-Scholes model and constitutes its extension to the two-dimensional form [70, 100]. In [62], Heston derived a semi-closed formula for the model, however, its implementation is not a straightforward exercise because of the oscillatory behavior of the complex integrand which comes into play through the Fourier-type inversion formula. Therefore we turn to numerical methods to approximate these option pricing problems.

Most of numerical methods for evaluating the Heston model are based on the method-of-line approach which consists of two steps. Firstly, the PDE is discretize in space thus generating a system of ordinary differential equation. Secondly, the subsequent semi-discrete problem is solved in time by applying a suitable time integrator method. This is the approach followed in some of the numerical methods we review below.

In't Hout and Foulon [77] used the method-of-line approach to solve the Heston model. They first, discretized the PDE using a non-uniform grid to capture the important region around the strike price. Then they integrated the resulting semi-discrete problem by using three different alternating direction implicit (ADI) methods in time. As ADI methods, they considered the Douglas [38, 99] , Craig-Sneyd [34], the Modified Craig-Sneyd [34, 76] and the Hundsdorfer-Verwer [72, 73] schemes. They demonstrated through various numerical examples with realistic data set from the literature combined with theoretical analysis and stability results obtained previously, that their approach was very effective. This approach was latter extended to the more complex Heston-Hull-White PDE in [56].



In [74], Ikonen and Toivanen studied the accuracy of the operator splitting methods for solving American options with stochastic volatility. In their numerical experiments, they compared the accuracy of their approach with conventional implicit projective successive over relaxation (PSOR) time discretization method [106, 150]. The results obtained demonstrated that the additional error due to the splitting does not increase the time discretization error.

Zhu and Chen [147] applied singular perturbation method to price European put option with stochastic volatility model, and derived a simple analytical formula as an approximation for the valuation of European put options. In'T Hout and Weideman [75] used finite difference to semi-discretize the Heston model in space and subsequently used contour integral method for time integration. They compared the efficiency of the contour integral approach with the ADI splitting schemes for solving this problem. The numerical experiments showed that the contour integral method was superior for the

range of medium to high accuracy requirements.

In this chapter, we apply the spectral method based on Chebyshev point to discretize the PDE in each spatial direction. Then we use a tensor product of the one-dimensional polynomials to represent the two-dimensional basis functions. For the time discretization, we consider the contour integral methods. Some other works related to numerical methods of multi-asset options pricing can be found in [10, 90, 112, 118, 124].

The rest of this chapter is organized as follows. In Section 7.2, we discuss the Heston model problem. In Section 7.3, we discuss the application of spectral methods to solve the model problem. Numerical results of our experiments are presented in Section 7.4 and finally the summary and conclusions are given in Section 7.5.

## 7.2 Description of the model problem

Let $V \equiv V(s, \varphi, \tau)$ denotes the price of a European option described by the Heston's stochastic volatility model at time $\tau = T - t$. Then, $V$ satisfies the following PDE

$$\frac{\partial V}{\partial \tau} = \frac{1}{2}\sigma^2 s\varphi \frac{\partial^2 V}{\partial s^2} + \rho\sigma s\varphi \frac{\partial V^2}{\partial s \partial \varphi} + \frac{1}{2}\sigma^2 \varphi \frac{\partial^2 V}{\partial \varphi^2} + r\frac{\partial V}{\partial s} + \tilde{\kappa}(\varsigma - \varphi)\frac{\partial V}{\partial \varphi} - rV, \quad (7.2.1)$$

where $0 \leq \tau \leq T$, $s > 0$ and $\varphi > 0$. The parameter $\tilde{\kappa} > 0$ is the mean-reversion rate, $\varsigma > 0$ is the long-term mean, $\sigma > 0$ is the volatility-of-variance, $\rho \in [-1, 1]$ is the correlation between the two underlying Brownian motion, $r$ denotes the risk free interest rate.

For a European style put option, the payoff yields the initial condition

$$V(s, \varphi, 0) = \max(K - s, 0), \quad (7.2.2)$$

where $K > 0$ is the strike price of the option. In numerical practice, a bounded spatial domain $[0, s_{\max}] \times [0, \varphi_{\max}]$ is chosen with fixed values $s_{\max}$, $\varphi_{\max}$ taken sufficiently

large. The boundary conditions are

$$\left.\begin{aligned} V(0,\varphi,t) &= K, && (0 \le \varphi < \varphi_{\max}, 0 \le t \le T), \\ \frac{\partial V}{\partial s}(s_{\max},\varphi,\tau) &= 0, && (0 \le \varphi \le \varphi_{\max}, 0 \le \tau \le T), \\ \frac{\partial V}{\partial \varphi}(s,\varphi_{\max},\tau) &= 0, && (0 \le s < s_{\max}, 0 \le \tau \le T). \end{aligned}\right\} \tag{7.2.3}$$

We use the spectral domain approach for discretization of (7.2.1)-(7.2.3) in the next section.

## 7.3 Spectral discretization

We discretize the two dimensional problem (7.2.1) by using spectral method. To this end, as a basis, we recall the discretization of a one dimensional function and then we extend the discretization to the two dimensional problem by using tensor product.



To begin with, let us note that the rational approximation of a function $u$, defined on $[-1,1]$, at the Chebyshev points $\xi_k$, $k = 0, 1..., N$ is given by

$$u_N(\xi) = \frac{\sum_{k=0}^{N} \frac{w_k}{\xi - \xi_k} u(\xi_k)}{\sum_{k=0}^{N} \frac{w_k}{\xi - \xi_k}}, \tag{7.3.1}$$

where $w_k$, $k = 0, 1, ..., N$ are the barycentric weights defined by $w_0 = 1/2$, $w_N = (-1)^N/2$, and $w_k = (-1)^k$; $k = 1, ..., N-1$. For the rational spectral method, the $m^{th}$

order differentiation matrix associated with the rational interpolant (7.3.1) is given by

$$u_N^{(m)}(\xi_k) = \sum_{k=0}^{N} \frac{d^m}{d\xi^m} \left( \frac{\sum_{k=0}^{N} \frac{w_k}{\xi - \xi_k} u(\xi_k)}{\sum_{k=0}^{N} \frac{w_k}{\xi - \xi_k}} \right). \tag{7.3.2}$$

Similar to the one-dimensional approximation, the rational approximation for a two dimensional function defined on $[-1,1] \times [-1,1]$ is given by

$$u_N(\xi, \tilde{\xi}) = \frac{\sum_{j=0}^{N} \sum_{k=0}^{\tilde{N}} \frac{w_j w_k}{(\xi - \xi_j)\left(\tilde{\xi} - \tilde{\xi}_k\right)} u(\xi_k, \tilde{\xi}_k)}{\sum_{j=0}^{N} \sum_{k=0}^{\tilde{N}} \frac{w_j w_k}{(\xi - \xi_j)\left(\tilde{\xi} - \tilde{\xi}_k\right)}}, \tag{7.3.3}$$

where $w_j$, $j = 0, 1, ..., N$ and $w_k$, $j = 0, 1, ..., \tilde{N}$ are the barycentric weights defined by $w_0 = 1/2$, $w_N = (-1)^N/2$, and $w_j = (-1)^j$; $j = 1, ..., N-1$, and $w_{\tilde{N}} = (-1)^{\tilde{N}}/2$, and $w_k = (-1)^k$; $k = 1, ..., \tilde{N} - 1$.



In this chapter, we proceed differently to discretize the two dimensional problem (7.2.1). We set up a grid based on Chebyshev points independently in each direction $s$ and $\varphi$, called the tensor grid [60, 79, 132].

**Definition 7.3.1** *Let $P \in \mathbb{R}^{\ell \times k}$ and $Q \in \mathbb{R}^{m \times n}$. The tensor product, also called Kronecker product, of $P$ and $Q$ is the matrix defined by*

$$P \otimes Q = \begin{pmatrix} p_{11}Q & \dots & p_{1k}Q \\ \vdots & \ddots & \vdots \\ p_{\ell 1} & \dots & p_{\ell k}Q \end{pmatrix} \in \mathbb{R}^{\ell m \times kn}. \tag{7.3.4}$$

On the tensor grid, the discretization of other derivatives reads

$$\left.\begin{aligned} \frac{\partial V}{\partial s} &:= \left(D_s^{(1)} \otimes I_\varphi\right) V, \\ \frac{\partial V}{\partial \varphi} &:= \left(I_s \otimes D_\varphi^{(1)}\right) V, \\ \frac{\partial^2 V}{\partial s^2} &:= \left(D_s^{(2)} \otimes I_\varphi\right) V, \\ \frac{\partial^2 V}{\partial \varphi^2} &:= \left(I_s \otimes D_\varphi^{(2)}\right) V, \\ \frac{\partial^2 V}{\partial s \partial \varphi} &:= \left(D_s^{(1)} \otimes D_\varphi^{(1)}\right) V, \end{aligned}\right\} \tag{7.3.5}$$

where $\otimes$ denotes the Kronecker product, $I_s$ and $I_\varphi$ are the identity matrices in $s$ and $\varphi$ direction, respectively; $D_s^{(1,2)}$, $D_\varphi^{(1,2)}$ are the first and second order differentiation matrices in the corresponding variable.

To discretize (7.2.1), we map each domain to the reference interval $[-1, 1]$ by the linear transformations

$$\left.\begin{aligned} s &= \tfrac{s_{\max}}{2}(\xi + 1) \qquad s \in [0, s_{\max}], \\ \varphi &= \tfrac{\varphi_{\max}}{2}(\xi + 1) \qquad \varphi \in [0, \varphi_{\max}]. \end{aligned}\right\} \tag{7.3.6}$$

On the tensor grid, (7.2.1) becomes

$$\begin{aligned} V_\tau \;=\; & \beta_1 (D_s^{(2)} \otimes I_\varphi) V + \beta_2 (D_s^{(1)} \otimes D_\varphi^{(1)}) V + \beta_3 (I_s \otimes D_\varphi^{(2)}) V \\ & + r (D_s^{(1)} \otimes I_\varphi) V + \beta_4 (I_s \otimes D_\varphi^{(1)}) V - r I_s \otimes I_\varphi V, \end{aligned} \tag{7.3.7}$$

where

$$\begin{aligned}\beta_1 &= \frac{1}{2}\sigma^2 s^2 I_s \otimes \varphi I_\varphi,\\ \beta_2 &= \rho\sigma s I_s \otimes \varphi I_\varphi,\\ \beta_3 &= \frac{1}{2}\sigma^2 \varphi I_\varphi \otimes I_\varphi,\\ \beta_4 &= \tilde{\kappa}(\varsigma - \varphi) I_\varphi \otimes I_\varphi.\end{aligned}$$

The equation (7.3.7) can be written in the form of a global matrix as

$$V_\tau = AV, \tag{7.3.8}$$

where

$$\begin{aligned}A &= \beta_1(D_s^{(2)} \otimes I_\varphi) + \beta_2(D_s^{(1)} \otimes D_\varphi^{(1)}) + \beta_3(I_s \otimes D_\varphi^{(2)})\\ &\quad + r(D_s^{(1)} \otimes I_\varphi) + \beta_4(I_s \otimes D_\varphi^{(1)}) - rI_s \otimes I_\varphi.\end{aligned} \tag{7.3.9}$$



We solve (7.3.8) by the Laplace transform method discuss earlier in previous chapter. Below we discuss the numerical results.

## 7.4 Numerical results

In this section, we compute put option prices for the Heston model (7.3.8) with boundary conditions (7.2.3) using the spectral method in space and contour integral method in the time direction. The parameter values used in the simulation are $K = 10$; $\sigma = 0.9$; $r = 0.1$; $\rho = 0.1$; $\varsigma = 0.16$; $T = 0.25$, $s_{\max} = 20$, $\varphi_{\max} = 1$. The prices are presented in Tables 7.4.1 and 7.4.2 for asset values $s = 8$; 9; 10; 11; 12 and for the variance values $\varphi = 0.0625$ and $\varphi = 0.25$. In the first column we have the values of the asset, the second column contains the exact values obtained in [74], the third column contains the values obtained from our inverse Laplace transform (ILT) approach and the last

column represents the estimated error.

From tables 7.4.1 and 7.4.2, we observe that the direct application of the spectral method combined with the ILT method produces results which are second order accurate.

Table 7.4.1: Values of the European put option associated with the Heston's volatility model using $\varphi = 0.0625$, $K = 10$; $\sigma = 0.9$; $r = 0.1$; $\rho = 0.1$; $\varsigma = 0.16$; $T = 0.25$, $s_{\max} = 20$, $\varphi_{\max} = 1$.

| s | Exact values [74] | ILT | Error |
|---|---|---|---|
| 8 | 2.0000 | 2.0984 | 0.0984 |
| 9 | 1.1080 | 1.1523 | 0.0443 |
| 10 | 0.5316 | 0.5422 | 0.0106 |
| 11 | 0.2261 | 0.1502 | 0.0759 |
| 12 | 0.0907 | 0.0788 | 0.0119 |

Table 7.4.2: Values of the European put option associated with the Heston's volatility model using $\varphi = 0.25$, $K = 10$; $\sigma = 0.9$; $r = 0.1$; $\rho = 0.1$; $\varsigma = 0.16$; $T = 0.25$, $s_{\max} = 20$, $\varphi_{\max} = 1$.

| s | Exact values [74] | ILT | Error |
|---|---|---|---|
| 8 | 2.0733 | 2.0930 | 0.0197 |
| 9 | 1.3290 | 1.3460 | 0.0170 |
| 10 | 0.7992 | 0.6974 | 0.1018 |
| 11 | 0.4536 | 0.4699 | 0.0163 |
| 12 | 0.2502 | 0.2611 | 0.0109 |

## 7.5 Summary and discussions

We proposed spectral method combined with the Laplace transform method for pricing European options using Heston's stochastic volatility model. In this approach, a direct spectral method is applied for discretization in space. To approximate the derivatives in both $s$ and $v$ directions, we set up a grid based on Chebyshev points independently in both directions and then considered a new grid which is the tensor product of these two grids. Our computational results show that the proposed method gives the option prices that are very close to the exact values.

Currently, we are investigating the possibility of using the multi-domain decomposition method in space to further improve the accuracy.

# Chapter 8

# Concluding remarks and scope for future research



In this thesis, we investigated the application of Laplace transform method for solving different option pricing models. We particularly applied this method to price options under the Black-Scholes model such as the European and American options. Then we extended the approach to the jump-diffusion model, barrier options and the Heston's stochastic volatility model. To discretize in space, we use decomposition method based on spectral method. The method uses piecewise rational expansions to approximate the option price represented on a Chebyshev grid within each sub-domain. It is the piecewise rational approximation that allows an exact representation of the non-smooth initial condition of these options. Numerical results have shown that by dividing the domain into sub-domain at the discontinuity (strick price $K$), the spectral method gives exponential convergence.

In Chapter 2, we investigated two efficient numerical methods for solving the Black-Scholes equation for pricing the European options. We used spectral methods to discretize the associated partial differential equation with respect to space and generated a system of ODEs which was then solved by applying two contour integral methods. The first one was the exponential time differencing Runge-Kutta method of order 4.

The second one was based on the application of the trapezoidal rule to approximate a Bromwich integral. We gave a comparative discussion on these two methods and compared the numerical results with conventional methods such as the MATLAB solver ode15s and Crank-Nicholson's method.

In Chapter 3, we investigated a new approach to improve the results obtained in Chapter 2. The approach was based on spectral domain decomposition and the Laplace transform method. The spectral domain decomposition method approximated the solution using piecewise high order rational interpolant on the Chebyshev mesh points within each sub-domain with the boundary domain placed at the strike price where the discontinuity was located. The resulting system was then solved by applying Laplace transform method. To assess the accuracy and efficiency of this method, the solutions obtained by using this approach were compared with those obtained with conventional methods such as Crank-Nicholson and finite difference methods.

Ideas explored in Chapter 2 and 3 were extended to design a robust numerical method to price American options in Chapter 4. Due to the non-smooth initial condition associated with the American options, we used spectral domain decomposition method to approximate the option price which was represented pointwise on a Chebyshev grid within each sub-domain. To avoid the computation of the unknown free boundary associated with the American option, we used an updating procedure. Numerical results of the proposed method were presented for the solution and the Greeks.



In Chapter 5, we considered options with jumps on a single asset. We took advantage of the suitability of the Chebyshev grid point for Gauss-Legendre quadrature to efficiently approximate the convolution integral. The resulting discrete problem was solved by the inverse Laplace transform using the Bromwich contour integral approach. The numerical results obtained were compared with those obtained from Crank-Nicholson and finite difference methods.

In Chapter 6, we solved problems for pricing exotic options. In particular, we solved a single barrier European down-and-out and a double barrier European knock-out option. We compared the results obtained from our approach with those seen in

the literature.

To see the further applicability of the methods proposed in previous chapters, in Chapter 7, we applied them to solve the Heston's volatility model. To approximate the associated two-variable PDE, we constructed a grid which was the tensor product of the two grids each of which were based on the Chebyshev points in the two directions in space. The resulting semi-discrete problem was then solved by applying Laplace transform method.

From all the numerical experiments, we see that Laplace transform method is very efficient and robust for solving the option pricing problems in computational finance.

As far as the scope of the future work is concerned, we are currently investigating the extensions of this approach to price more complicated model such as American jump-diffusion model. We are also investigating whether the preconditioning of the block matrix in SDDM can produce better results. Furthermore, we think the method can be potentially extended to price other complex options, for example,

- Improved Heston's stochastic volatility,
- Arithmetic Asian options,
- Asian Basket options.

Additionally, we note that the domain decomposition approach proposed and used to solve some of the problems in this thesis can be made more efficient so that it can be used to solve problems for pricing multi-asset options.

# Bibliography


[1] J. Abate and P.P. Valko, Multi-precision Laplace transform inversion, *International Journal for Numerical Methods in Engineering* **60 (5)** (2004) 979–993.

[2] J. Ahn, S. Kang and Y. Kwon, A Laplace transform finite difference method for the Black-Scholes equation, *Mathematical and Computer Modelling* **51 (3-4)** (2010) 247–255.

[3] L. Andersen and J. Andreasen, Jump-diffusion processes: Volatility smile fitting and numerical methods for option pricing, *Review of Derivatives Research* **4** (2000) 231–262.

[4] U.M. Ascher, S.J. Ruuth and B.T.R. Wetton, Implicit-explicit methods for time-dependent partial differential equations, *SIAM Journal on Numerical Analysis* **32** (1995) 797–823.

[5] R. Baltensperger, J.P. Berrut and B. Noël, Exponential convergence of a linear rational interpolant between transformed Chebyshev points, *Mathematics of Computation* **68** (1999) 1109–1120.

[6] E. Banks and P. Siegel, *The Options Applications Handbook: Hedging and Speculating Techniques for Professional Investors*, McGraw-Hill, 2006.

[7] G. Barone-Adesi and E. Whaley, Efficient analytic approximation of American option values, *The Journal of Finance* **XLII (2)** (1987).

[8] J. Barraquand and D. Martineau, Numerical valuation of high dimensional multivariate American securities, *Journal of Financial and Quantitative Analysis* **30** (1995) 383–405.

[9] A. Battauz and M. Pratelli, Optimal stopping and American options with discrete dividends and exogenous risk, *Insurance: Mathematics and Economics* **35** (2004) 255–265.

[10] C. Bernard, O. Le Courtois and F. Quittard-Pinon, Pricing derivatives with barriers in a stochastic interest rate environment, *Journal of Economic Dynamics and Control* **32 (9)** (2008) 2903–2938.

[11] J.P. Berrut and H.D. Mittelmann, Rational interpolation through the optimal attachment of poles to the interpolating polynomial, *Numerical Algorithms* **23 (4)** (2000) 315–328.

[12] F. Black and M. Scholes, The pricing of options and corporate liabilities, *The Journal of Political Economy* **81 (3)** (1973) 637-654.

[13] J.P. Boyd, *Chebyshev and Fourier Spectral Methods* 2*nd ed.*, Dover, New York, 2000.

[14] P.P. Boyle, Options: A Monte-Carlo approach, *Journal of Financial Economics* **4 (3)** (1977) 323–338.

[15] P.P. Boyle and Y.S. Tian, An explicit finite difference approach to the pricing of barrier options, *Applied Mathematical Finance* **5** (1998) 17–43.

[16] M. Brennan and E. Schwartz, The valuation of American put options, *Journal of Finance* **32** (1977) 449–462.

[17] M. Brennan and E. Schwartz, Finite difference methods and jumps processes arising in the pricing of contingent claims: A synthesis, *Journal of Financial and Quantitative Analysis* **13 (3)** (1978) 461–474.

[18] M. Broadie, P. Glasserman and S.G. Kou, A continuity correction for discrete barrier options, *Mathematical Finance* **7** (1997) 325–349.

[19] P. Carr, R. Jarrow and R. Myneni, Alternative characterizations of the American put, *Mathematical Finance* **2** (1992) 87–106.

[20] Z. Cen and A. Le, A robust finite difference scheme for pricing American put options with Singularity-Separating method, *Numerical Algorithms* **53** (2010) 497–510.

[21] T. Chan, Pricing contingent claims on stocks driven by Lévy processes, *Annals of Applied Probability* **9 (2)** (1999) 504–528.

[22] S. Chao, Y. Jing-Yang and L. Sheng-Hong, On barrier option pricing in binomial market with transaction costs, *Applied Mathematics and Computation* **189** (2007) 1505–1516.

[23] X. Chen, J. Chadam and R. Stamicar, The optimal exercise boundary for American put option: analytic and numerical approximation, Preprint, 2000.

[24] C. Chiarella, B. Kang and G. Meyer, The evaluation of barrier option prices under stochastic volatility, *Computers and Mathematics with Applications,* to appear.

[25] M.M. Chwala, M.A. Al-Zanaidi and D.J. Evans, Generalize trapezoidal formulas for the Black-Scholes equation of option pricing, *International Journal of Computer Mathematics* **12** (2003) 1521–1526.

[26] M.M. Chwala, M.A. Al-Zanaidi and D.J. Evans, Generralized trapezoidal formulas for valuing American options, *International Journal of Computer Mathematics* **81 (3)** (2004) 375–381.

[27] N. Clarke and K. Parrott, Multigrid for American option pricing with stochastic volatility, *Applied Mathematical Finance* **6** (1999) 177–195.

[28] R. Company, A.L. Gonzalez and L. Jodar, Numerical solution of modified Black-Scholes equation pricing stock options with discrete dividend, *Mathematical and Computer Modelling* **44** (2006) 1058–1068.

[29] J.C. Cortés, L. Jódar and P. Sevilla-Peris, Exact and numerical solution of Blck-Scholes equations matrix equation, *Applied Mathematics and Computing* **160** (2005) 607–613.

[30] M. Costabile, I. Massab and E. Russo, An adjusted binomial model for pricing Asian options, *Review of Quantitative Finance and Accounting* **27** (2006) 285–296.

[31] J.C. Cox, S.A. Ross and M. Rubinstein, Option pricing: A simplified approach, *Journal of Financial Economics* **7 (3)** (1979) 229–264.

[32] J.C. Cox and M. Rubinstein, *Options Markets*, Prentice-Hall, Englewood Cliffs, New Jersey, 1985.



[33] S.M. Cox and P.C. Mathews, Exponential time differencing for stiff system, *Journal of Computational Physics* **176** (2002) 430–455.

[34] I.J.D. Craig and A.D. Sneyd, An alternating-direction implicit scheme for parabolic equations with mixed derivatives, *Computational Mathematics and Applications* **16** (1988) 341–350.

[35] S.H. Crandall, An optimal implicit recurrence formula for the heat conduction equation, *Quarterly of Applied Mathematics* **13** (1955) 318–320.

[36] B. Davies and B. Martin, Numerical inversion of Laplace transform: a survey and comparison of methods, *Journal of Computational Physics* **33 (1)** (1979) 1–32.

[37] G. Doetsch, *Introduction to the Theory and Application of the Laplace Transformation*, Springer-Verlag, New York, 1970.

[38] J. Douglas and H.H. Rachford, On the numerical solution of heat conduction problems in two and three space variables, *Transaction of the American Mathematical Society* **82** (1956) 421–439.

[39] D.G. Duffy, On the numerical inversion of Laplace transform: comparison of the three new methods on characteristic problems from applications, *ACM Transactions on Mathamatical Software* **19** (1993) 333–359.

[40] D.G. Duffy, *Transform Methods for Solving Partial Differential Equations, 2nd ed.*, Chapman & Hall/CRC, Boca Raton, FL, 2004.

[41] F. Fang and C.W. Oosterlee, Pricing Early-Exercise and Discrete Barrier Options By Fourier-Cosine Series Expansions, *Numerische Mathematik* **114 (1)** (2009) 27–62.

[42] F. Fang and C.W. Oosterlee, A Fourier-based Valuation Method for Bermudan and Barrier Options under Heston′s Model, *SIAM Journal on Financial Mathematics* **2** (2011) 439–463.



[43] G.E. Fasshauer, A.Q.M. Khaliq and D.A. Voss, Using meshfree approximation for multi-asset American option, *Journal of the Chinese Institute of Engineers* **27 (4)** (2004) 563–571.

[44] L. Feng and V. Linetsky, Pricing discretely monitored barrier options and defaultable bonds in Lévy process models: A fast Hilbert transform approach, *Mathematical Finance* **18 (3)** (2008) 337–384.

[45] S. Figlewski and B. Gao, The adaptive mesh model: a new approach to efficient option pricing, *Journal of Financial Economics* **53** (1999) 313–351.

[46] E.O. Fischer, Analytic approximation for the valuation of American put options on stocks with known dividends, *International Review of Economics and Finance* **2 (2)** (1993) 115–127.

[47] B. Fornberg, *A Spectral Guide to Pseudospectral Methods*, Cambridge University Press, Cambrigde, 1996.

[48] P.A. Forsyth and K.R. Vetzal, Quadratic convergence for valuing American options using a penalty method, *SIAM Journal on Scientific Computing* **23 (6)** (2002) 2095–2122.

[49] G. Fusai and M. C. Recchioni, Analysis of quadrature methods for pricing discrete barrier options, *Journal of Economic Dynamics and Control* **31 (3)** (2007) 826–860.

[50] I.P. Gavrilyuk and V.L. Makarav, Exponentially convergent parallel discretization methods for the first order evolution equations, *Computational Methods in Applied Mathematics* **1** (2001) 333–355.

[51] I.P. Gavrilyuk and H. Hackbush and B.N. Khoromskij, H-matrix approximation for the operator exponential with applications, *Numerische Mathematik* **92** (2002) 83–111.



[52] R. Gesk and H.E. Johnson, The American put options valued analytically, *Journal of Finance* **39 (5)** (1984) 1511–1524.

[53] R. Gesk and K. Shastri, Valuation by approximation: A comparison of alternative option valuation techniques, *Journal of Financial and Quantitative Analysis* **20** (1985) 45-71.

[54] G.H. Golub and C.F. van Loan, *Matrix Computations*, 3rd ed., Johns Hopkins University Press, Baltimore, 1996.

[55] Y. Goto, Z. Fei, S. Kan and E. Kita, Options valuation by using radial basis function approximation, *Engineering Analysis with Boundary Elements* **31** (2007) 836–843.

[56] T. Haentjens and K. In't Hout, ADI Finite Difference Discretization of the Heston-Hull-White PDE, *ICNAAM 2010: International Conference of Numerical Analysis and Applied Mathematics 2010. AIP Conference Proceedings* **1281** (2010) 1995–1999.

[57] N. Hale, On the Use of Conformal Maps to Speed Up Numerical Computations, PhD Thesis, Oxford University, 2009.

[58] H. Han and X. Wu, Fast numerical method for the Black-Scholes equations of American options, *SIAM Journal on Numerical Analysis* **41** (2003) 2081–2095.

[59] E. Haug, Closed form valuation of American barrier options, *International Journal of Theoretical and Applied Finance* **4** (2001) 355–359.

[60] W. Heinrichs, Improved condition number of spectral methods, *Mathematics of Computation* **53 (187)** (1989) 103–119.

[61] J.S. Hesthaven, S. Gottlieb and D. Gottlieb, *Spectral Method for Time-Dependent Problems*, Cambridge University Press, Cambridge, 2007.

[62] S.L. Heston, A closed-form solution for options with stochastic volatility with applications to bond and currency options, *Review of Financial Studies* **6 (2)** (1993) 327–343.

[63] N.J. Higham, *Accuracy and Stability of Numerical Algorithms*, SIAM, Philadelphia, 1996.

[64] J.D. Higham, *An Introduction to Financial Option Valuation*, Cambridge University Press, Cambridge, 2004.

[65] M. Hochbruck, C. Lubich and H. Selhofer, Exponential integration for large systems of differential equations, *SIAM Journal on Scientific Computing* **19** (1998) 1552–1574.

[66] M. Hochbruck and A. Ostermann, Explicite exponential Runge-Kutta methods for semilinear parabolic problems, *SIAM Journal on Numerical Analysis* **43** (2005) 1069–1090.

[67] Y.C. Hon, A quasi-Radial basis functions methods for American options pricing, *Computer and Mathematics with Applications* **43** (2002) 513–524.

[68] E.N. Houstis, K. Pantazopoulos and S. Kortesis, A front-tracking finite difference method for the valuation of American options, *Computational Economics* **12 (3)** (1998) 255–273.

[69] W.Z. Huang and M.D. Sloan, The pseudospectral method for solving differential eigenvalue problems, *Journal of Computational Physics* **111** (1994) 399–409.

[70] J.C. Hull and A. White, The pricing of options on assets with stochastic volatility, *The Review of Financial Studies* **42** (1987) 281–300.

[71] J.C. Hull, *Options Futures and Others Derivatives*, 4th ed., Prentice-Hall International, New Jersey, 2000.



[72] W. Hundsdorfer, Accuracy and stability of splitting with stabilizing corrections, *Applied Numerical Mathematics* **42** (2002) 213–233.

[73] W. Hundsdorfer and J.G. Verwer, *Numerical Solution of Time-Dependent Advection-Diffusion-Reaction Equations*, Springer, Berlin, 2003.

[74] S. Ikonen and J. Toivanen, Operator splitting methods for pricing American options under stochastic volatility, *Numerische Mathematik* **113** (2009), 299–324.

[75] K.J. In't Hout and J.A.C. Weideman, Appraisal of a contour integral method for the Black-Scholes and Heston equations, *SIAM Journal on Scientific Computing* **33** (2011) 763–785.

[76] K.J. In't Hout and B.D. Welfert, Unconditional stability of second-order ADI schemes applied to multi-dimensional diffusion equations with mixed derivative, *Applied Numerical Mathematics* **59 (3-4)** (2009) 677–692.

[77] K.J. In't Hout and S. Foulon, ADI finite difference schemes for option pricing in the Heston model with correlation, *International Journal of Numerical Analysis and Modeling* **7 (2)** (2010) 303–320.

[78] K.R. Jackson, S. Jaimungal and V. Surkov, Fourier space time-stepping for option pricing with Lévy models, *Journal of Computational Finance* **12 (2)** (2008) 1–28.

[79] K. Julien and M. Watson, Efficient multi-dimensional solution of PDEs using Chebyshev spectral methods, *Journal of Computational Physics* **228 (5)** 1480–1503.

[80] I. Karatzas and S.E. Shreve, *Brownian Motion and Stochastic Calculus*, Graduate Texts in Mathematics, vol.113, Springer-Verlag, New York, 1991.

[81] A. Kassam and L.N. Trefethen, Fourth-order time stepping for stiff PDEs, *Journal of Computational Physics* **176** (2002) 430–455.

[82] A.Q.M. Khaliq, D.A. Voss and S.H.K. Kazmi, A linearly implicit predictorcorrector scheme for pricing American options using a penalty method approach, *Journal of Banking and Finance* **30** (2006) 489–502.

[83] A.Q.M. Khaliq, D.A. Voss, and K. Kazmi, Adaptive $\theta$-methods for pricing American options, *Journal of Computational and Applied Mathematics* **222** (2008) 210–227.

[84] I.J. Kim, The analytic valuation of American options, *The Review of Financial Studies* **3 (4)** (1990) 547–572.

[85] M. Kindelan, F. Bernal, P. Gonzalez-Rodriguez and M. Moscoso, Application of the RBF meshless method to the solution of the radiative transport equation, *Journal of Computational Physics* **229** (2010) 1897–1908.

[86] R.W. Klopfenstein, Numerical differentiation formulas for stiff systems of ordinary differential equations, *RCA Review* **32** (1971) 447–462.

[87] S.G. Kou and H. Wang, First passage times of a jump diffusion process, *Advances in Applied Probability* **35** (2003) 504–531.

[88] R.E. Kuske and J.B. Keller, Optimal exercise boundary for American put option, *Applied Mathematical Finance* **5 (2)** (1998) 107–116.

[89] Y.K. Kwok, *Mathematical Models of Financial Derivatives*, Springer-Verlag, New York, 1998.

[90] E. Larsson, K. Ahlander and A. Hal, Multi-dimensional option pricing using radial basis functions and the generalized Fourier transform, *Journal of Computational and Applied Mathematics* **222** (2008) 175–192.

[91] A.J. Laub, *Matrix Analysis for Scientists and Engineers*, SIAM, Philadelphia, PA, 2005.

[92] W. Liao and A.Q.M. Khaliq, High-order compact scheme for solving non-linear Black-Scholes equation with transaction cost, *International Journal of Computer Mathematics* **86 (6)** (2009) 1009–1023.

[93] M. López-Fernández and C. Palencia, On the numerical inversion of the Laplace transform of certain holomorphic mappings, *Applied Numerical Mathematics* **51 (2-3)** (2004) 289–303.

[94] L.W. Macmillan, An analytic approximation for the American put price, *Advances in Futures and Options Research* **1** (1986) 119–139.

[95] R. Mallier and G. Alobaidi, Laplace transforms and American options, *Applied Mathematical Finance* **7** (2000) 241–256.

[96] V.E. Martensen, Zur numerischen Auswertung uneigentlicher Integrale, *Zeitschrift für Angewandte Mathematik und Mechanik* **48** (1968) T83–T85.

[97] B.J. McCartin and S.M. Labadie, Accurate and efficient pricing of vanilla stock options via the Crandall-Douglas scheme, *Appliend Mathematics and Computation* **143** (2003) 39–60.

[98] H.P. McKean, Appendix: A free boundary problem for the heat equation arising from a problem in mathematical economics, *Industrial Management Review* **6** (1965) 32–39.

[99] S. McKee, D.P. Wall and S. K. Wilson, An alternating direction implicit scheme for parabolic equations with mixed derivative and convective terms, *Journal Computational Physics* **126 (1)** (1996) 64–76.



[100] R.C. Merton, Option pricing when underlying stock returns are discontinous, *Journal of Financial Economics* **3** (1976) 125–144.

[101] G.H. Meyer, Numerical investigation of early exercise in American puts with discrete dividends, *Journal of Computational Finance* **5 (2)** (2002) 37–53.

[102] G.V. Narayanan and D.E. Beskos, Numerical operational methods for time-dependent linear problems, *International Journal for Numerical Methods in Engineering* **18 (12)** (1982) 1829–1854.

[103] J.C. Ndogmo and D.B. Ntwiga, High-Order accurate implicite methos for barrier option pricing, *Applied Mathematics and Computation* **218** (2011) 2210–2224.

[104] B.F. Nielsen, O. Skavhaug and A. Tveito, Penalty and front-fixing methods for the numerical solution of American option problems, *Journal of Computation Finance* **5** (2002) 69–97.

[105] G. Ökten, E. Salta and A. Göncü, On pricing discrete barrier options using conditional expectation and importance sampling Monte Carlo, *Mathematical and Computer Modelling* **47** (2008) 484–494.

[106] C.W. Oosterlee, On multigrid for linear complementarity problems with application to American-style options, *Electronic Transaction on Numerical Analysis* **15** (2003) 165–185.

[107] C.W. Oosterlee, C.C.W. Leentvaar and X. Huang, Accurate american option pricing by grid stretching and high-order finite differences, *Technical report: Delft University of Technology*, The Netherlands, 2005.

[108] A. Pelsser, Pricing double barrier options using Laplace transforms, *Finance and Stochastics* **4** (2000) 95–104.

[109] J. Persson and L. Sydow, Pricing American options using a space-time adaptive finite difference method, *Mathematics and Computers in Simulation* **80** (2010) 1922–1935.



[110] G. Petrella, An extension of the Euler Laplace method transform inversion algoritm with application in option pricing, *Operation Research Letter* **32** (2004) 380–389.

[111] G. Petralla and S. Kou, Numerical pricing of discrete barrier and lookback options via Laplace transforms *The Journal of Computational Finance* **8 (1)** (2004) 1–37.

[112] U. Pettersson, E. Larsson, G. Marcusson and J. Persson, Improved radial basis function methods for multi-dimensional option pricing, *Journal of Computational and Applied Mathematics* **222** (2008) 82–93.

[113] P. Phelim, B.Y. Tian, An explicit finite difference approach to the pricing of barrier options, *Applied Mathematics Finance* **5** (1998) 17–43.

[114] D. Rich, The mathematical foundations of barrier option pricing theory, *Advances in Futures and Options Research* **7** (1994) 267–311.

[115] P. Ritchken, On pricing barrier options, *Journal of Derivatives* **3** (1995) 9–28.

[116] L.C.G. Rogers and Z. Shi, The Value of an Asian Option, *Journal of Applied Probability* **32 (4)** (1995) 1077–1088.

[117] H. Sak, S.Ozekici and I. Boduroglu, Parallel computing in Asian option pricing, *Parallel Computing* **33** (2007) 92–108.

[118] S. Sanfelici, Galerkin infinite element approximation for pricing barrier options and options with discontinuous payoff, *Decisions in Economics and Finance* **27** (2004) 125–151.

[119] C. Schneider and W. Werner, Some aspect of rational interpolation, *Mathematics of Computation* **47** (1986) 285–299.

[120] D. Ševčovič, An iterative algorithm for evaluating approximations to the optimal exercise boundary for a non-linear Black-Scholes equation, *Computational Finance* arXiv:0710.5301v1 [q-fin.CP] 28 Oct 2007.

[121] D. Ševčovič, Transformation methods for evaluating approximations to the optimal exercise boundary for linear and non-linear Black-Scholes, *Computational Finance* arXiv:0805.0611v1 [q-fin.CP] 5 May 2008.

[122] A. Sheen, I.H. Sloan, and V. Thomée, A Parallel method for time-discretization of parabolic problems based on contour integral representation and quadrature, *Mathematics of Computation* **69** (2000) 177–195.

[123] M.R. Spiegel, *Theory and Problems of Laplace Transforms*, McGraw-Hill, New York, 1965.

[124] C. Sun, J.Y. Yang and S.H. Li, On barrier option pricing in binomial market with transaction costs, *Applied Mathematics and Computation* **189 (2)** (2007) 1505–1516.

[125] A. Talbot, The accurate numerical inversion of Laplace transforms, *IMA Journal of Applied Mathematics* **23 (1)** (1979) 97–120.

[126] D.Y. Tangman, A. Gopaul and M. Bhuruth, Exponential time integration and Chebychev discretisation schemes for fast pricing of options, *Applied Numerical Mathematics* **58 (9)** (2008) 1309–1319.

[127] D.Y. Tangman, A. Gopaul and M. Bhuruth, Numerical pricing of option using high-order compact finite difference schemes, *Journal of Computational and Applied Mathematics* **218 (2)** (2008) 270–280.

[128] D.Y. Tangman, A. Gopaul and M. Bhuruth, A fast high-order finite difference algorithm for pricing American option, *Journal of Computational and Applied Mathematics* **222** (2008) 17–29.



[129] D.Y. Tangman, A. Gopaul and M. Bhuruth, Numerical pricing of option using high-order compact finite difference schemes, *Journal of Computational and Applied Mathematics* **218 (2)** (2008) 270–280.

[130] W. Tee, A rational collocation with adaptively transformed Chebyshev grid points, *SIAM Journal on Scientific Computing* **28 (5)** (2006) 1798–1811.

[131] J. Toivanen, A high-order front-tracking finite difference method for pricing American options under jump-diffusion models, *Journal of Computational Finance* **13 (3)** (2010) 61–79.

[132] L.N. Trefeten, *Spectral Method in MATLAB*, SIAM, Philadelphia, PA, 2000.

[133] B.A. Wade, A.Q.M. Khaliq, M. Yousuf, J. Vigo-Aguiar and R. Deininger, On smoothness of the Crank-Nicholson scheme and higher order scheme for pricing

barrier options, *Journal of Computational and Applied Mathematics* **204** (2007) 144–158.

[134] J.Z. Wei, A front-fixing finite difference method for the valuation of Americain options, *Journal of Financial Engineering* **6 (2)** (1997).

[135] J.A.C. Weideman, L.N. Trefethen, The eigenvalues of second-order spectral differentiation matrices, *SIAM Journal on Numerical Analysis* **25** (1988) 1279–1298.

[136] J.A.C. Weideman and S.C. Reddy, A MATLAB differentiation matrix suit, *ACM Transaction on Mathematics Software* **26** (2000) 465–519.

[137] J.A.C. Weideman, Optimizing Talbot's contours for the inversion of the Laplace transform, *SIAM Journal on Numerical Analysis* **44** (2006) 2342–2362.

[138] J.A.C. Weideman and L.N. Trefethen, Parabolic and hyperbolic contours for computing the Bromwich integral, *Mathematics of Computation* **76 (259)** (2007) 1341–1356.



[139] D.B. Welfert, Generation of pseudospectral differentiation matrices I, *SIAM Journal on Numerical Analysis* **34** (1997) 1640–1657.

[140] R.E.Whaley, Valuation of American call options on dividend-paying stocks, *Journal of Financial Economics* **10** (1982) 29–58.

[141] P. Wilmot, J. Dewynne and S. Howison *Options Pricing, Mathematical Models and Computation*, Oxford Financial Press, Oxford, 1993.

[142] P. Wilmot *Theory and Practice of Financial Engineering*, John Wiley & Sons, 1998.

[143] L. Wu. and Y.K. Kwok, A front-fixing finite difference method for the valuation of Americain options, *Journal of Financial Engineering* **6 (2)** (1997) 83–97.

[144] W. Zewen and X. Dinghua, Numerical inversion of multimensional Laplace transforms using moment methods, *Journal of Chinese Universities* **14 (3)** (2005) 267–275.

[145] J. Zhao, M. Davison and R.M. Corless, Compact finite difference method for American option pricing, *Journal of Computational and Applied Mathematics* **206** (2007) 306–321.

[146] S.P. Zhu, An exact and explicit solution for the valuation of American put options, *Quantitative Finance* **6** (2006) 229–242.

[147] S.P. Zhu and W.T. Chen, A new analytical approximation for European puts with stochastic volatility, *Applied Mathematics Letters* **23** (2010) 687–692.

[148] W. Zhu and D.A. Kopriva, A spectral element approximation to price european options. II. The Black-Scholes model with two underlying assets, *Journal of Scientific Computing* **39 (3)** (2009) 323–339.



[149] Y.L. Zhu, X. Wu and I.L. Chern, *Derivative Securities and Difference Methods*, Springer, New York, 2004.

[150] R. Zvan, P.A. Forsyth and K.R. Vetzal, Penalty methods for American option with stochastic volatility, *Journal of Computational and Applied Mathematics* **91 (2)** (1998) 199–218.

[151] R. Zvan, K.R. Vetzal and P.A. Forsyth, PDE methods for pricing barrier options, *Journal of Economic Dynamics and Control* **24** (2000) 1563–1590.